Universidad Autónoma de San Luis Potosí
Facultad de Ingeniería
Centro de Investigación y Estudios de Posgrado

Título de la tesis

Low-order controllers for time-delay systems. Singularities and implementation issues.

Controladores de orden reducido para sistemas con retardo. Singularidades y problemas de implementación

Que para obtener el grado de:

Doctor en Ingeniería Eléctrica

En la especialidad de:

Cibernética, Control y Robótica

Presenta: Juan Diego Torres García

Asesor: César Fernando F. Méndez Barrios

Co-asesor: Silviu Iulian Niculescu

San Luis Potosí, S. L. P. Marzo de 2025

UASLP
Universidad Autónoma de San Luis Potosí

FACULTAD DE INGENIERÍA

CENTRO DE INVESTIGACIÓN Y ESTUDIOS DE POSGRADO

UNIVERSIDAD AUTÓNOMA DE SAN LUIS POTOSÍ
FACULTAD DE INGENIERÍA
Área de Investigación y Estudios de Posgrado

DECLARACIÓN

El presente trabajo que lleva por título:

Low-order controllers for time-delay systems.
Singularities and implementation issues.
Controladores de orden reducido para sistemas con retardo.
Singularidades y problemas de implementación

se realizó en el periodo 03 de 2022 a 03 de 2025 bajo la dirección de los Doctores Cesar Fernando Francisco Mendez Barrios y Silviu Iulian Niculescu

Originalidad

Por este medio aseguro que he realizado el trabajo reportado, y la escritura de este documento de tesis para fines académicos sin ayuda indebida de terceros y sin utilizar otros medios más que los indicados.

Las referencias e información tomadas directa o indirectamente de otras fuentes se han definido en el texto como tales y se ha dado el debido crédito a las mismas.

El autor exime a la UASLP de las opiniones vertidas en este trabajo escrito y asume la responsabilidad total del mismo.

Este trabajo no ha sido sometido como tesis o trabajo terminal a ninguna otra institución nacional o internacional en forma parcial o total, exceptuando el caso cuando existe un convenio específico de doble titulación celebrado entre ambas instituciones.

Se autoriza a la UASLP para que divulgue este documento para fines académicos.

El autor del trabajo escrito, Juan Diego Torres García

UASLP
Universidad Autónoma de San Luis Potosí

FACULTAD DE INGENIERÍA

21 de noviembre de 2024

M.I. JUAN DIEGO TORRES GARCÍA
P R E S E N T E.

En atención a su solicitud de Temario, presentada por los **Dres. César Fernando Francisco Méndez Barrios y Silviu-Iulian Niculescu,** Asesor y Coasesor de la Tesis que desarrollará Usted con el objeto de obtener el Grado de **Doctor en Ingeniería Eléctrica**, me es grato comunicarle que en la sesión del H. Consejo Técnico Consultivo celebrada el día 21 de noviembre del presente año, fue aprobado el Temario propuesto:

TEMARIO:

"Controladores de orden reducido para sistemas con retardo. Singularidades y problemas de implementación"

Introducción
1. Estabilidad de sistemas con retardo: Un enfoque basado en eigenvalores
2. Implementación de una acción derivativa: Un problema mal planteado
3. Caso general de la implementación de la acción derivativa a través de operadores en diferencias
4. Controladores PI para sistemas LTI SISO con retardos

Conclusiones y perspectivas
Apéndice A
Apéndice B
Bibliografía

"MODOS ET CUNCTARUM RERUM MENSURAS AUDEBO"

A T E N T A M E N T E

DR. EMILIO JORGE GONZÁLEZ GALVÁN
DIRECTOR

UNIVERSIDAD AUTONOMA DE SAN LUIS POTOSI
FACULTAD DE INGENIERIA
DIRECCION

Copia. Archivo.
*etn.

www.uaslp.mx

Av. Manuel Nava 8
Zona Universitaria • CP 78290
San Luis Potosí, S.L.P.
tel. (444) 826 2330 al39
fax (444) 826 2336

Contents

Statement of Originality

I, **Juan Diego Torres García**, hereby declare that this thesis, entitled:

Low-Order Controllers for Time-Delay Systems.

Singularities and Implementation Issues

and the work presented within it, are entirely my own.

To my wife, Cecilia, for all the love and support.

All stable processes we shall predict. All unstable processes we shall control.

-Von Neumann

Acknowledgements

First, I want to thank my wife, whose support and love helped me through my path and who was a source of strength and inspiration. *Gracias por todo, Ceci. Te amo.*

I want to thank my parents, for all the support and love, without them I would not be here. *Papá, donde sea que estés, gracias. Gracias Mamá, por todo el apoyo.*

I want to thank Professor César Méndez Barrios for always supporting me and contributing strongly to my academic and personal training and for all the talks, both academic and non-academic. *Gracias por cada consejo y café compartidos.*

I also want to thank Professor Silviu Niculescu, for all the support during these three years, and for teaching me a lot about academia. *Un grand merci pour votre soutien.*

I would like to extend a special thank you to Professor Hitay Özbay and Professor Rifat Sipahi for their invaluable insights and constructive comments, which significantly contributed to enhancing the quality of my manuscript.

I am also grateful to all the members of my thesis committee, Professors Raúl Balderas, Wim Michiels, Sabine Mondié, Belem Saldivar, Tomas Vyhlídal, Emilio González, Miguel Lastras, and Ricardo Álvarez, for their valuable comments and suggestions, which greatly contributed to the improvement of this work. Thank you very much.

I want to thank all my colleagues in Mexico and France. In particular, thanks to Julian and Erick, who shared great memories with me. *Gracias a los dos.* I also want to thank all my friends at L2S, Thibault, Anas, Jeanne, Dora, Benoit, Gabriel, Miguel, Nihed, Flavio, Edwin, Cyprien, and all the other members, for all the talks, coffees, and memories we shared. *Merci beaucoup!*

I also want to thank all the staff members in both the UASLP and L2S. In particular, I want to thank Stephanie, Catherine, and Caroline for all the support and help.

Thanks to all my professors in Mexico and France. I have learned so much.

I am grateful to the *Consejo Nacional de Humanidades, Ciencia y Tecnología* (CONAHCYT) for the financial support provided, without which this project would not have been possible. I also want to thank the *ADI 2022* project, funded by the *IDEX Paris-Saclay, ANR-11-IDEX-0003-02"* for the additional financial support during my stay in France. Finally, I am thankful for the financial support received from CONAHCyT–México, under the grant *Ciencia Básica y de Frontera:* CBF2023–2024–2696.

Abstract

This thesis investigates two key problems related to the stability of dynamical systems with time delays.

The first problem addresses the impact of approximating the derivative action in a closed-loop system with PD controllers using a delay-difference approximation in a frequency-domain framework. The systems under consideration are linear time-invariant (LTI) and single-input/single-output (SISO). Specifically, the study explores the conditions under which such an approximation can destabilize the system, referred to as an improperly-posed scenario. This problem is analyzed in two parts:

1. For approximations involving one or two delays, necessary and sufficient conditions are derived to ensure the system remains *properly-posed*, meaning it preserves stability when the derivative action is replaced by the delay-difference approximation with sufficiently small delays. A *parameter-based approach* is employed, focusing on the system's behavior with respect to such parameters (control gain, delays). It should be mentioned that the delay used in the approximation can also be interpreted and used as a *control parameter*.

2. For cases with an arbitrary number of delays, the effects of increasing the number of delays on properly-posedness conditions are examined. As in the first part, a parametric approach is used to analyze the system. A key tool in both cases is the Newton's diagram method, which enables the expression of characteristic equation solutions as formal power series. This facilitates insights into how specific parameters influence system stability.

The second part of the thesis examines the stabilization of systems with non-minimum phase behavior and input-output delays using PI controllers. These systems are of particular interest due to their relevance in various physical applications, including electrical circuits and aircraft dynamics. The analysis leverages the continuity property of characteristic roots with respect to system parameters. Using the $\mathcal{D}$-partition technique, a methodology is developed to identify stability regions in the control parameter space and determine control gains that achieve the fastest decay rate. The implicit function theorem is applied to detect the movement direction of characteristic roots in the complex plane. The effectiveness of the proposed methodology is validated through numerical simulations and one real-world application, namely a DC-DC power electronics converter.

Besides the frequency-domain framework, both problems share several commonalities:

1. **Parameter-based Analysis of LTI SISO systems with Low-Order Controllers**: Both approaches rely

on low-order controllers with a reduced number of control parameters. More precisely, in the first problem, two control gains and one delay are considered; in the second, two control gains are used.

2. **Singular Behavior**: Both problems exhibit singular behaviors. In the first problem, it arises from the sensitivity of characteristic roots to the delay parameter with the important remark that, in some cases, a "small" delay in the approximation can induce instability for the closed-loop system. In the second, it stems from the spectral abscissa, the rightmost root of the characteristic function, where singularities occur due to multiplicities greater than one, often corresponding to optimal cases.

This work contributes to the understanding and control of delayed dynamical systems, providing both theoretical insights and practical tools for stability analysis.

Resumen

Esta tesis investiga dos problemas clave relacionados con la estabilidad de sistemas dinámicos con retardos temporales.

El primer problema aborda el impacto de aproximar la acción derivativa en un sistema en lazo cerrado con controladores del tipo proporcional-derivativo (PD) mediante una aproximación basada en diferencias con retardo. Los sistemas considerados son lineales invariantes en el tiempo (LTI) y de una sola entrada y una sola salida (SISO). En particular, el estudio explora las condiciones bajo las cuales dicha aproximación puede desestabilizar el sistema, un escenario conocido como mal planteado. Este problema se analiza en dos partes:

1. Para aproximaciones que involucran uno o dos retardos, se derivan condiciones necesarias y suficientes para garantizar que el sistema siga siendo bien planteado, es decir, que conserve la estabilidad al reemplazar la acción derivativa con la aproximación de diferencias con retardos suficientemente pequeños. Se emplea un enfoque paramétrico que analiza el comportamiento del sistema en función de los parámetros de control.

2. Para casos con un número arbitrario de retardos, se examinan los efectos de aumentar el número de retardos sobre las condiciones de mal plantemiento. Al igual que en la primera parte, se utiliza un enfoque paramétrico para analizar el sistema. Una herramienta clave en ambos casos es el método del diagrama de Newton, que permite expresar las soluciones de la ecuación característica como series formales de potencias, facilitando observaciones sobre cómo los parámetros específicos influyen en la estabilidad del sistema.

La segunda parte de la tesis examina la estabilización de sistemas con comportamiento de fase no mínima y retardos en el canal entrada-salida utilizando controladores PI. Estos sistemas son de particular interés debido a su relevancia en diversas aplicaciones físicas, incluyendo circuitos eléctricos y dinámicas de aeronaves. El análisis aprovecha la propiedad de continuidad de las raíces características respecto a los parámetros del sistema. Mediante la técnica de $\mathcal{D}$-particiones, se desarrolla una metodología para identificar regiones de estabilidad en el espacio de parámetros de control y determinar los valores de ganancia que logran la tasa de decaimiento más rápida. El teorema de la función implícita se utiliza para detectar la dirección del movimiento de las raíces características en el plano complejo. La efectividad de la metodología propuesta se valida mediante simulaciones numéricas y una aplicación, en este caso un convertidor DC-DC de electrónica de potencia.

Ambos problemas comparten varios puntos en común:

1. **Análisis Paramétrico con Controladores de Orden Reducido**: Ambos enfoques se basan en controladores de bajo orden con un número reducido de parámetros de control. En el primer problema, se consideran dos ganancias de control y un retardo; en el segundo, dos ganancias de control.

2. **Comportamiento Singular**: Ambos problemas presentan un comportamiento singular. En el primer problema, esto surge de la sensibilidad de las raíces características al parámetro de retardo. En el segundo, proviene de la abscisa espectral, la raíz más a la derecha de la función característica, donde ocurren singularidades debido a multiplicidades mayores a uno, que frecuentemente corresponden a casos óptimos.

Este trabajo contribuye al entendimiento y control de sistemas dinámicos con retardos, proporcionando tanto perspectivas teóricas como herramientas prácticas para el análisis de estabilidad.

Résumé

Cette thèse explore deux problèmes clés liés à la stabilité des systèmes dynamiques en présence des retards.

Le premier problème examine l'impact de l'approximation de l'action dérivative dans un système en boucle fermée avec des contrôleurs de type proportionnel-dérivé (PD), en utilisant une approximation par différences retardées. On considère des systèmes linéaires invariant dans le temps (LTI), à mono entrée/mono sortie (SISO). En particulier, l'étude identifie les conditions sous lesquelles cette approximation peut déstabiliser le système, situation appelée *"improprement posée"*. L'étude est organisé en deux parties :

1. Pour les approximations impliquant un ou deux retards, des conditions nécessaires et suffisantes sont établies pour garantir que le système reste proprement posé, c'est-à-dire qu'il conserve sa stabilité lorsque l'action dérivative est remplacée par une approximation par différences retardées avec des retards *"suffisamment"* petits. Une approche paramétrique est adoptée pour étudier le comportement du système en fonction des gains du contrôleur.

2. Dans le cas où on a un nombre arbitraire de retards, les effets de l'augmentation du nombre de retards sur les conditions pour lesquelles le système est proprement posé sont examinés. Comme dans la première partie, une approche paramétrique est utilisée pour analyser le système. Un outil clé dans les deux cas est la méthode du diagramme de Newton, qui permet d'exprimer les solutions de l'équation caractéristique sous forme de séries formelles, fournissant des informations sur l'influence des paramètres spécifiques sur la stabilité du système.

La deuxième partie de la thèse s'intéresse à la stabilisation de systèmes présentant un comportement à phase non-minimale et des retards (dans le canal entrée-sortie) à l'aide de contrôleurs PI. Ces systèmes sont particulièrement intéressants en raison de leur pertinence dans diverses applications dans les science physiques et de l'ingénieur, notamment les circuits électriques et la dynamique des aéronefs. L'analyse repose sur la propriété de continuité des racines caractéristiques par rapport aux paramètres du système. En utilisant la technique des $\mathcal{D}$-partitions, une méthodologie est développée pour identifier les régions de stabilité dans l'espace des paramètres de contrôle et déterminer les gains permettant d'obtenir le taux de décroissance le plus rapide. Le théorème de la fonction implicite est utilisé pour détecter la direction du déplacement des racines caractéristiques dans le plan complexe. L'efficacité de la méthodologie proposée est validée par des simulations numériques et une application à un convertisseur DC-DC

d'électronique de puissance.

Les deux problèmes partagent plusieurs points communs :

1. **Analyse Paramétrique avec des Contrôleurs d'Ordre Reduit** : Les deux approches s'appuient sur des contrôleurs d'ordre reduit avec un nombre reduit de paramètres de contrôle. Dans le premier cas, deux gains de contrôle et un retard sont considérés ; dans le second, deux gains pour la loi de commande.

2. **Comportement Singulier** : Les deux problèmes présentent un comportement singulier. Dans le premier cas, cela découle de la sensibilité des racines caractéristiques au paramètre de retard. Dans le second, cela provient de l'abscisse spectrale, la racine de la fonction caractéristique localisée la plus à droite dans le plan complexe, où des singularités se produisent en raison de multiplicités supérieures à un, souvent associées aux cas optimaux.

Ce travail contribue à la compréhension et au contrôle des systèmes dynamiques à retards, fournissant à la fois des perspectives théoriques et des outils pratiques pour l'analyse de la stabilité.

Contents

List of Figures

List of Tables

List of symbols

Sets

$\mathbb{C}$	The set of complex numbers
$\mathbb{C}_+(\mathbb{C}_-)$	The set of complex numbers with strictly positive (negative) real part
$\mathbb{R}$	The set of real numbers
$\mathbb{R}^n$	The n dimensional euclidean space
$\mathbb{R}_+$	The set of non-negative real numbers
$\mathbb{Z}$	The set of integers
$\mathbb{Z}_+$	The set of non-negative integers
$\mathbb{N}$	The set of natural numbers
$\mathbb{Q}$	The set of rational numbers
$\mathbb{P}C$	The set of the piecewise continuous functions
$\Re$	Real axis of the complex plane
$\Im$	Imaginary axis of the complex plane
$\mathcal{C}[a,b]$	Space of continuous functions $f:[a,b]\to\mathbb{R}^n$
$\mathcal{C}^m[a,b]$	Space of m continuously differentiable functions $f:[a,b]\to\mathbb{R}^n$
$\mathcal{A}^*$	For a given set $\mathcal{A}$, $\mathcal{A}^* := \mathcal{A}\setminus\{0\}$
$\overline{\mathcal{A}}$	For a given set $\mathcal{A}$, $\overline{\mathcal{A}} := \mathcal{A}\cup\{0\}$

Operators and constants

$\boldsymbol{i} := \sqrt{-1}$	Imaginary unit
$\mathcal{L}$	Laplace transform operator
$\langle \vec{x}, \vec{y} \rangle$	Scalar product between two n-dimensional real vectors $\vec{x} \in \mathbb{R}^n$ and $\vec{y} \in \mathbb{R}^n$
$\mathrm{Arg}(z)$,	The argument of $z \in \mathbb{C}$, also noted as $\angle z$ and defined as $\arctan\left(\frac{\Im(z)}{\Re(z)}\right)$
$\mathrm{Card}(\mathcal{A})$	Cardinality of the set $\mathcal{A}$
$\mathrm{sign}(x)$	For $x \in \mathbb{R}$, $\mathrm{sign}(x) \in \{-1, 0, 1\}$ denotes the sign of x
$\Re(z)$	For $z \in \mathbb{C}$, $\Re(z)$ represents its real part
$\Im(z)$	For $z \in \mathbb{C}$, $\Im(z)$ represents its imaginary part

Abbreviations

HOT	Higher order terms
LHP	Left-half plane (equivalent to $\mathbb{C}_-$)
RHP	Right-half plane (equivalent to $\mathbb{C}_+$)
LTI	Linear time-invariant
SISO	Single-input single-output
PI	Proportional-Integral (controller)
PD	Proportional-Derivative (controller)
PID	Proportional-Integral-Derivative (controller)

List of Publications

Journal Articles

J1 Méndez-Barrios, C.-F., **Torres-García, J.-D.**, and Niculescu, S.-I. (2024), Delay-difference approximations of PD-controllers. Improperly-posed systems in multiple delays case, International Journal of Robust and Nonlinear Control. 34(10), 6431-6454.

J2 Mazenc, F., Niculescu, S. I., and **Torres-Garcia, D**. (2024). Stability analysis for linear systems with a switched rapidly varying delay. Automatica. 169, 111862.

J3 **Torres-García, D**, Méndez-Barrios, F., Niculescu, S.-I. (2024) Stabilization of second-order non-minimum phase system with delay via PI controllers. Spectral abscissa optimization. IEEE Access.

Book Chapters

B1 **Torres-García, D.**, Hernández-Gallardo J.-A., Méndez-Barrios, F., Niculescu, S.-I. (2024, March) Exploring Delay-Based Controllers. A Comparative Study for Stabilizing Angular Positioning. In: Cardona, M.N., Baca, J., Garcia, C., Carrera, I.G., Martinez, C. (eds) Advances in Automation and Robotics Research. LACAR 2023. Lecture Notes in Networks and Systems. (pp. 123-136).

Conferences

C1 **Torres-García, D.**, Méndez-Barrios, F., Niculescu, S.-I., Martínez-González, A. (2022, November). Delay-difference approximation of pd-controllers. insights into improperly-posed closed-loop systems. In IFAC Workshop on Control of Complex Systems 2022, IFAC-PapersOnLine 55(40), 79–85.

C2 **Torres-García, D.**, Méndez-Barrios, F., Niculescu, S.-I. (2023, June). Some Remarks on the Implementation of a Derivative Action via a Delay-Difference Approximation. ECC 2023 - European Control Conference, European Control Association.

C3 **Torres-García, D.**, Méndez-Barrios, F., Niculescu, S.-I. (2024) Impact of Delay-Difference Approximation on PID Controllers: Stability and Performance Insights. 32nd Mediterranean Conference on Control and Automation (MED), 616-621 IEEE.

C4 **Torres-García, D.**, Méndez-Barrios, F., Niculescu, S.-I., Hernández-Gómez, M. (2024)PI Control for Optimal Spectral Abscissa in General Non-Minimum Phase Systems with Time Delay. 2024 10th International Conference on Control, Decision and Information Technologies (CoDIT), 1358-1363 IEEE.

C5 **Torres-García, D.**, Méndez-Barrios, C. F., and Niculescu, S. I. (2024, September). Insights into the Stabilization of a Chain of Integrators via Delay-Difference Approximations. In IFAC Workshop on Time Delay Systems 2024, IFAC-PapersOnLine, 58(27), 19-24.

Introduction

If I have seen further than others, it is by standing upon the shoulders of giants.

Isaac Newton

0.1 Introduction and outline

0.1.1 Introduction

This thesis addresses two main problems related to linear time-delay systems:

1. The stability analysis of a closed-loop linear time-invariant (LTI) single-input single-output (SISO) system with a Proportional-Derivative (PD) controller, where the derivative action is approximated using a delay-difference operator.

2. The optimization of the decay rate for second-order LTI SISO time-delay systems using Proportional-Integral (PI) controllers.

The first problem investigates the impact of incorporating a derivative operator in a control scheme. Specifically, the derivative action is replaced with a delay-difference approximation, and the effect of this approximation on the closed-loop system's stability is analyzed. The results are presented in two parts.

In the first part, the approximation is constructed using either one or two delays, and necessary and sufficient conditions for the closed-loop system's stability are derived. The second part extends the analysis to a more general approximation scheme, where the delay-difference operator incorporates an arbitrary number of commensurate delays. The interest in this kind of approximation comes from the fact that, in theory, increasing the number of delays and, thereby, points produces a more precise approximation. Moreover, considering commensurate delays allows staying in the framework of low-order controllers, in the sense that we increase the number of parameters only by one, regardless of the number of points considered in the approximation scheme. In particular, it is shown that, contrary to what one may expect, increasing the number of delays reduces the interval of *properly-posedness* of the closed-loop system.

The second problem focuses on second-order LTI SISO systems with a delay in the input/output channel. In this context, we propose controlling the system in closed-loop using PI controllers. Moreover, we propose a methodology that allows tuning the control gains such that the system achieves its maximum decay rate (in closed-loop). Both numerical and experimental examples are included to illustrate the effectiveness of the proposed methodology.

0.1.2 Outline

The thesis is organized in four parts, as follows:

Part 1 In the remaining of this Chapter, we introduce the basic mathematical tools required for this work. It covers the fundamentals of time-delay systems and their solutions and discusses the concept of improperly-posedness and singularity. Additionally, Chapter 1 presents the stability analysis of time-delay systems using an eigenvalue-based approach, which is the approach considered in this work.

Part 2 Chapter 2 examines the improperly-posedness of the delay-difference approximation for the derivative action on the implementation of PD controllers, focusing on cases with one and two delays. In Chapter 3, this analysis is extended to cases involving an arbitrary number of delays.

Part 3 Chapter 4 addresses the optimization of the spectral abscissa for a second-order LTI SISO system with a delay in the input/output channel in closed-loop with a classical PI controller.

Part 4 Finally, Chapter 13 concludes the thesis with a summary of the findings and perspectives for future research.

It is worth mentioning that two appendices are also included at the end of the document. Appendix A includes the proof of the main results of the thesis, while Appendix B contains Python and Matlab codes used on different parts of the thesis.

0.2 Prerequisites and mathematical background

This section presents the basic mathematical theory for the development of this thesis. For comprehensiveness, the content provided herein should be sufficient to follow the main results. However, to gain a deeper understanding of the general ideas and the underlying theory, we strongly encourage the reader to consult the references provided at the end of each section.

0.2.1 The Implicit function theorem

The Implicit Function Theorem (Krantz and Parks, 2002) gives us a tool to find a velocity function for an implicit function $y = \phi(x)$ coming from an equation of the type $f(x, y) = 0$. We have the following Theorem, retrieved from (Canuto and Tabacco, 2015)

Theorem 0.2.1: Implicit Function Theorem

Let Ω be a non-empty open set in $\mathbb{R}^2$ and $f : \Omega \to \mathbb{R}^2$ a $\mathcal{C}^1$ map. Assume that for some point $(x_0, y_0) \in \Omega$ we have $f(x_0, y_0) = 0$. Then, if $\frac{\partial f}{\partial y}(x_0, y_0) \neq 0$ there exist a neighborhood $\mathcal{N}$ of x_0 and a function $\phi : I \to \mathbb{R}$ such that:

1. $(x, \phi(x)) \in \Omega$ for any $x \in \mathcal{N}$
2. $y_0 = \phi(x_0)$
3. $f(x, \phi(x)) = 0$ for any $x \in \mathcal{N}$
4. ϕ is a $\mathcal{C}^1$ map on $\mathcal{N}$ and its derivative is given by:

$$\phi'(x) = -\frac{\frac{\partial f}{\partial x}(x, \phi(x))}{\frac{\partial f}{\partial y}(x, \phi(x))}$$

in the neighborhood of (x_0, y_0).

Note that, for the sake of simplicity, Theorem 0.2.1 considers the two-dimensional case. Such a case is sufficient in the context of this work, but it should be mentioned that this result is already extended for higher dimensional cases.

Consider the following illustrative example:

Example 1. *Consider the following algebraic equation:*

$$x^3 + y^3 + 2x^2y = 1,$$

which has a solution given by $(x_0, y_0) = (1, 0)$. Now, we are interested in finding, if any, the behavior of the derivative of the solution in a neighborhood of (x_0, y_0). To such a task we define the following function $f : \mathbb{R}^2 \to \mathbb{R}$:

$$f(x, y) = x^3 + y^3 + 2x^2y - 1.$$

According to the above theorem, first, we verify that $f_y(1, 0) \neq 0$. Indeed, we can easily observe that $f_y(1, 0) = 2$. Therefore, we know that, for $\mathcal{N}$ a neighborhood of x_0, there exists a function $\phi : \mathcal{N} \to \mathbb{R}$ such that $\phi(1) = 0$ and the following must hold:

$$x^3 + (\phi(x))^3 + 2x^2(\phi(x)) = 1, \quad x \in \mathcal{N}.$$

Finally, one can easily compute $f_x(1, 0) = 3$, which means that the tangent $\phi'(1) = -2/3$; therefore, the map ϕ is decreasing at this point, and the corresponding tangent to its graph is $y = -\frac{2}{3}(x - 1)$.

For a comprehensive treatment of the Implicit Function Theorem and relevant historical insights, we refer the reader to Krantz and Parks (2002).

0.2.2 Perturbation theory: An introduction

One way to study the stability of linear dynamical systems relies on studying its associated characteristic polynomials. In this context, we say that a *linear system* is exponentially stable if and only if all the roots of its characteristic polynomial have negative real part. In this spirit, let us consider the following characteristic polynomial $\Delta : \mathbb{C} \times \mathbb{R}^m \to \mathbb{C}$:

$$\Delta(s; \vec{p}) = s^n + a_{n-1}(\vec{p})s^{n-1} + \cdots + a_0(\vec{p}), \tag{1}$$

where $a_i(\vec{p})$ for $i \in \{0, 1, 2, \ldots, n-1\}$ are real coefficients that smoothly depend on the vector of m real parameters $\vec{p} = [p_1, p_2, \ldots, p_m]$. Note that, for a given $\vec{p} \in \mathcal{P} \subset \mathbb{R}^m$, where $\mathcal{P}$ is a compact set, the polynomial $\Delta(s; \vec{p})$ has n roots, counting multiplicities. With this in mind, we refer to the set of vectors $\vec{p}$ such that the polynomial (1) is stable as its stability domain. Additionally, the set of points $\vec{p}$ for which the polynomial (1) has zero, or purely imaginary roots (i.e., roots of the form $s = \pm \boldsymbol{i}\omega$, where $\omega \in \mathbb{R}$), while all other roots have negative real part, is referred to as the *stability boundary*. We aim to illustrate these ideas with the following example.

Example 2 (Stability domain)**.** *Consider the polynomial function $\Delta : \mathbb{C} \times \mathbb{R}^2 \to \mathbb{C}$:*

$$\Delta(s; \vec{p}) = s^2 + p_1 s + p_2. \tag{2}$$

It is clear that, depending on the values of p_1 and p_2, the roots of $\Delta(s; \vec{p})$ will change their location on $\mathbb{C}$. However, for a polynomial of degree two, it is well known that, in order to be stable, all the coefficients of the polynomial must be positive. Therefore, the stability domain will correspond to the region in the parameters plane (see Figure 1) (p_1, p_2) such that the following inequalities hold:

$$p_1 > 0, \quad p_2 > 0.$$

This means that, for any pair of parameters $\vec{p} = (p_1, p_2) \in \mathbb{R}^2_+$, the characteristic polynomial $\Delta(s; \vec{p})$ will remain stable.

This example illustrates that the stability of the characteristic polynomial depends on its parameters $\vec{p}$. In particular, this parametric approach is of interest in the context of control systems, as it allows analysis of the system's stability in terms of control parameters. In this context, the core concept of perturbation theory is to analyze how the characteristic roots behave as one or more parameters p_i are varied. In this spirit, the Implicit Function Theorem, previously introduced, can be useful in characterizing the behavior of the roots as the parameters

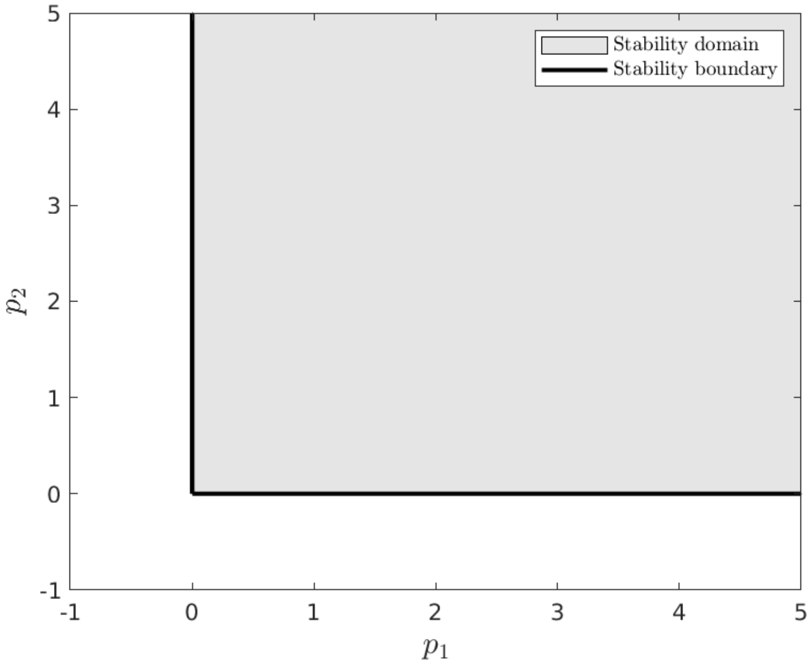

Figure 1: Stability region and boundary of $\Delta(s;\vec{p})$.

$\vec{p}$ change.

Remark 1. *Note that one of the assumptions in the Implicit Function Theorem is that* $\frac{\partial f}{\partial y}(x_0, y_0) \neq 0$*. In this case, with* $y = s$ *and* $x = p_i$*, the primary implication is that the root in question is simple. Therefore, when a combination of parameters leads to a double root, additional considerations may be required.*

To illustrate this idea, let us consider the same $\Delta(s;\vec{p})$ as in Example 2.

Example 3 (Perturbation of simple roots)**.** *Let us consider a root* s *of the characteristic polynomial* $\Delta(s;\vec{p})$*, given in* (2)*. From the Implicit Function Theorem, such a root is a function of the parameter vector* $\vec{p}$*, which means that there exists a map* $s(\vec{p})$*. Consider the derivative of the characteristic equation* $\Delta(s;\vec{p}) = 0$*, with respect to* $\vec{p}$*. We obtain the following:*

$$\frac{\partial \Delta}{\partial s}\frac{\partial s}{\partial \vec{p}} + \frac{\partial \Delta}{\partial \vec{p}} = 0,$$

which leads us to the same writing as the Implicit Function Theorem:

$$\frac{\partial s}{\partial \vec{p}} = -\frac{\frac{\partial \Delta}{\partial \vec{p}}}{\frac{\partial \Delta}{\partial s}}.$$

From this last expression, it is clear that a multiple root is a nonsmooth function of $\vec{p}$*. It is worth noting that this last expression also allows us to analyze the behavior of a given root* s*, as a parameter* p_i *varies. To illustrate how the roots behave as the parameters vary, let us fix* $p_2 = 1$ *and allow* p_1 *to change. When* $p_1 = 2$*, the polynomial* $\Delta(s;\vec{p})$ *has a root of multiplicity two at* $s^* = -1$*. At this point, the implicit function theorem no longer applies. Figure 2*

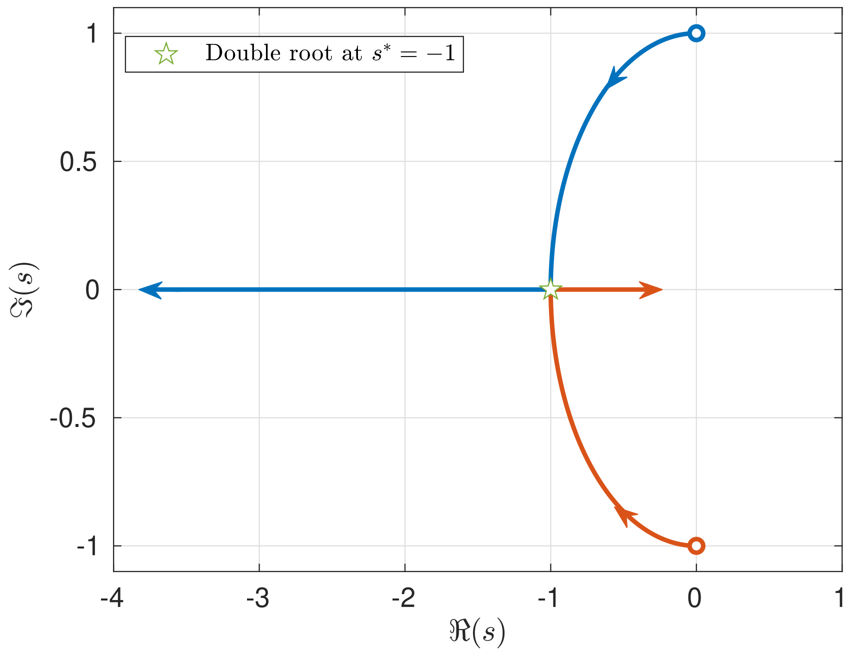

Figure 2: Evolution of the roots of $\Delta(s;\vec{p}$ as $p_1 \in (0,4)$ increases.

illustrates the behavior of the roots as p_1 varies. Notably, once the root reaches a multiplicity of two, the polynomial's roots transition from a pair of complex conjugates to two distinct real roots. This bifurcation, which occurs when two roots collide *and then separate, is a key challenge in characterizing the behavior of roots at points where their multiplicity exceeds one. Such points complicate the analysis due to the nonsmooth nature of the root trajectories.*

For an in-depth discussion and theoretical development of Perturbation Theory, we refer the reader to Seyranian and Mailybaev (2003) and the thesis by Martínez González (2021).

0.2.2.1 $\mathcal{D}$-partition method

As has already been mentioned, the stability properties of a dynamical system can be studied by the location of its characteristic roots in the complex plane. In that sense, let us consider a characteristic polynomial $\Delta(s;\vec{p})$ of given degree $n \in \mathbb{N}$ with $\vec{p} \in \mathbb{R}^m$ being the set of real parameters $(p_1, p_2, \ldots, p_m)$. Given a fixed $\vec{p}^*$, it is clear that the polynomial $\Delta(s;\vec{p}^*)$ has a total of n roots, which can be further divided into r stable roots and q unstable roots, such that $n = r + q$. With this in mind, the $\mathcal{D}$-partition method is a methodology, originally presented by Neimark in (Neimark, 1948) that allows *decomposing* the parameter space into n different domains characterized by the number of stable roots within them. It is also worth mentioning that, in a different context, similar ideas to those of Neimark were discussed by Pinney in (Pinney, 1958). The key property of the characteristic roots that allows the development of this methodology is their continuity with respect to the parameters of the characteristic function. This implies, as extensively discussed in the literature (see, for example, Michiels and Niculescu (2014) and the references therein), that stability can only be lost if a root crosses the imaginary axis. In other words, this occurs when a root takes the form $s = \boldsymbol{i}\omega$, i.e., the root is located over the imaginary axis. Example 2 is the application of the $\mathcal{D}$-partition method. In the following, we present a generalization of this method for the cases of one and two real parameters.

First, consider the family of polynomials defined in the following way:

$$\Delta(s;k) = P_1(s) + kP_2(s), \quad k \in \mathbb{R}, \tag{3}$$

where $P_1(s)$ and $P_2(s)$ are polynomials in the complex variable s and real coefficients. The following result (retrieved from Gryazina and Polyak (2006)), while intuitive, is crucial for the subsequent discussion:

Theorem 0.2.2

Let $P_1(s)$ and $P_2(s)$ be polynomials of degree n and m, respectively, with $n \geq m$. Then, the polynomial $\Delta(s;k) = P_1(s) + kP_2(s)$, where $k \in \mathbb{R}$, has exactly n roots, counted with multiplicity. Moreover, $\Delta(s;k)$ has at most $n+1$ $\mathcal{D}$-decomposition segments, and no more than $\lceil \frac{n}{2} \rceil$ stable segments, where $\lceil \cdot \rceil$ denotes the ceiling operator.

Remark 2. *Note that any values for which roots pass from one segment to the other are given by:*

$$k = -\frac{P_1(\boldsymbol{i}\omega)}{P_2(\boldsymbol{i}\omega)} \quad \wedge \quad \Im(k) = 0.$$

Remark 3. *Since the considered polynomials Δ have real coefficients, the existence of a root given by $s = \boldsymbol{i}\omega$, implies that $s = -\boldsymbol{i}\omega$ is also a root. Therefore we can reduce the analysis to consider only $\omega \in [0, +\infty)$.*

We now illustrate these concepts through the following example:

Example 4 (Algorithm of the $\mathcal{D}$-partition method for polynomials with one real parameter)**.** *Let us consider the characteristic function $\Delta : \mathbb{C} \times \mathbb{R} \to \mathbb{C}$:*

$$\Delta(s;k) = s^2 + ks + 1.$$

As mentioned earlier, a stability switch can only occur if one or more roots cross the imaginary axis. Therefore, as a ***first step****, we set $s = \boldsymbol{i}\omega$, leading to the following equation:*

$$\Delta(\boldsymbol{i}\omega;k) = -\omega^2 + \boldsymbol{i}\omega k + 1 = 0.$$

Since it is evident that $\Delta(\boldsymbol{i}\omega;k) = 0 \implies \Delta(-\boldsymbol{i}\omega;k) = 0$, we restrict our consideration to $\omega \in [0, +\infty)$, as previously mentioned. As a ***second step****, we seek values of k such that there exists an ω for which a stability switch occurs. These values are given by:*

$$k = \frac{\omega^2 - 1}{\boldsymbol{i}\omega} = \frac{(1-\omega^2)\boldsymbol{i}}{\omega} \quad \wedge \quad \Im(k) = 0.$$

*In this case, it is clear that for any value of $\omega \neq 0$, $k \in \boldsymbol{i}\mathbb{R}$, which means that the only possible crossing occurs at $k = 0$. For the **third step**, a natural question would be* how to determine the direction of the crossing. *For such a task, the ideas presented in the two previous sections may be useful. In this sense, using the Implicit Function Theorem, we can obtain:*

$$\frac{ds}{dk} = -\frac{\frac{\partial \Delta}{\partial k}}{\frac{\partial \Delta}{\partial s}} = -\frac{s}{k+2s}.$$

Note that at $k = 0$, $sign(ds/dk) = -1$, indicating that the crossing occurs from right to left or, in other words, that the root s is decreasing its value. This is consistent with what we would expect since, similarly to Example 2, we have a second-order polynomial, which means that stability will only be preserved if $k > 0$. Moreover, as expected from Theorem 0.2.2, there is only one stable region ($n/2 = 1 \geq 1$).

Next, we want to consider the following family of polynomials:

$$\Delta(s; k_1, k_2) = P_0(s) + k_1 P_1(s) + k_2 P_2(s), \quad k_2, k_2 \in \mathbb{R}, \tag{4}$$

which correspond to polynomials with two different real parameters. We have the following results, retrieved from Gryazina and Polyak (2006):

Theorem 0.2.3

Let $P_0(s)$, $P_1(s)$, and $P_2(s)$ be polynomials of degree n with real coefficients. Then, the polynomial $\Delta(s; k_1, k_2) = P_0(s) + k_1 P_1(s) + k_2 P_2(s)$ has no more than $(2n(n-1)+3)$ $\mathcal{D}$-decomposition regions on the parameter plane (k_1, k_2).

Clearly, in this case, we have regions divided by parametric curves instead of segments. In particular, such a curve is characterized by the equation:

$$\Delta(\boldsymbol{i}\omega; k_1, k_2) = 0,$$

which implies:

$$\Re\{\Delta(\boldsymbol{i}\omega; k_1, k_2)\} = 0 \quad \wedge \quad \Im\{\Delta(\boldsymbol{i}\omega; k_1, k_2)\} = 0,$$

from where we can solve for k_1 and k_2, obtaining:

$$k_1 = -\frac{\Delta_1}{\Delta_0}, \quad k_2 = -\frac{\Delta_2}{\Delta_0}, \tag{5}$$

where:

$$\Delta_0 = \begin{vmatrix} U_{P_1} & U_{P_2} \\ V_{P_1} & V_{P_2} \end{vmatrix}, \quad \Delta_1 = \begin{vmatrix} U_{P_0} & U_{P_2} \\ V_{P_0} & V_{P_2} \end{vmatrix}, \quad \Delta_2 = \begin{vmatrix} U_{P_1} & U_{P_0} \\ V_{P_1} & V_{P_0} \end{vmatrix},$$

where:

$$\begin{aligned} U_{P_0} &= p_{0,0} - p_{0,2}\omega^2 + p_{0,4}\omega^4 + \dots, \\ U_{P_1} &= p_{1,0} - p_{1,2}\omega^2 + p_{1,4}\omega^4 + \dots, \\ U_{P_2} &= p_{2,0} - p_{2,2}\omega^2 + p_{2,4}\omega^4 + \dots, \\ V_{P_0} &= p_{0,1} - p_{0,3}\omega^2 + p_{0,5}\omega^4 + \dots, \\ V_{P_1} &= p_{1,1} - p_{1,3}\omega^2 + p_{1,5}\omega^4 + \dots, \\ V_{P_2} &= p_{2,1} - p_{2,3}\omega^2 + p_{2,5}\omega^4 + \dots, \end{aligned}$$

where the coefficients $p_{i,j}$ correspond to the coefficients of the term s^j in P_i. For $\Delta_0 \neq 0$, the parameters in (5) describe a parametric curve. Moreover, crossing such a curve in the parametric plane implies a complex conjugate root crossing the imaginary axis in the complex plane. The $\mathcal{D}-$decomposition curve, which corresponds to the stability crossing curve, also includes the following lines:

$$p_{0,0} + k_1 p_{0,1} + k_2 p_{0,2} = 0, \quad \wedge \quad p_{0,n} + k_1 p_{1,n} + k_2 p_{2,n} = 0, \tag{6}$$

which correspond to crossing through $\omega = 0$ and, as a consequence, correspond to crossing of simple real roots. Note that if (k_1, k_2) corresponds to control parameters and the system associated with the characteristic function $\Delta(s; k_1, k_2)$ is strictly proper, then $p_{1,n} = p_{2,n} = 0$. We illustrate this methodology with the following example:

Example 5 (Algorithm of the $\mathcal{D}$-partition method for polynomials with two real parameters)**.** *Consider the following two-parameter polynomial:*

$$\Delta(s; k_1, k_2) = s^2 + k_1(s+1) + k_2(2s+3).$$

First, we can identify that $P_0(s) = s^2$*,* $P_1(s) = s+1$ *and* $P_2(s) = 2s+3$*. By considering* $s = \boldsymbol{i}\omega$ *such that* $\Delta(\boldsymbol{i}\omega; k_1, k_2) = 0$ *with* $\omega \in \mathbb{R}_+^*$ *we obtain:*

$$k_1(\omega) = -2\omega^2 \quad \wedge \quad k_2(\omega) = \omega^2,$$

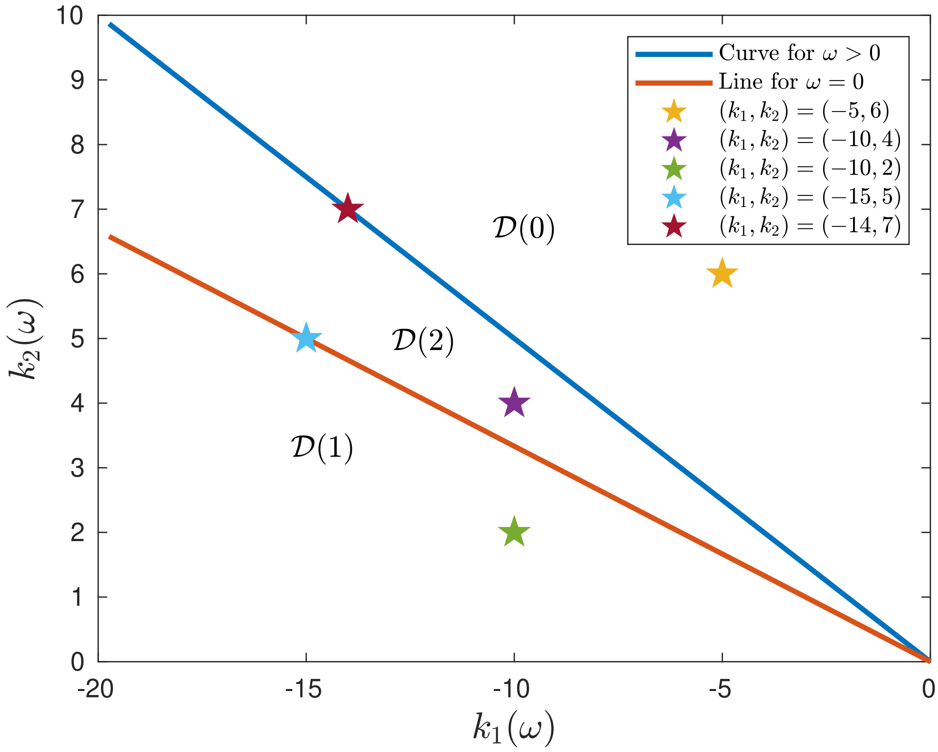

Figure 3: $\mathcal{D}$-decomposition curves and regions on the parameter space (k_1, k_2).

and for $\omega = 0$:

$$k_2 = -\frac{k_1}{3}.$$

The corresponding curve is depicted in 3, where we indicate by $\mathcal{D}(q)$ the regions with q unstable roots. In particular, the region $\mathcal{D}(0)$ is referred to as a stable region.

Since $\Delta(s; k_1, k_2)$ is a second-degree polynomial, it always has two different roots. Table 1 summarizes the location of such roots for different parameters located either inside one of the regions $\mathcal{D}(q)$ or over the corresponding curves, as depicted in Figure 3.

Table 1: **Location of the roots of $\Delta(s; k_1, k_2)$ for different parameter values.**

(k_1, k_2)	Corresponding region	Roots locations	Number of unstable roots
$(-5, 6)$	$\mathcal{D}(0)$	$s = (-7 \pm \sqrt{3}\boldsymbol{i})/2$	0
$(-10, 4)$	$\mathcal{D}(2)$	$s = 1 \pm \boldsymbol{i}$	2
$(-10, 2)$	$\mathcal{D}(1)$	$s = 3 \pm \sqrt{13}$	1
$(-15, 5)$	–	$s = 0 \wedge s = 5$	1
$(-14, 7)$	–	$s = \pm\sqrt{7}\boldsymbol{i}$	–

For a complete description of the $\mathcal{D}$ method and a collection of compelling examples, we refer the reader to Gryazina et al. (2008).

0.2.2.2 Newton diagram method

Consider the *simple*, yet complicated, question in the realm of solutions of polynomials: given a polynomial equation of the form $f(x, y) = 0$, where f is a polynomial in the two variables x and y, how can we determine y as a function of x such that $f(x, y(x)) = 0$? To address this question, Sir Isaac Newton provided us with a geometric instrument: the *Newton Polygon*. This powerful tool enables us to express y as a power series in x, a series frequently referred to as a Puiseux series. Notably, analogous to the Taylor series, one can shift any point x_0 to the origin by the translation $x \to x - x_0$. This methodology, known as the *Newton Diagram Method*, is one of the main tools employed in the development of this thesis. We have the following result, retrieved from Wall (2004):

Theorem 0.2.4: Puiseux Theorem

Any equation of the form $f(x, y) = 0$ where f is a polynomial with zero constant term admits at least one solution in formal power series with the following form:

$$x = t^q, \quad y = \sum_{1}^{\infty} a_r t^r, \quad q \in \mathbb{N}.$$

Theorem 0.2.4, in essence, only states that there is some solution of $f(x, y)$ such that $y = a_0 x^{\beta} +$ Higher order terms (HOT) where $\beta \in \mathbb{Q}$. But how do we find β? For the sake of clarity and comprehension, this is presented through an example.

Example 6. *Consider the function $f : \mathbb{R}^2 \to \mathbb{R}$ defined as:*

$$f(x, y) = y^2 + xy + y - x^2, \tag{7}$$

Our goal is to find a representation of y as a power series in x, such that $f(x, y(x)) = 0$. To simplify the analysis, we note that, as already mentioned, any point can be translated to the origin by applying a simple transformation $x \to x - x_0$. Without loss of generality, we will perform the power series expansion at $x = 0$. Note that, as mentioned, there must be a solution of the form $y = a_1 x^{\beta_1} + HOT$. Substituting such a solution on $f(x, y)$, we note that each term of the form $c_{q,r} x^r y^q$ will produce a term $c_{q,r} a_1^q x^{r+q\beta_1}$, plus the terms of higher order. It is clear that any term of order lower than $r + \beta_1 q$ must be canceled. Next, we need to identify the possible values of β_1. To this end, we consider a plane (q, r), where q and r represent the powers of elements of the form $c_{q,r} x^r y^q$, and mark *those pairs $p_{q,r} = (q, r) \in \Pi := \{p_{q,r} : c_{q,r} \neq 0\}$. In this case, it is clear that $\Pi = \{(0, 2), (1, 0), (1, 1), (2, 0)\}$. Next, the lines $r + \beta_1 q = constant$ all have the same slope, and we consider those that pass through one of the points we included. We continue by considering the segment until the line passes through another marked point (as we need the terms to cancel, we need at least two points). Finally, for a slope μ, $\beta_1 = -\mu$. Following this procedure, we obtain Figure 4. Here, we introduce the concept of the Newton Diagram, which is the convex hall above and to the right of the points*

$p_{q,r} \in \Pi$. Next, the lower boundary, composed of the line segments obtained by connecting the points, is the Newton Polygon of f. After obtaining β_1, we must find the corresponding coefficient a_1. The non-trivial solutions of the following equation give such coefficients:

$$\sum_{l=i}^{j} c_i(x)w^l = 0,$$

where $a_i(x)$ corresponds to $c_{q,r}x^r$, and the values of l are all values of q that are part of the line segment of the given slope β_1. From Figure 4 we observe two different slopes $\beta_{1,0} = 0$ and $\beta_{1,1} = 2$. Moreover, the horizontal length of the corresponding line segment indicates the number of roots with structure given by $y(x) = ax^{\beta_1} + HOT$. Let us first consider $\beta_{1,0} = 0$. The corresponding equation is:

$$w^2 + w = 0,$$

which has two solutions. As mentioned, we are interested in the non-trivial ones, which in this case is only $w = -1$. This indicates that there is a solution $y(x) = -1 * x^0 + \mathcal{O}(x) = -1$, for $x = 0$. Next, for $\beta_{1,1} = 2$ we have the following equation:

$$w - x^2 = 0,$$

which has a solution $w = x^2$. This means that the following solutions exist:

1. $y(x) = -1 + \mathcal{O}(x)$.

2. $y(x) = x^2 + \mathcal{O}(x^3)$.

As expected, we have one root with each corresponding slope β_i and constants a_i. Finally, to obtain the corresponding higher-order terms, we repeat the above process for the polynomial obtained after replacing y with the corresponding series.

Algorithm 1 summarizes the procedure presented in the above example.

For an introduction to the Newton diagram method and historical insights into Newton's work on algebraic equations, see Christensen (1996). Technical details on the contention of the Puiseux Theorem can be found in the second part of Puiseux (1850). Additionally, some of Sir Isaac Newton's early ideas on algebraic equations are discussed in Newton and Whiteside (2008).

0.2.3 Chebyshev polynomials

Just as Fourier did with the theory of Fourier series, which gives us a tool to represent a function as a trigonometric series in the following way:

$$F(\theta) \approx \frac{1}{2}\sum_{k=0}^{n} c_k(e^{\boldsymbol{ik\theta}} + e^{-\boldsymbol{ik\theta}}), \quad \theta \in [-\pi, \pi], \tag{8}$$

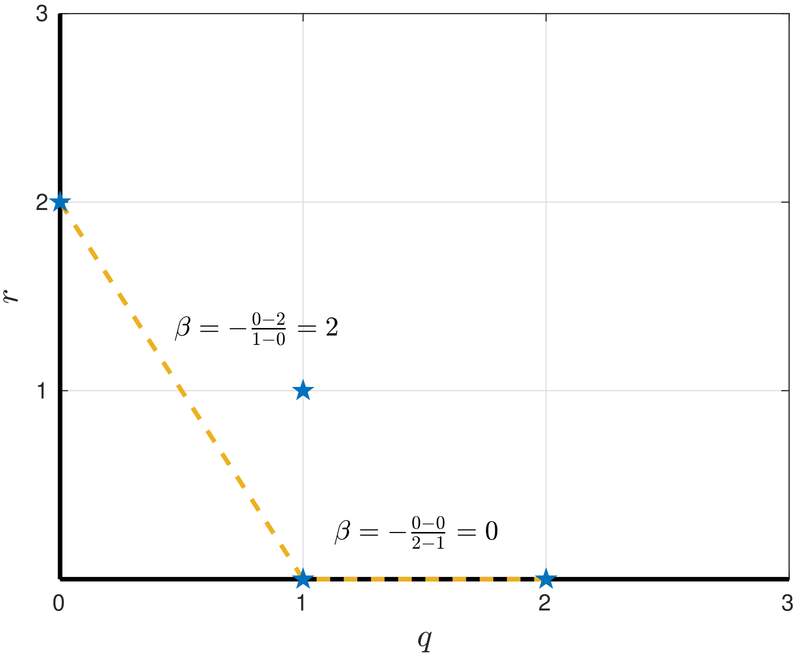

Figure 4: Newton Polygon of f.

Algorithm 1: Newton Diagram Method for Determining Asymptotic Solutions.

Data: $f(x, y) = \sum_{i=0}^{n} \sum_{j=0}^{m} c_{j,i} x^i y^j$: Polynomial with real coefficients.

Result: Set of possible solutions $y(x) = a_i x^{\beta_{1,i}} + \text{HOT}$ (Higher Order Terms).

Initialization: Initialize an empty set Π (to store exponent pairs);
for $i = 0$ *to* n **do**
  for $j = 0$ *to* m **do**
    if $c_{j,i} \neq 0$ **then**
      Add the point (j, i) to the set Π; `// Points represent exponents in` $c_{j,i}x^i y^j$ `terms.`

Construct Newton Polygon.
Plot all points in Π in the (q, r) plane.
Find the lower bound convex hull of Π as the Newton Polygon N. `// Lower boundary of the convex hull is key.`
Identify Edge Slopes.
for *each edge* e_k *of* N **do**
  Compute the slope $\beta_{1,k}$ of the edge e_k. `// Slopes represent candidate exponents of` x `in solutions.`

Solve for Leading Order Coefficients
for *each slope* $\beta_{1,k}$ **do**
  Find the non-trivial solution of $\sum_{l=i}^{j} c_i(x) w^l = 0$, where $c_i(x)$ are the terms associated with the points in the corresponding edge e_k.
  Add the solution $y(x) = a_k x^{\beta_{1,k}} + \text{HOT}$ to the result set, where a_k correspond to the non-trivial solutions found.
Output: Return the set of possible solutions $\{y(x) = a_k x^{\beta_{1,k}} + \text{HOT}\}$.

Chebyshev (or Tchebyshev in French, Tschebyschow in German) provides us with a tool to represent a function as:

$$f(x) \approx \sum_{k=0}^{n} a_k T_k(x), \quad x \in [-1, 1]. \tag{9}$$

In this case, the polynomial T_k is known as the $k-th$ Chebyshev polynomial (of the first kind), which was introduced by Chebyshev in the 1850s (for further details, see Tchébychev (1858)). We shall next explain how such polynomials are defined. Indeed, the $k-th$ Chebyshev polynomial of the first kind can be seen as the real part of the function z^k on the unit circle, namely:

$$x = \Re(z) = \frac{1}{2}(z + z^{-1}) = \cos(\theta) \tag{10}$$

$$T_k(x) = \Re(z^k) = \frac{1}{2}(z^k + z^{-k}) = \cos(k\theta). \tag{11}$$

Some interesting properties of these polynomials are the following:

1. T_k always satisfies $-1 \leq T_k(x) \leq 1$ for $x \in [-1, 1]$.

2. For any $k \in \mathbb{N}$ the following relationship allows computing the kth Chebyshev polynomial by induction (i.e. in a recursive way):

$$T_{k+1}(x) = 2xT_k(x) - T_{k-1}(x).$$

   It is clear that the corresponding initial conditions are $T_0(x) = 1$ and $T_1(x) = x$.

Next, for the $k-th$ Chebyshev polynomial of the second kind U_k we consider the imaginary part of z^k on the unit circle, namely:

$$z^k = T_k(x) + \boldsymbol{i}yU_{k-1}(x),$$

where $z = x + \boldsymbol{i}y$, and U_k is defined as:

$$U_k(x) = \frac{\sin((k+1)\theta)}{\sin(\theta)},$$

and satisfies the recurrent relationship:

$$U_{k+1}(x) = 2xU_k(x) - U_{k-1}(x),$$

but with the initial conditions given by $U_0(x) = 1$ and $U_1(x) = 2x$.

We summarize the first 3 iterations, namely $k = 2, 3, 4$, for T_k and U_k in Table 2

Table 2: **Some examples of Chebyshev polynomials of the first and second kind.**

k	$T_k(x)$	$U_k(x)$
2	$T_2(x) = 2x^2 - 1$	$U_2(x) = 4x^2 - 1$
3	$T_3(x) = 4x^3 - 3x$	$U_3(x) = 8x^3 - 4x$
4	$T_4(x) = 8x^4 - 8x^2 + 1$	$U_4(x) = 16x^4 - 12x^2 + 1$

For a complete characterization of Chebyshev polynomials in the context of interpolation methods, we refer to Trefethen (2019), which also includes historical notes and introduces the MATLAB package *Chebfun* (see the official website at https://www.chebfun.org/).

0.3 Time-delay systems: A brief introduction

Time-delay systems are a class of *infinite-dimensional* systems (see Remark 4), described by *functional differential equations* of the form:

$$\frac{dx(t)}{dt} = f(t, x(t), x(t-\tau)), \tag{12}$$

with the initial condition:

$$x(t_0 + \theta) = \phi(\theta), \quad \theta \in [-\tau, 0], \quad \phi \in \mathcal{C}[t_0 - \tau, t_0].$$

Time-delay dynamical systems have a particular feature: they incorporate the influence of the past into the present state. This feature makes them particularly relevant in modeling real-world scenarios since control systems often operate in the presence of delays. Examples span across diverse fields, including biology, physics, engineering, and economics (Sipahi et al., 2011). To further understand the need for an initial condition that covers a full interval of time, we illustrate the *solution* of a delay differential equation in Figure 5

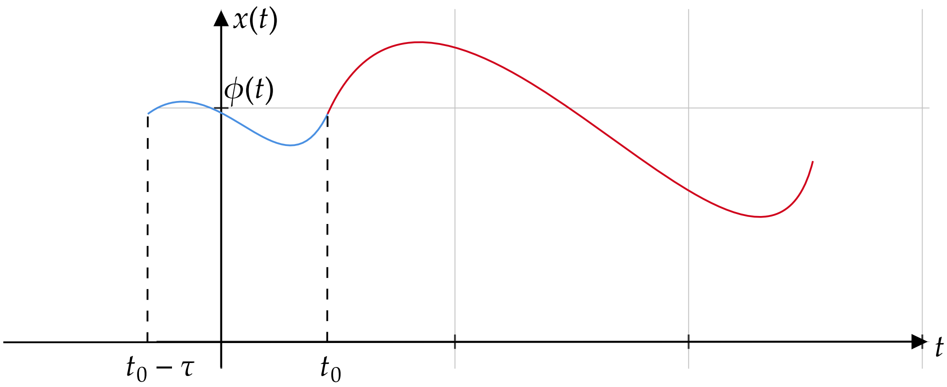

Figure 5: Time-delay systems and their initial condition.

Remark 4. *In a finite-dimensional dynamical system, the system's evolution can be fully determined by specifying a finite set of initial conditions. This finite set cardinality defines the system's dimension. However, in systems with delays, the present state depends continuously on past states over an interval, meaning that an entire function, rather than a finite collection of values, is required to describe the initial condition. This reliance on a continuous past history places delay systems in the realm of infinite-dimensional systems.*

In the rest of this chapter, we aim to present and understand the fundamental principles of time-delay systems. We will explore how these systems are modeled, examine some of their stability properties, and discuss some of the techniques used to analyze them. Furthermore, we will delve into the complex dynamics they exhibit, as well as some of the different kinds of time-delay systems we might encounter.

0.3.1 Dynamical systems with time delays

The following examples illustrate how delays naturally and intuitively emerge in the dynamics of various systems. These examples serve as a compelling motivation to explore the impact of delays on dynamical systems and highlight their significant influence on system behavior.

Example 7 (Supply chain)**.** *Some of the key components of a supply chain include production, inventories, transportation, communication, and decision-making. It is easy to observe that each of these components involves processes that* take time*, meaning the corresponding actions within the supply chain are not instantaneous.*

One of the main objectives of such a system is to maintain sufficient production to meet customer demand while avoiding excess that could lead to losses. Achieving this balance is clearly influenced by the presence of delays, which directly impact the system's ability to respond efficiently to changes in demand. Figure 6 illustrates in a general way how all these processes interact and how delays appear in between them. In particular, in Delice and Sipahi (2009), the authors discuss three different ways that delay may be considered when modeling supply chain dynamics: constant, distributed, and time-varying delays. In particular, for the case of constant delays, the Riddalls's model (see Riddalls and Bennett (2002)) is considered, namely:

$$\frac{dO(t)}{d(t)} = \alpha(L(t) - O(t - \tau)),$$

where $O(t)$ is the orders rate, τ correspond to a constant delay, $L(t)$ is the loss rate, and α is a constant.

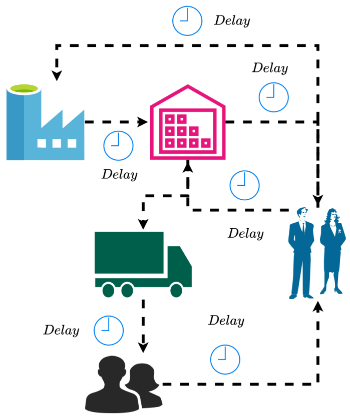

Figure 6: Supply chain diagram.

List of references:

1. *Delice and Sipahi (2009)*

2. *Ivanov et al. (2018)*

3. Wu et al. (2024)

Example 8 (Networked Control Systems (NCS))**.** *In modern control problems, controlling a plant via a communication network is very common due to the popularity of emerging technologies, such as the Internet of Things. In this sense, the information from sensors, controllers, and actuators* flows *through a network. Naturally, these exchanges of information and computations require time, introducing delays in the network. We illustrate this kind of system in Figure 7.*

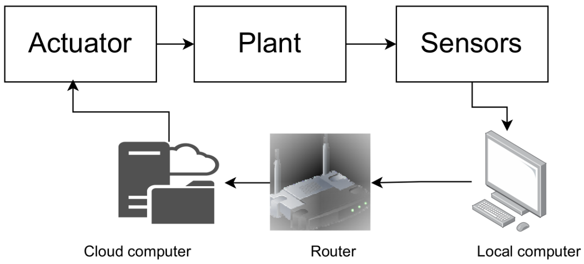

Figure 7: Networked control system.

In the simplest case, a linear networked system of the form:

$$\dot{x}(t) = Ax(t) + Bu(t),$$

where $x(t)$ is the state and $u(t)$ is the control input, the control input will be presented in the following way:

$$u(t) = Kx(t - \tau(t)),$$

where K correspond to static control gains, and $x(t - \tau(t))$ is the delayed state. This kind of model arises naturally as we never have instantaneous access to the state of the system through the network.

List of references:

1. Zhang et al. (2001)

2. Tipsuwan and Chow (2003)

3. Egaji et al. (2020)

Example 9 (Traffic flow)**.** *When modeling traffic flow, it is essential to account for how drivers (human or autonomous systems) sense, perceive, and react to their surroundings. This sequence of actions introduces a delay, which can impact the overall stability of the traffic system. In this context, traffic flow stability refers to the ability of the system to maintain a collision-free state. A common approach to modeling traffic dynamics is by using the following equation:*

$$\ddot{x}_a(t) = k(\dot{x}_b(t - \tau) - \dot{x}_a(t - \tau)),$$

where x_a and x_b denote the positions of two different vehicles, and τ is a time delay (see Figure 8).

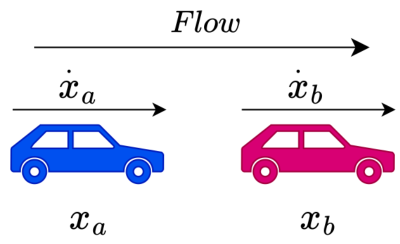

Figure 8: Traffic flow system.

List of references:

1. *Keyvan-Ekbatani et al. (2021)*
2. *Hossain and Tanimoto (2022)*

0.3.2 Types of time-delay systems

Through this section, we present a review of one of the existent classifications of time-delay systems. It is worth mentioning that we focus on *linear* time-delay systems.

0.3.2.1 Retarded delay differential equations

Time-delay systems with the delayed state are referred to as *retarded* time-delay systems and can be written as follows:

$$\dot{x}(t) = Ax(t) + \sum_{k=1}^{m} A_k x(t - \tau_k), \tag{13}$$

where the $x(t) \in \mathbb{R}^n$ is the system's state, A and A_k for $k \in \{1, 2, \ldots, m\}$ are real matrices, and $\tau_k > 0$ for $k \in \{1, 2, \ldots, m\}$ are time delays. One of the most important properties of *retarded* type time-delay systems is that, although they are infinite dimensional systems and therefore have an infinite number of eigenvalues, their *eigenvalues asymptotic chains* go *deep* into the left-half plane. In other words, the amount of unstable characteristic roots of the associated characteristic function is always finite.

In order to understand delay differential equations, it is always helpful to take a look at the simplest, yet effective, method to find solutions to such kinds of differential equations, namely the *step* method. We illustrate such a method through the following example.

Example 10 (Step method for retarded delay differential equations)**.** *Consider the following differential equation:*

$$\dot{x}(t) = x(t - \tau), \quad x(t) \in \mathbb{R}, \tau > 0 \tag{14}$$

with the following initial conditions:

$$x(t) = \phi(t), \quad \forall t \in [-\tau, 0], \tag{15}$$

where $\phi(\theta) = 1 - \theta$. The interest is to find a solution $x(t)$, such that (14) holds. With the information we have, it is easy to observe that one can explicitly obtain the solution in the interval $t \in [0, \tau)$:

$$x(t) = x(0) + \int_0^t x(s-\tau)ds = x(0) + \int_0^t \phi(s-\tau)ds.$$

For the sake of simplicity, assume that $\tau = 1$. Then, as the first step, we find the solution in the interval $t \in [0, 1)$:

$$x(t) = 1 + \int_0^t (2-s)ds = -\frac{t^2}{2} + 2t + 1.$$

What this means is that, for $t \in [0, 1]$, the behavior of the solution is given by $x(t) = -\frac{t^2}{2} + 2t + 1$. With this information, we can proceed to compute the solution for another interval, namely $t \in [\tau, 2\tau) = [1, 2)$:

$$x(t) = x(1) + \int_1^t (-\frac{s^2}{2} + 3s - \frac{3}{2})ds = \frac{1}{6}\left(-t^3 + 9t^2 - 9t + 16\right).$$

Note that this procedure can be repeated indefinitely for any interval of the form $[t_0 + k\tau, t_0 + (k+1)\tau]$, where $k = 0, 1, 2, \ldots$, and t_0 is the initial time. In this case, t_0 was considered to be 0, but the process can be generalized as long as the initial condition is defined for $t \in [t_0 - \tau, t_0]$. Repeating the process for $t \in [2, 3)$ we obtain:

$$x(t) = \frac{1}{24}\left(-t^4 + 16t^3 - 60t^2 + 140t - 48\right).$$

Matlab has a delay differential equations solver called dde23. The details on how to use such a solver are out of the scope of this thesis, but the reader may consult them at the official documentation site. In Figure 9 we observe the solution obtained using the step method and the one obtained using the dde23 Matlab function.

The solution can be implemented and plotted in Matlab or Python as shown in the Appendix B.

0.3.2.2 Neutral delay differential equations

Systems with delays on the derivative of the state are called *neutral* time-delay systems.

$$\dot{x}(t) + \sum_{k=1}^{N} D_k \dot{x}(t - \tau_k) = Ax(t) + \sum_{k=1}^{m} A_k x(t - \tau_k), \tag{16}$$

Time-delay systems of the *neutral* type, similarly to those of the retarded type, also have properties associated with the roots of their corresponding characteristic functions. However, in this case these *asymptotic chains*, which might be infinite, lie on a vertical strip on the complex plane, therefore, situations where a system has an infinite

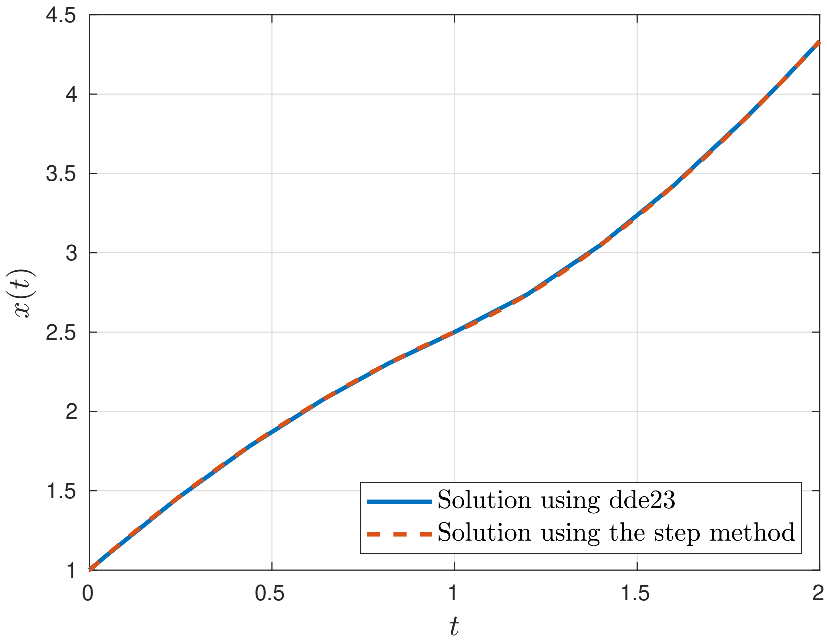

Figure 9: Comparisson of the computed solution via dde23 and the step method.

number of unstable roots may arise. This situation demands additional considerations when analyzing neutral time-delay systems. Just as for retarded type delay differential equations, one can find solutions to neutral type ones using the already presented *step* method, as shown in the following example:

Example 11 (Step method for neutral delay differential equations). *Consider the following differential equation:*

$$\dot{x}(t) - \frac{1}{2}\dot{x}(t-1) = -x(t) + x(t-1). \tag{17}$$

For the sake of simplicity we consider the initial condition $x(t) = \phi(t)$ for all $t \in [-1, 0]$, with $\phi(\theta) = 1$. In the first interval $t \in [0, 1)$ we can easily obtain the solution by noting that $\dot{x}(t-1) = \dot{\phi}(t-1) = 0$. Substituting into (17):

$$\dot{x}(t) = -x(t) + 1, \quad \forall t \in [0, 1),$$

which can be easily solved by noting that simple algebraic manipulation leads to:

$$e^t(\dot{x}(t) + x(t)) = e^t \implies x(t) = 1 + Ce^t, \quad \forall t \in [0, 1).$$

From the initial condition, it is easy to note that $x(0) = 1$ and thus, $C = 0$. In the next interval, $t \in [1, 2)$ we obtain:

$$\dot{x}(t) = -x(t) + 1, \quad \forall t \in [1, 2),$$

which is identical to the previous interval. Therefore, by induction, we can easily conclude that $x(t) = 1$ *for all* $t > 0$. *Similarly to the retarded case (with constant delays), Matlab has a neutral delay differential equations solver called ddensd. For any details related to such a solver, the reader may refer to the official documentation site.*

0.3.2.3 Other kinds of dynamical systems with delay

Although they are out of the scope of this thesis, there exist other types of delay systems apart from those of the Retarded and Neutral cases:

Advanced type Systems of the advanced type refer to a particular type of non-causal system with the following situation:

$$\dot{x}(t) = x(t + \tau).$$

Distributed delays A delay is said to be *distributed* if it appears in the following way:

$$\dot{x}(t) = \int_{-h}^{0} f(t, x(t + \theta))d\theta.$$

0.3.3 The Labyrinth of time-delay systems: Difficulties and advantages

0.3.3.1 Motivating examples

We start by showing the effect of delays on a system's performance and stability. Consider, for instance, the following examples:

Example 12 (Delay effect on stability)**.** *We have a system described by the following differential equation:*

$$\dot{x}(t) = -x(t - \tau). \tag{18}$$

In the case where there is no delay, i.e., when $\tau = 0$*, the system's solution is straightforwardly given by* $x(t) = Ce^{-t}$*, where* C *is a constant determined by the initial condition* $x(t_0)$*. This solution is exponentially stable. The question that naturally arises is whether the solution remains exponentially stable for any non-zero delay* $\tau \neq 0$*. To investigate this, let us consider the initial condition* $x(t) = \phi(t)$*, for all* $t \in [t_0 - \tau, t_0]$*, and let* $t_0 = 0$ *and* $\phi(\theta) = 1$*. Figure 10 illustrates the solution* $x(t)$ *for different values of the delay parameter. It is evident that the stability of the solution is influenced by the delay. Therefore, it is of interest to study the stability of a system considering the presence of the delay. The detailed analysis of this dependency will be discussed in subsequent chapters.*

As shown in the previous example, the stability of a system may depend on the delay parameter. However, this is not always the case, as we will observe in the following example.

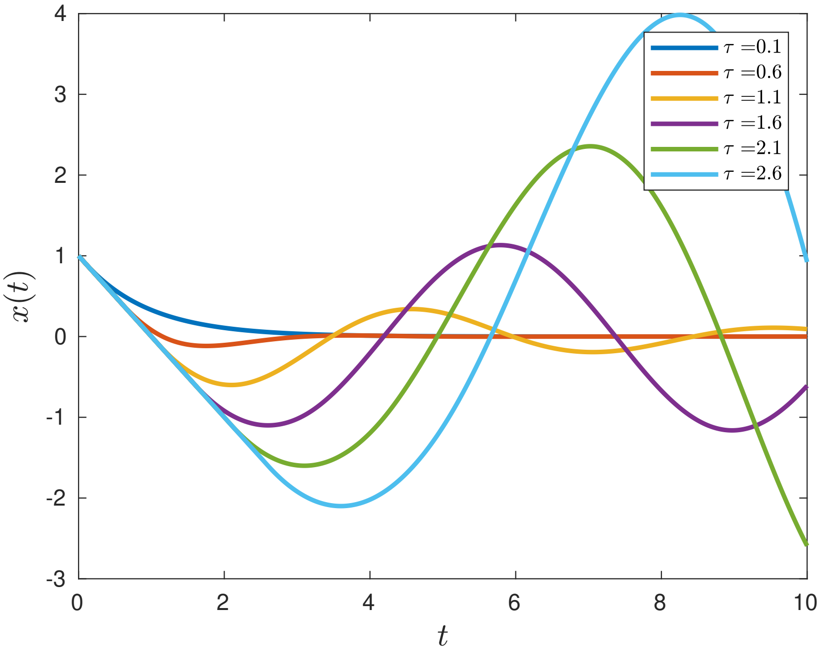

Figure 10: Solution $x(t)$ of Eq. (18) for different values of τ.

Example 13 (Stability independent of the delay)**.** *Let us consider the following differential equation:*

$$\dot{x}(t) = -x(t) + \frac{3}{4}x(t-\tau). \tag{19}$$

One way to study the stability of the given system is by the location of its characteristic roots. We will discuss how to find the corresponding characteristic function later, but for now, it is sufficient to know that the corresponding characteristic function is given by $\Delta : \mathbb{C} \times \mathbb{R}_+ \to \mathbb{C}$ *:*

$$\Delta(s;\tau) = s + 1 - \frac{3}{4}e^{-\tau s}.$$

The system is said to be stable (exponentially stable) if and only if all roots of $\Delta(s;\tau)$ *are located in* $\mathbb{C}_-$*. Since the system is of the retarded type and stable for* $\tau = 0$*, by continuity arguments, the only possible way stability can be lost is by crossing the imaginary axis. This means that there must exist a pair* (τ, ω) *such that* $\Delta(\boldsymbol{i}\omega;\tau) = 0$*. This implies the following:*

$$\Re(\Delta(\boldsymbol{j}\omega;\tau)) = 1 - \frac{3}{4}\cos(\tau\omega) = 0,$$
$$\Im(\Delta(\boldsymbol{j}\omega;\tau)) = \omega - \frac{3}{4}\sin(\tau\omega) = 0.$$

Observe that $1 - 3\cos(\tau\omega)/4 > 0$ *for any pair* $(\omega,\tau) \in \mathbb{R} \times \mathbb{R}_+$*, thus the system is stable for any value of* τ*. For* *illustration purposes, in Figure 11, we consider the initial condition $\phi(\theta) = 1$ and depict the solution $x(t)$ for different values of the delay parameter τ.*

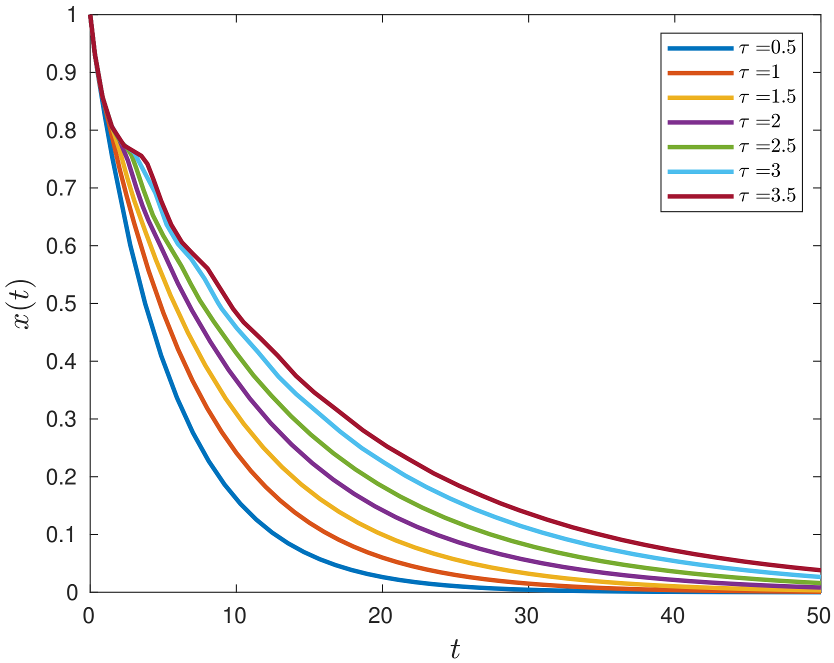

Figure 11: Solution $x(t)$ for different values of τ.

Example 14 (Stabilizing effect)**.** *As a final example, let us consider the following delay differential equation:*

$$\dot{x}(t) = x(t) + kx(t - \tau), \tag{20}$$

where $k \in \mathbb{R}^*$ is a constant gain. We already observed that the delay may or may not directly impact the closed-loop system's stability. Let $\tau = 0.1$, and the initial condition $x(t) = \phi(t)$ be $\phi(\theta) = 1$ for all $\theta \in [\tau, 0]$. In 12, we can observe how the behavior of the solution $x(t)$ changes depending on the value of k. In particular, note that the system without a delay term, i.e., $k = 0$, is unstable. In that sense, this illustrates how a delay term on the equation may have a beneficial effect on its stability.

0.3.4 The delay as a control parameter

Up to this point, we have examined how delays may influence a system's stability. However, our analysis has assumed that the delay is a fixed system parameter. However, a delay can be strategically utilized to stabilize a system or enhance its performance, similar to the situation presented in the last example of the previous section.

These ideas stem from the observation that a delay can approximate an average derivative through the following

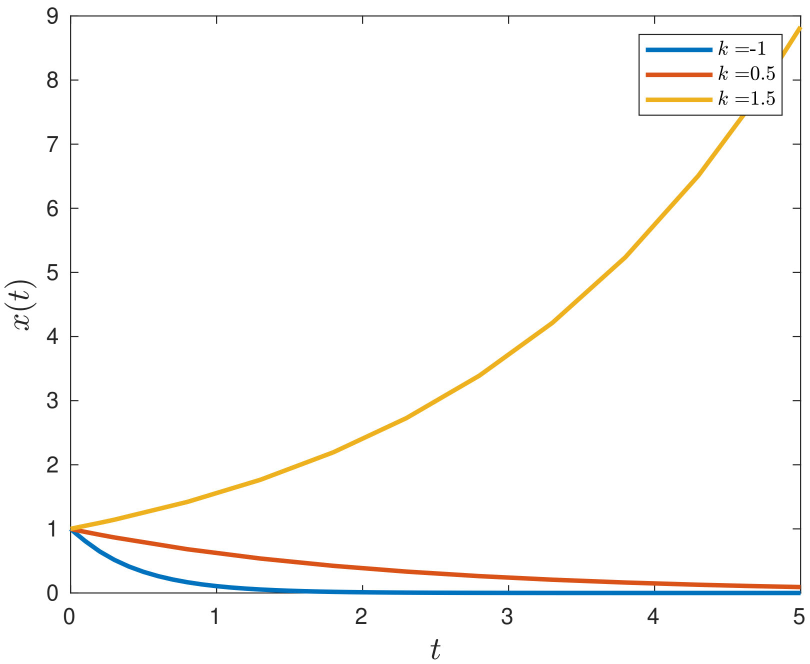

Figure 12: Solution $x(t)$ for different values of k in equation (20).

approximation scheme:

$$\dot{x}(t) = \frac{x(t) - x(t-\tau)}{\tau}.$$

This insight inspired the development of the control strategy known as Proportional Minus Delay (PMD) control (see, for instance, Suh and Bien (1979, 1980); Swisher and Tenqchen (1988)). Subsequent research expanded on this concept, as seen in works such as Kokame and Mori (2002). Further notable contributions based on this approach include the studies by Niculescu and Michiels (2004) and the authors of Kharitonov et al. (2005), which explored the potential of delay-based control methods in various contexts.

0.4 On the notion of singularity and well-posedness

We often refer to a *singularity* as a point where a mathematical object is either undefined or not *well-behaved*. In this thesis, we analyze singular behavior arising from two distinct sources.

First, singular behavior emerges from the sensitivity of a characteristic equation to the delay parameter. Specifically, in neutral-type systems, a phenomenon occurs where an infinitesimal perturbation in the delay parameter can destabilize the system. This phenomenon is also observed in the context of the delay-difference approximation of the derivative action. A specific structure of this approximation was characterized in Méndez-Barrios et al. (2022). In this thesis, we extend these results to a more general case where the approximation may involve multiple delays. This characterization is crucial because such approximations are often necessary for implementing controllers in real-world applications.

Second, singular behavior appears when optimizing the spectral abscissa of a system. In such cases, the optimal value frequently corresponds to a root of multiplicity $m > 1$. As discussed in earlier sections, this leads to singular behavior because the first $m - 1$ derivatives of the characteristic function vanish at the point of interest, resulting in a non-smooth solution.

The concept of singularity is closely tied to the notion of *well-posedness* in mathematical problems. But what does it mean for a problem to be well-posed? According to classical mathematics, a problem is well-posed if it has a unique solution that varies *continuously* with the initial conditions. In Hadamard (1902), Hadamard argued that ill-posed problems, that is, those that fail to meet these criteria, cannot reliably model "real-world" phenomena and, consequently, lack practical applications. However, Tikhonov (1977) later expanded on this perspective, demonstrating methods to "regularize" ill-posed problems and highlighting their practical relevance. In Tikhonov (1977), it is also mentioned that, in some contexts, such problems are referred to as *improperly-posed*.

In this thesis, we use the term improperly-posedness to describe the non-continuous and singular behavior of solutions to delay-differential equations for infinitesimally small delay parameters. Although this concept differs slightly from the classical notion of ill-posedness, it is closely related. Following Tikhonov's perspective, we demonstrate that such problems are indeed of practical interest.

For a discussion on how filtering can induce instability in closed-loop systems, see Michiels (2022). The characterization of the behavior of critical characteristic roots based on the Weierstrass preparation theorem is presented in Martínez-González et al. (2019). One of the earliest discussions on the sensitivity of delay systems to variations in the delay parameter can be found in Datko (1998). For a more general discussion on singularities and ill-posed problems, see Georgiou and Smith (1989).

0.5 Chapter summary

This chapter provides a comprehensive overview of the mathematical tools and theoretical foundations necessary for the development of this thesis. In particular, it provides some insights into how to analyze and solve delay-differential equations (DDEs). It also includes a brief introduction to the significance of time-delay systems in various engineering applications, highlighting their prevalence in real-world phenomena. The chapter then presents some of the basic mathematical techniques for addressing DDEs, including analytical and numerical methods, and discusses their applicability to different types of systems. Key concepts of time-delay systems are introduced, such as the nature of delays, their impact on system dynamics and stability, and the challenges they pose in modeling and analysis. Several illustrative examples are provided to demonstrate the application of these tools and to offer insight into the behavior of systems with delays. Furthermore, the chapter explores topics of special interest in this work, such as the notion of ill-posedness, referred to in this work as *improperly-posedness*, and its implications. Overall, this chapter serves as a foundational resource for understanding the complexities of delay-differential equations and presents the necessary tools to tackle the problems of this thesis to the reader.

Chapter 1

Time-delay systems stability: An eigenvalue-based approach

Mathematical analysis is as extensive as nature itself.

Joseph Fourier

Contents

1.1 Stability of time delay systems

The main objective of this section is to present a stability analysis for linear time-delay systems of the retarded type. The approach adopted in this thesis is based on the eigenvalues of the system. This implies that we will not consider systems with delays in the highest-order derivative (or, equivalently, in the derivative of the state). Additionally, we will focus on the system's characteristic function to study its stability.

To begin, consider the second-order differential equation of the form:

$$\ddot{y}(t) + a\dot{y}(t) + by(t) = cu(t), \tag{1.1}$$

where $y(t)$ is the system's output, $u(t)$ is an input, and a, b and c are real constant parameters. We can represent this system in state-space form by defining:

$$\begin{aligned} x_1(t) &= y(t), \\ x_2(t) = \dot{x}_1(t) &= y'(t), \\ x(t) &= [x_1, x_2]^T. \end{aligned}$$

Thus, the system can be written as:

$$\dot{x}(t) = Ax(t) + Bu(t) = \begin{bmatrix} 0 & 1 \\ -b & -a \end{bmatrix} x(t) + \begin{bmatrix} 0 \\ c \end{bmatrix} u(t), \quad x \in \mathbb{R}^2. \tag{1.2}$$

The associated eigenvalue problem consists of finding $\lambda \in \mathbb{C}$ such that:

$$\Delta(\lambda) = \det(\lambda I - A) = \lambda^2 + a\lambda + b = 0. \tag{1.3}$$

Equation (1.3) is called the characteristic equation of the system, and $\Delta(\lambda)$ is its characteristic polynomial. There exists a strong relationship between the characteristic equation and the solution of the differential equation (1.1). Indeed, assuming zero initial conditions, we can derive the Laplace-domain[1] representation of the system (1.2) as follows:

$$\begin{aligned} \mathcal{L}(\dot{x}(t)) = sX(s) &= AX(s) + BU(s), \\ \implies X(s) &= (sI - A)^{-1} BU(s). \end{aligned}$$

Let $y(t) = Cx(t) + Du(t)$ be the system output. Its Laplace-domain representation is given by:

$$\begin{aligned} Y(s) &= CX(s) + DU(s) \\ &= \frac{1}{\det(sI - A)} \left[C \operatorname{adj}(sI - A) B + D\right] U(s). \end{aligned}$$

It follows that in the transfer function representation $H_{yu}(s) = Y(s)/U(s)$, the characteristic polynomial $\Delta(\lambda)$ appears as the denominator. Therefore, in analyzing the system's stability, we can interchangeably refer to both the state-space representation and the transfer function representation. In the remainder of this thesis, we will leverage this equivalence to address the stability problem of linear systems with time delays.

[1] Once the system is represented in the Laplace-domain, one can use the inverse of the Laplace transform to find the solution

1.1.1 Characteristic quasipolynomials

In the analysis of time-delay systems, the following property of the Laplace transform plays a fundamental role:

$$\mathcal{L}\left\{x(t-\tau)\right\} = X(s)e^{-\tau s},$$

where $\tau > 0$ is a time delay. Similarly, for a state-space representation of a system with time-delay, given by:

$$\dot{x}(t) = Ax(t) + A_1 x(t-\tau),$$

its corresponding characteristic function $\Delta : \mathbb{C} \times \mathbb{R}_+^* \to \mathbb{C}$ can be obtained in the following way:

$$\Delta(\lambda; \tau) = \det\left(\lambda I - A - A_1 e^{-\lambda\tau}\right).$$

The presence of the exponential term gives rise to characteristic functions with a specific structure, referred to as quasipolynomials[2]. In general, a quasipolynomial takes the following form:

$$\Delta(s) = \sum_{k=0}^{n} P_k(s) e^{-\tau_k s}. \tag{1.4}$$

where $P_k(s)$ are polynomials with real coefficients on the Laplace variable s and $\tau_k \geq 0$ are time delays. The presence of the exponential terms $e^{-\tau_k s}$ makes the eigenvalue problem associated with linear time-delay systems inherently nonlinear. Additionally, this structure introduces the complexity of an infinite number of roots for the characteristic quasipolynomial, which complicates the stability analysis.

To address this challenge, we introduce the following key definition from Michiels and Niculescu (2014):

Definition 1.1.1: Spectral abscissa

For a closed-loop system with given characteristic function Δ, the spectral abscissa function $\rho : \mathcal{F}(\mathbb{C}; \mathbb{C}) \to \mathbb{R}$:

$$\rho(\Delta) = \max\left\{\Re(s_0) : s_0 \in \mathbb{C}, \Delta(s_0) = 0\right\}$$

The spectral abscissa $\rho(\Delta)$ represents the real part of the rightmost root of the characteristic quasipolynomial, which is crucial for determining the system's stability. The following result from Fridman (2014) formalizes the connection between the spectral abscissa and the solution behavior of linear time-delay systems:

[2] A quasipolynomial (or pseudopolynomial) generalizes polynomials. While polynomial coefficients come from a ring, quasipolynomials have coefficients that may involve exponential terms, such as $e^{-\tau s}$, which are periodic functions with an integral period in the complex plane.

Theorem 1.1.1

Let $\alpha_0 = \rho(\Delta)$. Then $\forall \alpha > \alpha_0$ there exist $C \geq 1$ such that for any $\phi \in \mathcal{C}[-\tau, 0]$, the solution $x(t)$ with $x_0 = \phi$ satisfies the following inequality:

$$||x(t)|| \leq Ce^{\alpha t}||\phi||, \quad t \geq 0.$$

From this result, the following corollary establishes the criterion for stability of linear time-delay systems of the retarded type:

Corollary 1.1.1: Stability of linear time-delay systems of the retarded type

A linear time-delay system of the retarded type is said to be exponentially stable if and only if all the roots of its characteristic quasipolynomial have negative real part.

Theorem 1.1.1 and Corollary 1.1.1 imply that the stability of a linear time-delay system can be determined by identifying the spectral abscissa $\rho(\Delta)$. Specifically, it is sufficient to check the location of the rightmost root of the characteristic quasipolynomial. Even though the quasipolynomial may have an infinite number of roots, stability is ensured as long as the spectral abscissa satisfies $\rho(\Delta) < 0$.

1.1.2 Continuity of the characteristic roots

As previously mentioned, linear time-delay systems have characteristic functions in the form of quasipolynomials, which generally possess an infinite number of roots. The system's stability can be analyzed by examining the location of these roots within the complex plane, similarly to the finite-dimensional case. A fundamental property in this stability study is the continuity of roots with respect to the parameters, which can be stated as follows: *Small variations in the system parameters induce small variations in its roots.* This concept is formalized below.

First, it is essential to introduce the following result, which will eventually serve as a key step toward proving the continuity of roots in quasipolynomials:

Theorem 1.1.2: Rouché's Theorem

Let $f(z)$ and $g(z)$ be two analytic functions within a simple closed contour $\mathcal{C}^a$. If $|g(z)| < |f(z)|$ for all $z \in \mathcal{C}$, then $f(z)$ and $f(z) + g(z)$ have the same number of zeros (including multiplicities) inside $\mathcal{C}$.

[a] In complex analysis, a simple contour is a differentiable curve with no self-intersections.

With Rouché's Theorem in mind, let us consider the following result:

Theorem 1.1.3

Let F, and D be polynomials with real coefficients and Δ a quasipolynomial defined as:

$$\begin{aligned}\Delta(s) &:= F(s) + D(s)e^{-hs}, \quad h \geq 0,\\ F(s) &:= f_0 + f_1 s + \cdots + f_n s^n, \quad f_n \neq 0,\\ D(s) &:= d_0 + d_1 s + \cdots + d_m s^m,\end{aligned}$$

where $n > m$. Let:

$$\begin{aligned}Q(s) &:= F_q(s) + D_q(s)e^{-hs},\\ F_q(s) &:= (f_0 + \epsilon_0) + (f_1 + \epsilon_1)s + \cdots + (f_n + \epsilon_n)s^n,\\ D_q(s) &:= (d_0 + \delta_0) + (d_1 + \delta_1)s + \cdots + (d_m + \delta_m)s^m,\end{aligned}$$

where ϵ_j, $\delta_\ell \in \mathbb{R}$ $\forall j \in \{0, 1, \ldots, n\} \wedge \forall \ell \in \{0, 1, \ldots, m\}$ such that $f_n + \epsilon_n \neq 0$. Consider a circle $\mathcal{C}_k$ of radius $r_k \in \mathbb{R}_+$ centered at $s_k \in \mathbb{C}$, which is a root of $\Delta(s)$ with multiplicity t_k. Assume additionally that r_k is fixed and satisfies the following condition:

$$0 < r_k < \min |s_k - s_j|, \quad j = 1, 2, \ldots, k-1, k+1, \ldots, m.$$

Then there exist positive numbers ϵ and δ, where $\epsilon > |\epsilon_i|$ for $i \in \{1, 2, \ldots, n\}$ and $\delta > |\delta_j|$ with $j \in \{1, 2, \ldots, m\}$, such that $Q(s)$ has exactly t_k zeros inside $\mathcal{C}_k$.

Proof. Let Δ be defined as in Theorem 1.1.3, and consider the following definitions:

$$\begin{aligned}R(s) &= F_r(s) + D_r(s)e^{-hs},\\ F_r(s) &= \epsilon_0 + \epsilon_1 s + \cdots + \epsilon_n s^n,\\ D_r(s) &= \delta_0 + \delta_1 s + \cdots + \delta_m s^m.\end{aligned}$$

On the one hand, since $\Delta(s)$ is continuous and non-zero for all s belonging to $\mathcal{C}_k$, we can define μ_k such that:

$$0 < \mu_k \leq |\Delta(s)|$$

On the other hand, we have the following:

$$
\begin{aligned}
|R(s)| &= |F_r(s) + D_r(s)e^{-hs}| \\
&\leq |F_r(s)| + |D_r(s)|e^{-h\Re(s)} \\
&= \sum_{i=0}^{n} |\epsilon_i||s^i| + e^{-h\Re(s)} \sum_{j=0}^{m} |\delta_j||s^j| \\
&\leq \epsilon \sum_{i=0}^{n} |s^i| + \delta e^{-h\Re(s)} \sum_{j=0}^{m} |s^j|.
\end{aligned}
$$

Since we are within a compact region in the complex plane, i.e., $s \in \mathcal{C}_k$, there exists an upper bound for $e^{-h\Re(s)}$, which we denote as γ, such that:

$$
\begin{aligned}
\epsilon \sum_{i=0}^{n} |s^i| + \delta e^{-h\Re(s)} \sum_{j=0}^{m} |s^j| &\leq \epsilon \sum_{i=0}^{n} (|s - s_k| + |s_k|)^i + \delta\gamma \sum_{j=0}^{m} (|s - s_k| + |s_k|)^j \\
&\leq \epsilon \sum_{i=0}^{n} (r_k + |s_k|)^i + \delta\gamma \sum_{j=0}^{m} (r_k + |s_k|)^j.
\end{aligned}
$$

Now let $\epsilon_m = \max\{\epsilon, \delta\}$, thus:

$$
\epsilon \sum_{i=0}^{n} (r_k + |s_k|)^i + \delta\gamma \sum_{j=0}^{m} (r_k + |s_k|)^j \leq \epsilon_m \left(\sum_{i=0}^{n} (r_k + |s_k|)^i + \gamma \sum_{j=0}^{m} (r_k + |s_k|)^j \right).
$$

By choosing $\epsilon_m < \dfrac{\mu_k}{\sum_{i=0}^{n} (r_k + |s_k|)^i + \gamma \sum_{j=0}^{m} (r_k + |s_k|)^j}$, we can guarantee $|\Delta(s)| > |R(s)|$ for all s on $\mathcal{C}_k$. By a direct application of Rouché's Theorem, $Q(s) = \Delta(s) + R(s)$ has the same zeros inside $\mathcal{C}_k$ as $\Delta(s)$. □

From a direct application of the previous result, the following corollary holds:

Corollary 1.1.2

Let the quasipolynomial $\Delta(s) = F(s) + D(s)e^{-hs}$ have roots at $s_1, s_2, \ldots, s_k$ with multiplicities $t_1, t_2, \ldots, t_k$, respectively. Then there exist circles $\mathcal{C}_1, \mathcal{C}_2, \ldots \mathcal{C}_k$ for which, under sufficiently small perturbations in its parameters, the number of roots of $\Delta(s)$ inside circle $\mathcal{C}_\ell$ is exactly t_ℓ, with $\ell \in \{1, 2, \ldots, k\}$.

It is worth noting that the continuity property of the characteristic roots holds also for the delay parameter. For more details on such a property we refer to Michiels and Niculescu (2014).

1.1.3 Numerical solution of quasipolynomial equations

Due to the presence of exponential terms, equations of the form:

$$\sum_{k=0}^{n} P_k(s)e^{-\tau_k s} = 0,$$

may have an infinite number of solutions. Determining these solutions is a challenging task, but numerical tools are available to help in this process.

In this thesis, we use the Quasi-Polynomial Root-Finder (QPmR), initially introduced in Vyhlídal and Zítek (2003) and later updated in Vyhlídal and Zítek (2014). The original implementation of the algorithm was developed in MATLAB using symbolic computation, whereas the updated version employs a matrix-based approach. In this work, we utilize an adaptation of the symbolic version in Python, which is detailed in Appendix B.

This choice is motivated by the fact that, although the symbolic version is slower, it handles roots with higher multiplicity more effectively. For further details on this Python adaptation of QPmR, we refer to the repository at https://github.com/DSevenT/QPmR. Additionally, an alternative Python implementation of the algorithm is available at https://github.com/LockeErasmus/qpmr. It is worth noting that, in addition to QPmR, other toolboxes that facilitate working with the roots of quasilopolynomials include P3δ (Boussaada et al., 2020), DDE-Biftool (Engelborghs et al., 2000), and TDS-Control (Appeltans et al., 2022).

1.2 Scalar systems: The retarded case

In the following, we present some stability properties and examples of systems of the retarded type.

1.2.1 Direct method for stability

It is clear that finding the roots of a quasipolynomial is not a simple task. However, it is also clear that, at least in the retarded case, the infinite and yet countable number of roots *"go deep"* into the left-half plane. In other words, if a retarded type system is unstable, the number of unstable roots is finite. This observation, in conjunction with the fact that we can study the stability of a system by checking only its right-most characteristic root, facilitates the stability analysis.

In particular, Walton and Marshall (1987) propose what they refer to as a *direct method* to study the stability of a time-delay system. We will exploit their ideas in some of the next chapters, but for now, we present the methodology by first introducing the simple case when the system presents only one discrete delay. Next, we show how the idea is generalized to cases with multiple, yet commensurate, delays.

First, for a linear retarded system with a single delay, note that the characteristic quasipolynomial can be expressed as follows:

$$\Delta(s) = Q(s) + P(s)e^{-s\tau}, \tag{1.5}$$

where Q and P are polynomials in the Laplace variable s, of degrees n and m, respectively. Moreover, $n > m$ and $\tau > 0$. As discussed in the previous section, the characteristic roots are continuous functions of the system parameters, and, in particular, this property holds for the delay parameter. Therefore, the first step is to verify the stability of the system when $\tau = 0$, which corresponds to solving:

$$Q(s) + P(s) = 0. \tag{1.6}$$

If all the solutions of (1.6) have negative real parts, then, by the continuity property of the characteristic roots, there exists a sufficiently *small* value of τ such that all the roots of (1.5) lie in $\mathbb{C}_-$. Next, as mentioned earlier, a root will only cross from $\mathbb{C}_-$ to $\mathbb{C}_+$ by traversing the imaginary axis. Thus, we need to identify the values of τ for which a root lies on the imaginary axis, i.e., $s = \boldsymbol{i}\omega$, which also implies $s = -\boldsymbol{i}\omega$ is a solution. In this scenario, $\Delta(\boldsymbol{i}\omega) = \Delta(-\boldsymbol{i}\omega) = 0$, leading to the following equation:

$$f(\omega) = Q(\boldsymbol{i}\omega)Q(-\boldsymbol{i}\omega) - P(\boldsymbol{i}\omega)P(-\boldsymbol{i}\omega).$$

Clearly, $f(\omega)$ is a polynomial of degree $2n$ in ω and, more specifically, degree n in ω^2. Two important observations follow: 1. Only positive solutions of $f(\omega) = 0$ are relevant. If $f(\omega) = 0$ has no positive solutions, then the system's stability does not change with τ; the system is either always stable or always unstable, regardless of the delay. 2. $f(\omega)$ is independent of τ.

Once the positive roots ω of $f(\omega) = 0$ are determined, substituting $s = \boldsymbol{i}\omega$ into (1.5) yields:

$$\Delta(\boldsymbol{i}\omega) = 0 \implies \begin{cases} \cos(\tau\omega) = -\Re\left\{\dfrac{Q(\boldsymbol{i}\omega)}{P(\boldsymbol{i}\omega)}\right\}, \\ \sin(\tau\omega) = \Im\left\{\dfrac{Q(\boldsymbol{i}\omega)}{P(\boldsymbol{i}\omega)}\right\}. \end{cases} \tag{1.7}$$

Let $\tau_0 \in \mathbb{R}_+$ be the smallest value such that (1.7) is satisfied. Then, for all delays of the form $\tau = \tau_0 + 2\pi n/\omega$ where $n \in \mathbb{N}$, (1.7) holds.

At this stage, we have only identified the pairs (τ, ω) where a crossing occurs. The next task is to determine whether the crossing is from $\mathbb{C}_+$ to $\mathbb{C}_-$ or vice-versa. To address this, the Implicit Function Theorem is useful. Specifically, the direction of crossing can be determined by evaluating the sign of the real part of $ds/d\tau$, given by:

$$\frac{ds}{d\tau} = -\frac{\frac{d\Delta(s)}{d\tau}}{\frac{d\Delta(s)}{ds}} = -s\left[\frac{Q(s)}{Q'(s)} - \frac{P(s)}{P'(s)} + \frac{1}{\tau}\right].$$

For $s = \boldsymbol{i}\omega$, the term $\boldsymbol{i}\omega/\tau$ is purely imaginary. Thus, the crossing direction depends only on ω and is independent of τ.

Next, we aim to generalize this methodology to cases where the system, while still linear and of the retarded type, involves multiple yet commensurate delays. To this end, consider a characteristic quasipolynomial of the following form:

$$\Delta_n(s) = \sum_{k=0}^{n} P_k(s) e^{-k\tau s}. \tag{1.8}$$

Here, P_0 must have a higher degree than any P_k for $k \neq 0$, since the system is of the retarded type. As in the single delay case, the first step is to assess the stability of the delay-free system, i.e., when $\tau = 0$.

In the same spirit as the single delay scenario, the next step is to determine the values of τ for which a root lies on the imaginary axis. This leads to the following equation:

$$\Delta_n(\boldsymbol{i}\omega) = \sum_{k=0}^{n} P_k(\boldsymbol{i}\omega) e^{-k\tau \boldsymbol{i}\omega} = 0.$$

As noted earlier, this also implies $\Delta_n(-\boldsymbol{i}\omega) = 0$, which allows us to derive the following equation:

$$\Delta_{n-1}(\boldsymbol{i}\omega) = \Delta_n(\boldsymbol{i}\omega) P_0(-\boldsymbol{i}\omega) - e^{-\boldsymbol{i}n\tau\omega} P_n(\boldsymbol{i}\omega) \Delta_n(\boldsymbol{i}\omega) = 0,$$

where all terms involving $e^{\pm \boldsymbol{i}n\tau\omega}$ are eliminated.

Next, we take $\Delta_{n-1}(\boldsymbol{i}\omega)$ and apply the same procedure to eliminate all terms involving $e^{\pm \boldsymbol{i}(n-1)\tau\omega}$. Repeating this process iteratively allows us to derive an expression free of exponential terms. Furthermore, in the second-to-last iteration, we obtain an expression containing only a single exponential term, enabling us to formulate a condition analogous to the one in (1.7).

1.2.2 Illustrative examples

Example 15 (Multiple stability intervals)**.** *Let us consider the following quasipolynomial:*

$$\Delta(s) = s^2 + \frac{\gamma}{4} s + 1 - \gamma e^{-s\tau}.$$

We are interested in detecting values of τ such that, for a given γ, all the roots of Δ lie in $\mathbb{C}_-$. Observe that, for $\tau = 0$, $\gamma > 0$ is sufficient for the stability of Δ. Next, following the Direct method, we obtain:

$$f(\omega) = \frac{1}{16}\gamma^2 \left(\omega^2 - 16\right) + \left(\omega^2 - 1\right)^2 = 0,$$

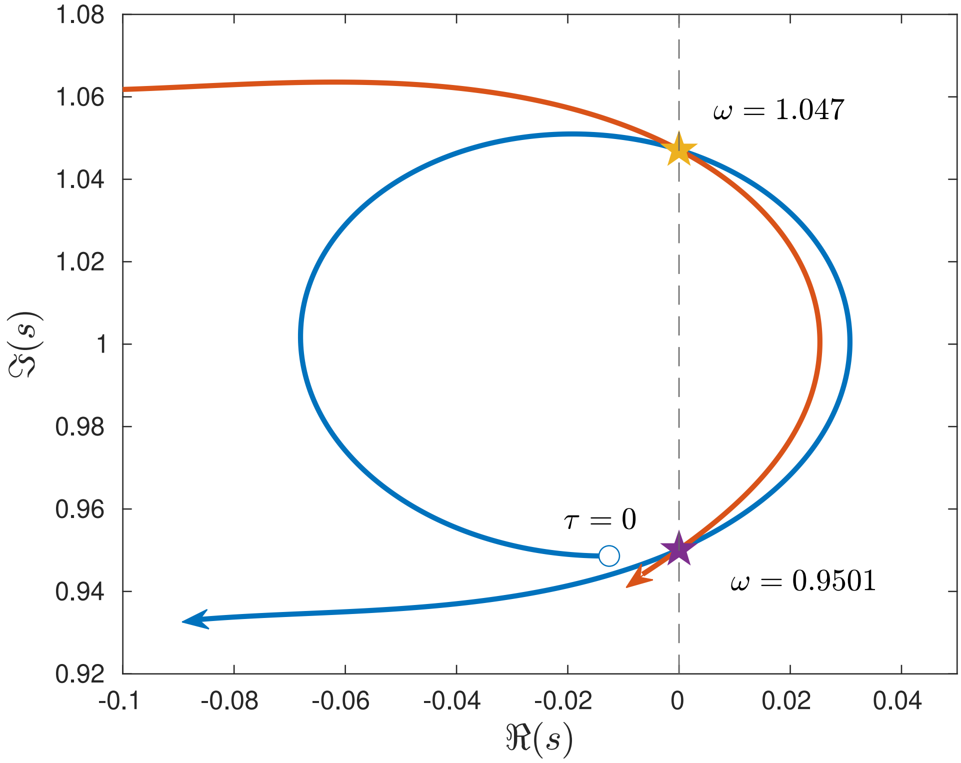

Figure 1.1: Evolution of the roots of $\Delta(s)$ with $\gamma = 1/10$ as $\tau \in (0, 13)$ increases.

from which we derive:

$$\omega = \pm\frac{1}{4}\sqrt{16 \pm \frac{1}{2}\gamma\left(\sqrt{\gamma^2+960}+\gamma\right)}.$$

As per the Direct Method, we only consider the positive values of ω*. Clearly, the stability crossing depends on the value of* γ*.*

Let $\gamma = 1/10$*. Under this assumption,* Δ *has all of its roots in* $\mathbb{C}_-$ *when* $\tau = 0$*. Notably, there are two positive solutions for* ω*, given by* $\omega = \{1.047, 0.9501\}$*. Using these values and applying* (1.7)*, we obtain* $\tau = 3.25 + 2\pi n/\omega$ *for* $n \in \mathbb{N}$*.*

Interestingly, by computing $ds/d\tau$ *and evaluating it at the corresponding points, we can verify the direction of the stability crossings. Specifically, crossings at* $\omega = 1.047$ *occur from left to right, leading to instability, while those at* $\omega = 0.9501$ *occur in the reverse direction, restoring stability.*

This phenomenon is illustrated in Figure 1.1, which demonstrates that multiple roots cross the imaginary axis for different values of τ*, but always at the same frequencies.*

Example 16 (Root tangent to the imaginary axis)**.** *For the next example, consider a quasipolynomial given by:*

$$\Delta(s) = s^2 + \frac{k}{2}s + 1 + \frac{k}{2}se^{-s\tau},$$

where $k \in \mathbb{R}$ is a real parameter. If $\tau = 0$, then the characteristic equation reads:

$$s^2 + ks + 1 = 0,$$

which has solutions at $\frac{1}{2}\left(\pm\sqrt{k^2-4} - k\right)$ with $k \in \mathbb{R}$, which implies that the system will conserve its stability as long as $k \in \mathbb{R}^+$. Next, for $\tau \neq 0$, we want to find the crossing frequencies which, by the direct method, correspond to the positive solutions of the following equation:

$$\left(\omega^2 - 1\right)^2 = 0.$$

Clearly, the crossings occur only at $\omega = 1$, independently of the value of k. Next, from (1.7) *we obtain*

$$\begin{aligned}\sin(\omega\tau) =& 2\frac{\omega^2 - 1}{k\omega}\\ \cos(\omega\tau) =& -1\end{aligned}$$

which only holds whenever $\tau = (2n+1)\pi$ with $n \in \mathbb{N}$ and $\omega = 1$. Since we are interested in observing whether or not stability is lost, we compute the derivative via the implicit function theorem and extract its real part:

$$\Re\left\{\frac{ds}{d\tau}\right\}\Big|_{s=\boldsymbol{i}\omega} = \Re\left\{-\frac{\frac{\partial\Delta}{\partial\tau}}{\frac{\partial\Delta}{\partial s}}\right\}\Big|_{s=\boldsymbol{i}\omega} = \frac{ks^2}{-sk\tau + (k+4s)e^{s\tau} + k} = \Re\left\{-\frac{\boldsymbol{i}k}{\pi k + 4}\right\} = 0.$$

Since sign($\Re\left\{\frac{ds}{d\tau}\right\}\big|_{s=\boldsymbol{i}\omega}$) $= 0$ we require a higher-order derivative to conclude on the direction the root is moving. We can compute the second derivative of s w.r.t. τ in a recursive way using the implicit function theorem, which yields:

$$\frac{d^2s}{d\tau^2} = -\frac{ks^3\left(k^2(2s\tau - 3) - 2k(k+2s)e^{s\tau} + (k+4s)^2e^{2s\tau}\right)}{\left(-sk\tau + (k+4s)e^{s\tau} + k\right)^3}$$

which evaluated at the point of interest gives:

$$\Re\left\{\frac{d^2s}{d\tau^2}\right\}\Big|_{s=\boldsymbol{i},\tau=\pi} = \Re\left\{\frac{2\boldsymbol{i}k(k(\pi k + 6) + 8\boldsymbol{i})}{(\pi k + 4)^3}\right\} = -16k.$$

Since the gain $k > 0$, we can conclude that sign($\Re\left\{\frac{d^2s}{d\tau^2}\right\}\big|_{s=\boldsymbol{i},\tau=\pi}$) $= -1$. Therefore, since we know that for $\tau = 0$, all the roots lie on the left-hand side, the root is not crossing the imaginary axis but rather touching it at $s = \boldsymbol{i}$ and $\tau = (2n+1)\pi$, but comes back to $\mathbb{C}_-$. In Figure 1.2, the behavior of the roots for $k = 1$ and $\tau \in (0, 3\pi)$ is depicted.

1.3 Delay-dependent coefficients: A new layer of complexity

To this point, the quasipolynomials have been in the form of (1.4), where each polynomial $P_k(s)$ depends only on s. One situation that may arise is the presence of polynomials that depend not only on s but also on the delay

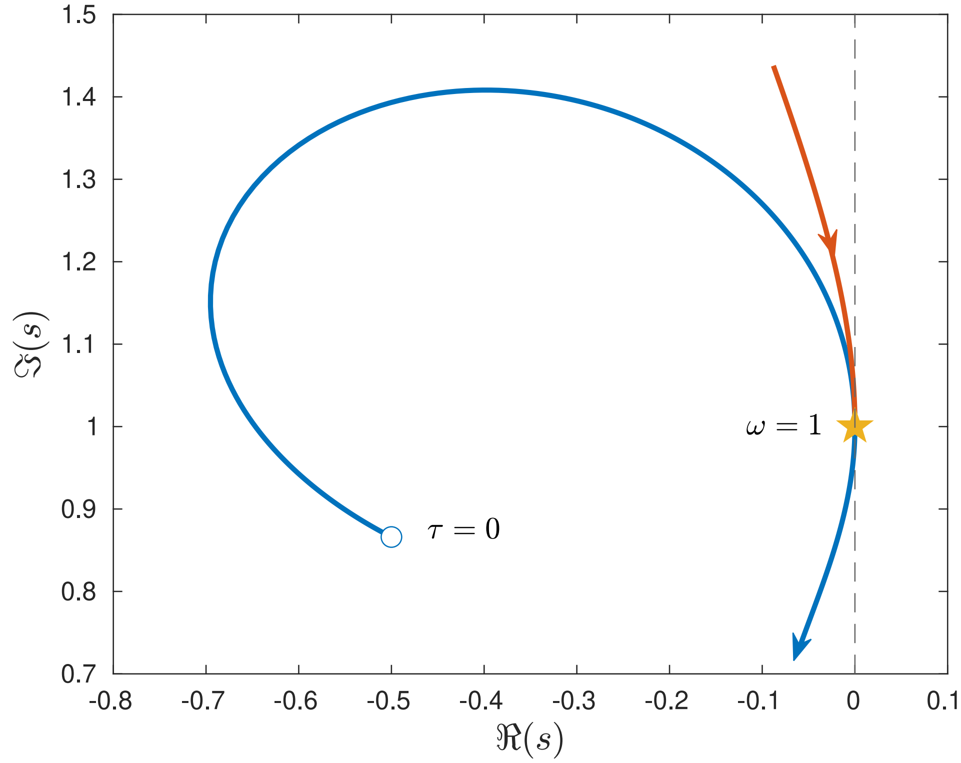

Figure 1.2: Roots of $\Delta(s)$ for $k = 1$ and $\tau \in (0, 3\pi)$ increasing.

parameter τ. As we will see later, this is one of the primary sources of difficulty in this thesis since classical results of time-delay systems might not apply under these conditions.

1.3.1 Motivating examples

We present some different scenarios where mathematical models with delay-dependent coefficients may arise.

1.3.1.1 TCP AQM networks

Congestion is a well-known classical issue in communication networks. When such networks operate under the Transmission Control Protocol (TCP), one established approach to mitigating congestion is the use of Active Queue Management (AQM) algorithms. These networks can be mathematically modeled by the following set of delay-differential equations (see Ünal et al. (2013) for further details on the modeling process):

$$\dot{W}(t) = \frac{1}{\tau(t)} - \frac{W(t)}{2}\frac{W(t-\tau(t))}{\tau(t-\tau(t))}p(t-\tau(t)),$$
$$\dot{q}(t) = \begin{cases} -C + \frac{N(t)}{\tau(t)}W(t) & q > 0 \\ \max\{0, -C + \frac{N(t)}{\tau(t)}W(t)\} & q = 0 \end{cases},$$

where $W(t)$ corresponds to the average size of the TCP window, $N(t)$ is the number of sessions, $\tau(t)$ is a delay, and $q(t)$ is the average queue length, i.e., the number of packets in the queue. Under suitable assumptions, the system can be linearized. When coupled with a classical PI controller $C(s) = k_p + k_i/s$, the closed-loop characteristic quasipolynomial is given by:

$$\Delta(s) = s^3 + \frac{1}{\tau_0}\left(1 + \frac{N_0}{\tau_0 C_0}\right)s^2 + \frac{2N_0}{\tau_0^3 C_0}s + \left(\frac{N_0}{\tau_0^2 C_0}s^2 + \frac{C_0^2}{2N_0}(k_p s + k_i)\right)e^{-\tau_0 s}, \tag{1.9}$$

where the subscript 0 refers to the nominal values at the equilibrium point. It is worth noting that the delay τ_0 not only appears in the exponential term but also influences the coefficients of the quasipolynomial $\Delta(s)$.

1.3.1.2 Derivative operator discretization

It is well-known that incorporating derivative action in control schemes often introduces various challenges. In particular, when the derivative of the output is not directly measurable, a discretization process becomes necessary. The simplest approach involves approximating the derivative operator using a delayed difference operator, as follows:

$$\dot{x}(t) \approx \frac{x(t) - x(t-\tau)}{\tau}.$$

Incorporating this type of discretization into a closed-loop system results in characteristic functions of the form:

$$\Delta(s) = Q(s) + P(s)\left(\frac{1 - e^{-\tau s}}{\tau}\right).$$

The implications and analysis of this structure are the main focus of Chapters 2 and 3 of this work.

1.4 Chapter summary

This chapter delves into the stability analysis of linear time-delay systems using a spectral approach, with a particular focus on the properties of quasipolynomials and their critical role in determining system stability. Quasipolynomials are introduced as the characteristic functions of time-delay systems, forming the main mathematical object involved in the stability analysis. Key properties of quasipolynomials, such as their structure and the continuity of their roots with respect to their coefficients, are discussed, laying the basis for stability analysis. Additionally, numerical tools for computing the roots of quasipolynomials are presented, providing practical methods for their analysis.

The chapter then introduces Walton's direct method as a powerful technique for assessing the stability of retarded-type linear time-delay systems. This method simplifies the problem by reducing it to a delay-free scenario, enabling the detection of roots crossing the imaginary axis. Stability is determined by the location of the roots of the characteristic quasipolynomial in the complex plane, with particular emphasis on the spectral abscissa, that is, the right-most root, which determines the system's stability. A notable advantage of this method is that, for retarded systems, the number of roots in the right-half plane is always finite. Combined with the continuity property of the characteristic roots, this allows for a systematic study of stability by checking crossings over the imaginary axis. The chapter includes illustrative examples to highlight specific phenomena and potential complications that may arise in the analysis.

Finally, the chapter addresses cases where the coefficients of the quasipolynomial explicitly depend on the delay parameter. This scenario introduces additional complexity and is explored further in Chapters 2 and 3 of this thesis, where advanced techniques are developed to tackle such challenges.

Chapter 2

Derivative action implementation: An improperly-posed problem

Singularity is almost invariably a clue.

Sherlock Holmes

Sir Arthur Conan Doyle

Contents

2.1 Introduction

It is well known that PID controllers are among the most common control strategies in real-world applications, both for the simplicity of their implementation and their capabilities to solve complex problems using a small number of parameters. However, there are essential drawbacks related to the derivative action. The first is high-frequency noise amplification, often solved through filters (see Michiels (2022) for a discussion on how filtering can induce instabilities to the system). Additionally, it is expected not to have access to the derivative of the state; that is, we cannot measure the derivative, and therefore, the controller cannot be implemented. One solution that can solve both these problems at the same time is the implementation of the derivative action via a delay-difference approximation. In this sense, the idea is to implement the controller by only using measurements from the past.

The above mentioned implementation has two main disadvantages. On the one hand, it produces a closed-loop characteristic function that presents time delays and has delay-dependent coefficients, making its stability analysis more complicated. Results on stability analysis of time-delay systems with delay-dependent coefficients exist in the literature. In particular, Beretta and Kuang (2002) and, more recently, An et al. (2019) present a geometric approach to study the stability of a quasipolynomial with two delays, including coefficients that depend on one of those delays. However, the main disadvantage of this approach is that as the number of delays increases, the geometric problem and the set of inequalities to be solved grow rapidly, making the results highly restrictive and computationally expensive. Other works, such as Jin et al. (2018), propose alternative approaches but are limited to systems with only a single delay.

On the other hand, as demonstrated in works like Georgiou and Smith (1989) and Michiels et al. (2004), instability can also arise from delay-difference approximations. In this sense, it is necessary to identify under which conditions such a situation arises, to guarantee a safe implementation of the control strategy.

In this spirit, in the following chapters, we focus our efforts on understanding the effect of the delay-difference implementation of the derivative action on the stability of the closed-loop system.

2.2 Finite dimension approximations and its limitations

2.2.1 Padé Approximation

The Padé approximation is often used to replace the exponential term that appears in the characteristic function of the system due to the delay term. The main idea is to approximate the infinite-dimensional system as a finite-dimensional one.

The approximation works in the following way: First, note that for a retarded type system, the characteristic function presents at least one term of the form $e^{-\tau s}$, where $\tau \in \mathbb{R}_+$. Next, we rewrite the exponential term as follows:

$$e^{-\tau s} = \frac{e^{-\tau s/2}}{e^{\tau s/2}}. \tag{2.1}$$

The Maclaurin series expansion (Taylor series at the origin) of each exponential term reads:

$$e^{-\tau s} = 1 - \tau s + \frac{\tau^2 s^2}{2} + \mathcal{O}(\tau^3).$$

The Padé approximation is then derived by reproducing the Maclaurin expansion up to a given order. Therefore, obtaining:

$$e^{-\tau s} = \frac{e^{-\tau s/2}}{e^{\tau s/2}} \approx \frac{1 - \frac{s\tau}{2} + \frac{s^2\tau^2}{8} + \dots}{1 + \frac{s\tau}{2} + \frac{s^2\tau^2}{8} + \dots}.$$

The order up to which we reproduce the Mclaurin series is called the order of the Padé approximation. The main disadvantage of this approach arises from the loss of spectral information. Specifically, since a finite-dimensional system approximates the infinite-dimensional time-delay system, the spectrum of the system is being modified. This limitation may lead to mistuning of the control gains, resulting in behavior that deviates from expectations and potentially introduces instability into the system. We illustrate this problem with the following example.

Example 17 (Loss of stability due to Padé Approximation)**.** *Consider the LTI SISO system described by the following transfer function:*

$$G(s) = \frac{1.6}{1 + 2.9s} e^{-0.24s}. \tag{2.2}$$

Replacing the exponential term by a second order Padé approximation, one obtain the following expression:

$$G_{p2}(s) = \frac{1.6s^2 - 40s + 333.3}{2.9s^3 + 73.5s^2 + 629.2s + 208.3}. \tag{2.3}$$

It is worth noting that the inclusion of the approximation is "adding" *a pair of complex conjugate unstable zeroes to the transfer function. Figure 2.1 depicts the step response of both systems, $G(s)$ and $G_p(s)$, given in* (2.2) *and* (2.3)*, respectively. Apart from the small oscillation and undershoot induced by the unstable zeroes that appears due to the approximation (see the zoom for $0 < t < 0.2$ in Figure 2.1), one can appreciate that the approximation method is very effective.*

It is worth noting that, the behavior presented in the initial response of the system will change depending on the considered approximation. Indeed, by considering a first-order approximation, one can reduce the number of unstable zeroes from two to only one:

$$G_{p1}(s) = \frac{4.5977 - 0.551724s}{s^2 + 8.67816s + 2.87356}. \tag{2.4}$$

The effect of the first order approximation on the initial response of the system is shown in Figure 2.2.

Next, assume that, in order to improve the performance of the system, we consider the classical PI controller $C(s) = k_p + k_i/s$. The corresponding closed-loop system will preserve stability if and only if the roots of the corresponding characteristic functions $\Delta(s) : \mathbb{C} \to \mathbb{C}$, $\Delta_{p1}(s) : \mathbb{C} \to \mathbb{C}$ and $\Delta_{p2}(s) : \mathbb{C} \to \mathbb{C}$ given by:

$$\Delta(s) = 2.9s^2 + s + 1.6e^{-0.24s}(k_p s + k_i), \tag{2.5}$$

$$\Delta_{p1}(s) = s(s^2 + 8.67816s + 2.87356) + (4.5977 - 0.551724s)(k_p s + k_i), \tag{2.6}$$

$$\Delta_{p2}(s) = s(2.9s^3 + 73.5s^2 + 629.2s + 208.3) + (1.6s^2 - 40s + 333.3)(k_p s + k_i), \tag{2.7}$$

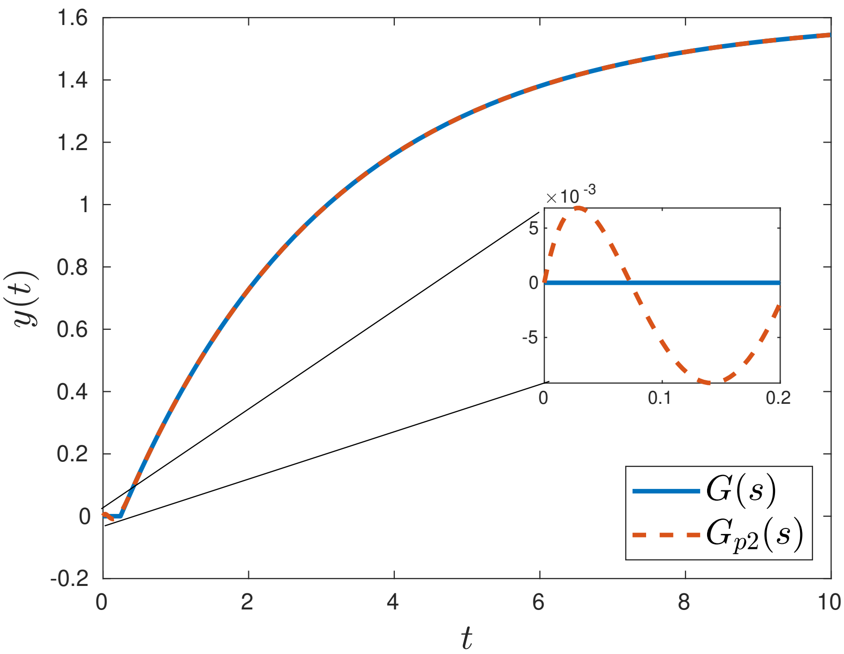

Figure 2.1: Step response of systems (2.2) and (2.3), respectively.

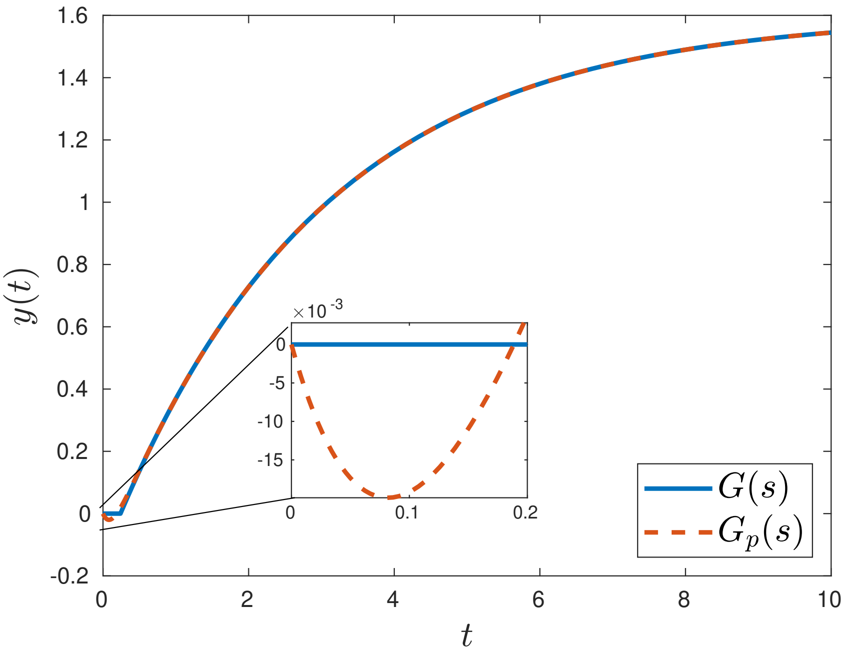

Figure 2.2: Step response of systems (2.2) and (2.4), respectively.

respectively, are in $\mathbb{C}_-$. *Intuitively, one might expect the stabilizing pairs* (k_p, k_i) *to be the same for the three different cases. However, as shown in Figure 2.3, the corresponding regions of* Δ, Δ_{p1}, *and* Δ_{p2} *differ. Moreover, while any stabilizing pair for the time-delay system also stabilizes the approximated systems, the reverse is not true. That is, for the approximated system, certain pairs may appear stabilizing but, in reality, are not. Naturally, one obtains a region*

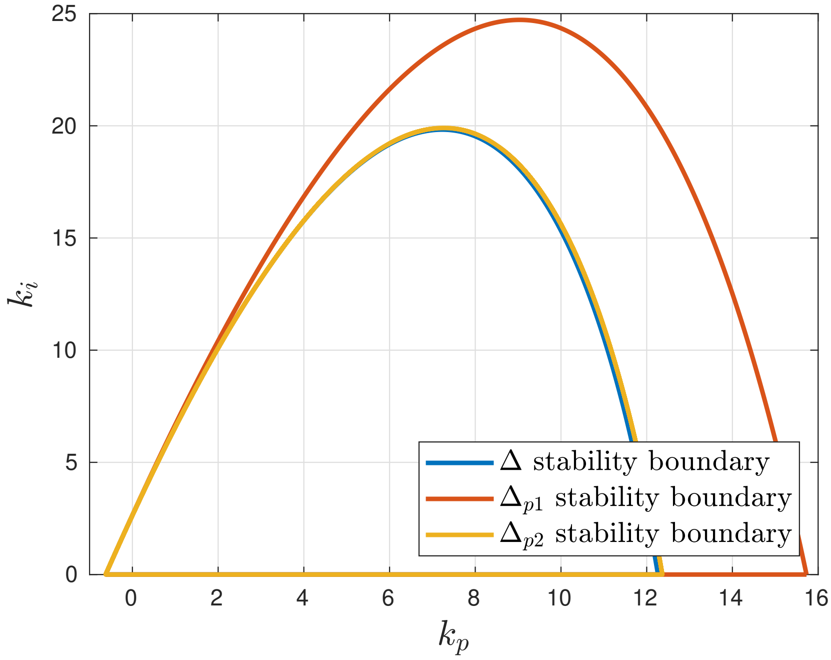

Figure 2.3: Stability boundary of the characteristic functions Δ, Δ_{p1} and Δ_{p2}.

that is "closer" *to the original one by increasing the order of the approximation. However, there exists a trade-off, as increasing the order of the approximation also increases the number of unstable zeroes that are being added. The only way to obtain the corresponding region and behavior of the actual system is by considering the exponential term in the characteristic function. For this reason, in this work, we do not replace the exponential term with its Padé approximation.*

2.3 Two and three points delay-difference approximation of PD-controllers.

In the following section, we only consider approximations of the derivative using two and three points in the sense of the finite-difference method.

2.3.1 Problem formulation

Consider *strictly proper* LTI SISO systems with the following form:

$$\Sigma : \begin{cases} \dot{x}(t) = \boldsymbol{A}x(t) + \boldsymbol{B}u(t), \\ y(t) = \boldsymbol{C}x(t), \end{cases} \tag{2.8}$$

which transfer function representation is given by:

$$H_{yu}(s) := \frac{P(s)}{Q(s)} \equiv \boldsymbol{C}(s\boldsymbol{I} - \boldsymbol{A})^{-1}\boldsymbol{B}, \tag{2.9}$$

where Q and P are polynomials in s, with real coefficients, given by:

$$Q(s) := s^n + \sum_{j=0}^{n-1} q_j s^j, \quad P(s) := \sum_{j=0}^{m} p_j s^j, \quad q_j, p_j \in \mathbb{R}, \tag{2.10}$$

such that $n := \deg(Q) > m := \deg(P)$. We also consider the classical PD-feedback law with the following structure:

$$u(t) = -k_p y(t) - k_d \dot{y}(t), \tag{2.11}$$

where $(k_p, k_d) \in \mathbb{R}^2 \setminus \{(0,0)\}$. In the Laplace domain, the corresponding PD controller will be denoted by C_0 and given by:

$$C_0(s) := k_p + k_d s, \tag{2.12}$$

such that, under unity feedback, the closed-loop characteristic function $\Delta : \mathbb{C} \to \mathbb{C}$ reads:

$$\Delta(s) = Q(s) + (k_d s + k_p)P(s). \tag{2.13}$$

In the following, we denote by $\mathrm{Stab}(H_{yu})$ the set of all stabilizing controllers and assume that this set is nonempty.

As has already been mentioned, there are several problems with the control law (2.11), such as not having access to the derivative of $y(t)$ or high-frequency noise amplification. To tackle these problems, we consider the following approximations based on the finite-difference method:

$$\dot{y}(t) \approx \frac{y(t) - y(t-\tau)}{\tau}, \tag{2.14}$$

$$\dot{y}(t) \approx \frac{1}{2\tau}\left(3y(t) - 4y(t-\tau) + y(t-2\tau)\right). \tag{2.15}$$

Under these approximations, the Laplace domain representation of the controller rewrites in the following way:

$$C_1(s) = k_p + \frac{k_d}{\tau}(1 - e^{-\tau s}), \tag{2.16}$$

$$C_2(s) = k_p + \frac{k_d}{2\tau}(3 - 4e^{-\tau s} + e^{-2\tau s}) \tag{2.17}$$

where the subindex $j \in \{1,2\}$ indicates the number of delays used on the approximation. It is clear that the approximation requires *sufficiently small* values of τ. Under this considerations, let $\Delta_j : \mathbb{C} \times \mathbb{R}_+ \to \mathbb{C}$ with $j \in \{1,2\}$

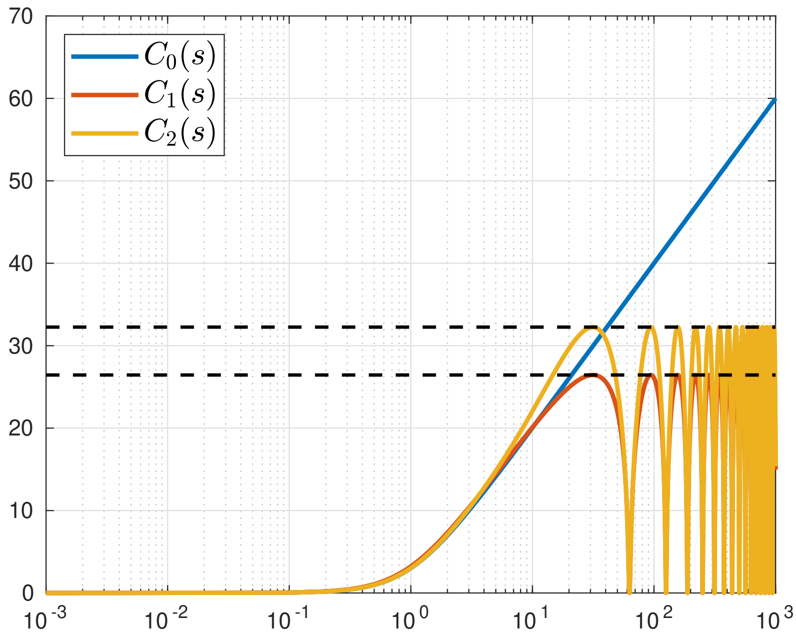

Figure 2.4: Bode magnitude plot of controllers $C_i(s)$, with $i \in \{0, 1, 2\}$ and $k_p = k_d = 1$ and $\tau = 0.1$.

be the corresponding closed-loop characteristic function given by:

$$\Delta_1(s;\tau) = Q(s) + P(s)\left(k_p + \frac{k_d}{\tau}\left(1 - e^{-\tau s}\right)\right), \tag{2.18}$$

$$\Delta_2(s;\tau) = Q(s) + P(s)\left(k_p + \frac{k_d}{2\tau}\left(3 - 4e^{-\tau s} + e^{-2\tau s}\right)\right). \tag{2.19}$$

The controller based on the approximation clearly avoids the problem of *measuring* the derivative since it requires only present and past measures of the output $y(t)$. To illustrate how the approximation also mitigates the high-frequency noise amplification, consider the Bode diagram of both (2.12) and its corresponding approximations (2.16)-(2.17), depicted in Figure 2.4, where we can observe that both $C_1(s)$ and $C_2(s)$ present an upper bound on its magnitude, which is not the case for the pure derivative action. While such an upper bound will depend on the chosen delay τ, we can mitigate the amplification problem by adequately choosing the parameter τ.

With these ideas in mind, the question we aim to answer in this chapter is the following: *"Are C_1 and C_2 always stabilizing controllers for a sufficiently small delay, given that $C_0 \in stab(H_{yu})$?"*.

2.3.2 Motivating example

Before continuing, we might wonder *"Why do we even have to ask the question?"*. Indeed, it might be counterintuitive to imagine that for $\tau \to 0$, the approximation itself can, in a way, destabilize the system. To clarify the problem, consider the following example:

Example 18. *Consider a system described by the following transfer function:*

$$H_{yu}(s) = \frac{-2}{s-2}. \tag{2.20}$$

Under unity feedback, the closed-loop with a classical PD controller $C_0(s)$ bears the following characteristic function $\Delta : \mathbb{C} \to \mathbb{C}$:

$$\Delta(s) = s - 2 - 2(k_d s + k_p). \tag{2.21}$$

By considering the gains $(k_p, k_d) = (1, 1)$, the only root of the characteristic equation is given by $s = -4$. Next, considering the one-delay approximation of the derivative action, one obtains the characteristic function $\Delta_1 : \mathbb{C} \times \mathbb{R}_+ \to \mathbb{C}$:

$$\Delta_1(s;\tau) = s - 2 - 2\left(\frac{k_d}{\tau}(1 - e^{-\tau s}) + k_p\right). \tag{2.22}$$

By considering the same gains, we obtain:

$$\Delta_1(s;\tau) = s - 4 + 2\frac{e^{-\tau s} - 1}{\tau}.$$

One can assume that, for $\tau \to 0$, $s = -4$ should be a solution of $\Delta_1(s;\tau) = 0$. Indeed, it is easy to verify that:

$$\lim_{\tau \to 0}\left(-8 + 2\frac{e^{4\tau} - 1}{\tau}\right) = 0.$$

However, due to the presence of the exponential term, there is an infinite number of characteristic roots of $\Delta_1(s;\tau)$. The question now is, "Is any of those roots located at $\mathbb{C}_+$?" To answer that question, observe that $\Delta_1(0;\tau) = -4$, and $\lim_{s\to\infty} \Delta_1(s;\tau) = \infty$ for any $\tau > 0$. This observation implies that there exists some $r \in \mathbb{R}_+^* \subset \mathbb{C}_+$ such that $\Delta(r;\tau) = 0$, meaning that the closed-loop system with the approximation is always unstable. In the following section, we fully characterize this behavior.

2.3.3 Improperly-posed case characterization

With the previous example in mind, we introduce the following definition from Méndez-Barrios et al. (2022):

Definition 2.3.1: Improperly-posed system

Consider the LTI SISO system with frequency domain representation given by the transfer function (2.9). Suppose that C_0 with the form (2.12) is a stabilizing controller, that is $C_0 \in \text{Stab}(H_{yu})$, and is replaced by C_j with $j \in \{1, 2\}$, given by (2.16) and (2.17), respectively. If there exists a sequence of real numbers $(\tau_n)_{n\in\mathbb{N}}$, $\tau_n \to 0^+$ when $n \to \infty$ such that for all $\epsilon > 0$, there exists some positive integer n_u, with $\tau_{n_u} < \epsilon$ and $C_{j_{n_u}} \notin Stab(H_{yu})$ the controller C_j is called an improperly-posed controller for "small" delays. In this case, the closed-loop system is improperly posed for "small" delays.

Definition 2.3.1 only states that if replacing the original stabilizing PD controller with one of the proposed approximations induces instability in the system regardless of how *"small"* the chosen τ is, the system is called improperly-posed. Naturally, in the opposite case, where stability can be preserved for a sufficiently small value of the delay parameter, we refer to the system as properly-posed.

Before continuing, consider the following representation of $\Delta_2(s;\tau)$:

$$\Delta_2(s;\tau) = Q(s) + P(s)\left(k_p + k_d\left(\frac{1-e^{-\tau s}}{\tau}\right)\left(\frac{3-e^{-\tau s}}{2}\right)\right). \tag{2.23}$$

As presented in the Introduction, the Newton diagram method allows us to represent a solution in the form of a Pusieux series. The Newton diagram can be constructed following the algorithm presented in the Introduction. To simplify this task, we express the characteristic function Δ_j, for $j \in \{1, 2\}$ in the following way:

$$\Delta_1(s;\tau) = Q(s) + \left(k_p + k_d \sum_{j=1}^{\infty} a_j s^j \tau^{j-1}\right) P(s), \tag{2.24}$$

$$\Delta_2(s;\tau) = Q(s) + \left(k_p + k_d \sum_{j=1}^{\infty} b_j s^j \tau^{j-1}\right) P(s), \tag{2.25}$$

where,

$$a_j = (-1)^{j-1}\frac{s^j\tau^{j-1}}{j!}, \quad b_j = -\frac{(-1)^j 2 + (-1)^{j+1}2^{j-1}}{j!}.$$

The Newton's Polygon of $\Delta_j(s;\tau)$ can be obtained using Algorithm 1, presented in the Introduction, page 25 (see Figure 2.5). From the Newton diagram method, Lemma 2.3.1 can be easily derived:

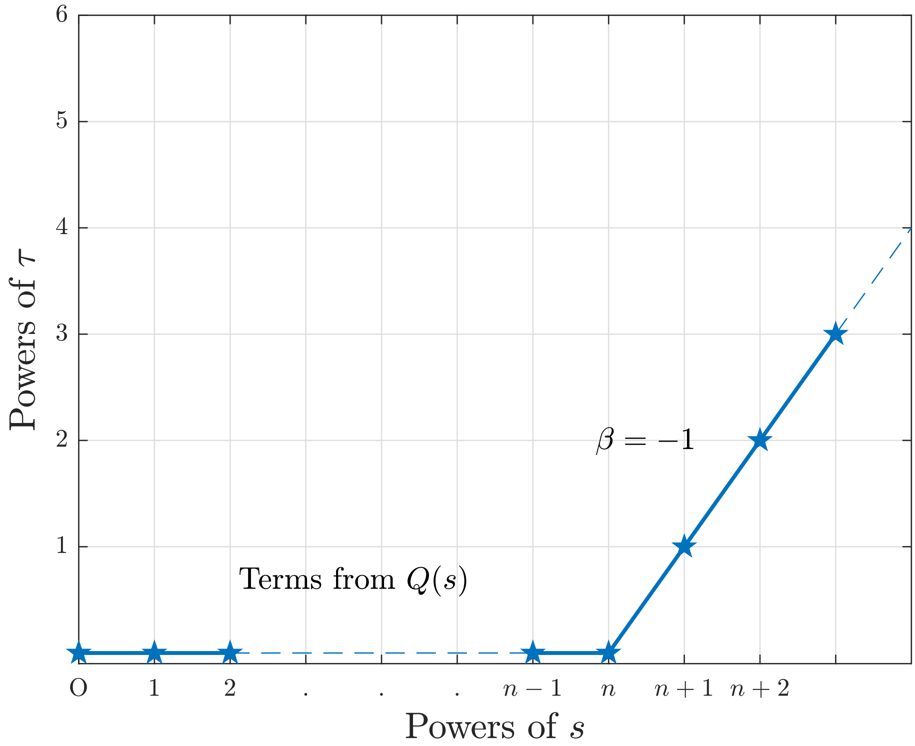

Figure 2.5: Newton polygon of $\Delta_j(s;\tau)$.

Lemma 2.3.1: Root structure

A closed-loop system with characteristic function given by $\Delta_j(s;\tau)$, with $j \in \{1,2\}$, may present roots $s^* : \mathbb{R}_+ \to \mathbb{C}$ with singular behavior given by:

$$s^*(\tau) = \frac{1}{\tau}\lambda^*(\tau), \tag{2.26}$$

where $\lambda(\tau)$ is an analytic function, such that $\lambda(0) \neq 0$.

Note that the only information on the root $s^*(\tau)$ that we have is that the root will present singular behavior for $\tau \to 0$. However, we can obtain information on the function $\lambda^*(\tau)$ from the Newton diagram method. In this spirit, we have the following results:

Proposition 2.3.1: Improperly-posedness of the closed-loop system

Let the characteristic function of a closed-loop system be given by $\Delta_j(s;\tau)$, with $j \in \{1,2\}$. Then, if $n = m+1$, where n and m represent the degrees of the polynomials Q and P respectively, the closed-loop system exhibits a singular characteristic root $s^* : \mathbb{R}_+ \to \mathbb{C}$ given by:

$$s^*(\tau) = \frac{1}{\tau} z^* + \mathcal{O}(1),$$

where $z^* \in \mathbb{R}$. Furthermore, $z^* > 0$ if and only if $k_d p_{n-1} < -1$, where p_{n-1} is the leading coefficient of $P(s)$. In this case, the system is improperly-posed.

The proof can be found on page 63 in Appendix A. It is worth noting that $n = m+1$ can be interpreted as having a relative degree equal to one in the open-loop system. We can summarize the result as follows: if the relative degree of the system is greater than one, that is $n > m+1$, the system is always properly-posed. This means that replacing the derivative action in a PD controller with its corresponding approximation will preserve stability, provided the delay parameter is *sufficiently small*. Conversely, if the relative degree of the system is exactly one ($n = m-1$), a properly-posed closed-loop system requires $k_d p_{n-1} > -1$. In other words, if $k_d p_{n-1} < -1$, the system will lose stability when the derivative action is replaced with its approximation, regardless of the delay parameter. This is illustrated in Figure 2.6. The following corollary allows the computation of z^*:

Corollary 2.3.1

Let the characteristic function of an improperly-posed closed-loop system be given by $\Delta_j(s;\tau)$, with $j \in \{1,2\}$. Then, the closed-loop system exhibits a singular characteristic root $s^* : \mathbb{R}_+ \to \mathbb{C}$ given by:

$$s^*(\tau) = \frac{1}{\tau} z^* + \mathcal{O}(1),$$

where $z^* \in \mathbb{R}$ is a non-trivial root of the auxiliary quasipolynomial:

$$\bar{f}_j(w) := \begin{cases} w + k_d p_{n-1}(1 - e^{-w}) & \text{if} \quad j = 1 \\ w + k_d p_{n-1}(1 - e^{-w}) \left(\frac{3 - e^{-w}}{2}\right) & \text{if} \quad j = 2 \end{cases}. \tag{2.27}$$

Proof. This result follows directly from the application of the Newton diagram method. The reasoning aligns with the steps detailed in the proof of Proposition 2.3.1 (see Appendix A, page 131). □

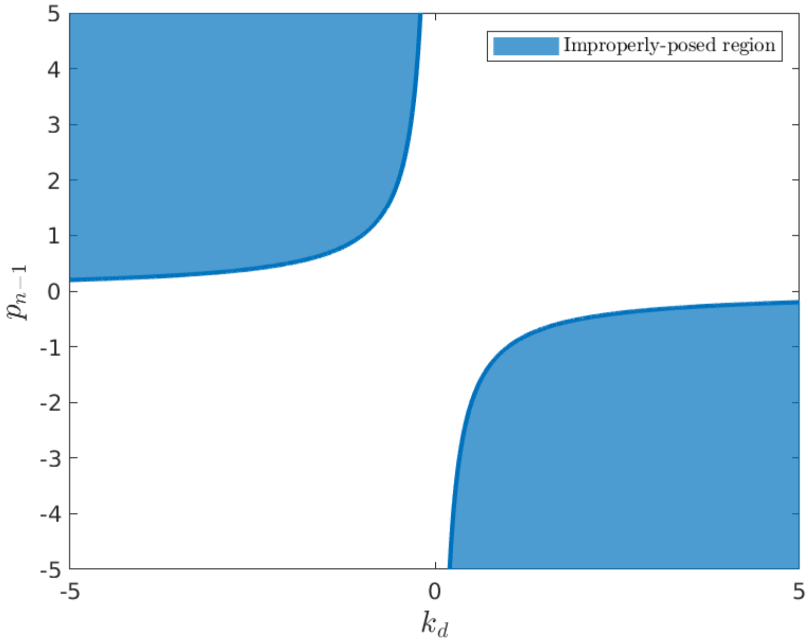

Figure 2.6: Properly-posed condition for delay-difference approximations considering one and two delays

2.4 Delay margin of the approximation

With the improperly-posed scenario characterized, a feature of interest is the delay margin of the approximation. That is, in the properly-posed case, how large can the delay be without compromising the stability of the closed-loop system? In this spirit, we define the delay margin of the approximation in the following way:

Definition 2.4.1: Delay margin of the approximation

Consider a properly-posed LTI SISO system with transfer function representation given by $H_{yu}(s)$ as in (2.9) in closed-loop with the controller $C_j(s)$ with $j \in \{1, 2\}$. The delay margin of the delay-difference approximation is defined by

$$\tau_{max} := \sup\{\beta \in \mathbb{R}_+ : C_j(\tau) \in \text{Stab}(H_{yu}) \quad \forall \tau \in (0, \beta)\}.$$

In the following, we present a methodology to find the delay margin of each approximation separately.

2.4.1 Delay margin in the single delay case

Let us analyze the single-delay approximation of the derivative action with fixed control gains $(k_p, k_d) = (k_p^\star, k_d^\star)$. We introduce the following function $F : \mathbb{R}_+ \times \mathbb{R}_+^* \to \mathbb{R}$:

$$F(\omega, \tau) = \frac{\left|\tau \left(Q(\boldsymbol{i}\omega) + k_p^\star P(\boldsymbol{i}\omega)\right) + k_d^\star P(\boldsymbol{i}\omega)\right|^2}{\left|k_d^\star P(\boldsymbol{i}\omega)\right|^2}. \tag{2.28}$$

Note that, regardless of Q and P, $F(\omega,\tau)$ is always quadratic in τ. Moreover, $F(\omega,0)=1$ for all $\omega\in\mathbb{R}$. Next, we define the set $\Omega\subset\mathbb{R}^2$ as the set of all pairs (ω,τ), with $\tau\in\mathbb{R}_+^*$ such that the following conditions are satisfied:

$$F(\omega,\tau)=1, \tag{2.29}$$

$$\mathrm{Arg}\left\{F(\omega,\tau)\right\}=-\omega\tau. \tag{2.30}$$

We also refer to Ω as a crossing set. We have the following result:

Proposition 2.4.1: Delay margin on the single delay case

Consider a properly-posed closed-loop system with characteristic function $\Delta_1(s;\tau)$ given by (2.18). Then, the delay margin τ_{max} of the closed-loop system is given by:

$$\tau_{max}:=\begin{cases}\min\limits_{(\omega,\tau)\in\Omega}\tau & \text{if} \quad \Omega\neq\emptyset\\ +\infty & \text{otherwise}\end{cases}, \tag{2.31}$$

and the corresponding crossing, if any, occurs at the given ω^* such that $(\omega^*,\tau_{max})\in\Omega$. If $\Omega=\emptyset$, we say that the stability of the closed-loop system is independent of the delay.

Proof. To derive $F(\omega,\tau)$, consider the characteristic equation $\Delta_1(s;\tau)=0$ evaluated at $s=\boldsymbol{i}\omega$. By separating terms with and without the exponential $e^{-\boldsymbol{i}\omega}$, we obtain $F(\omega,\tau)$ as the normalized magnitude of these terms. From the continuity of characteristic roots with respect to the system parameters, and given the properly-posed nature of the system, stability can only be lost if there exists a pair (ω,τ) such that Δ_1 has a root on the imaginary axis. Thus, finding such pairs corresponds to identifying the crossing set Ω. This ends the proof. □

Remark 5. *As previously noted, the function F is quadratic in τ and $F(0,\omega)=1$ for all $\omega\in\mathbb{R}$. This implies that, for a fixed ω, there are at most two solutions for τ satisfying $F(\tau,\omega)=1$. Among these, only one solution $\tau(\omega)$ is relevant for stability analysis. Specifically, if this solution is negative for all $\omega\in\mathbb{R}$, it follows that the system's stability is independent of the delay parameter τ.*

2.4.2 Delay margin in the three-points approximation case

Next, we consider the same problem but for the case of an approximation with two delays. To this end, let $\Delta_2(s;\tau)$ be defined as in (2.19), and introduce the following definitions:

$$\phi_0(\omega,\tau) = \tau Q(\boldsymbol{i}\omega) + \tau k_p P(\boldsymbol{i}\omega) + \frac{3k_d}{2}P(\boldsymbol{i}\omega), \tag{2.32}$$

$$\phi_1(\omega) = -2k_d P(\boldsymbol{i}\omega), \tag{2.33}$$

$$\phi_2(\omega) = \frac{k_d}{2}P(\boldsymbol{i}\omega). \tag{2.34}$$

Clearly, for any pair (ω,τ) such that $\Delta_2(\boldsymbol{i}\omega,\tau) = 0$, the following equation holds:

$$\phi_0(\omega,\tau) - 4\phi_2(\omega)e^{-\boldsymbol{i}\omega} + \phi_2(\omega)e^{-2\boldsymbol{i}\omega} = 0. \tag{2.35}$$

We next define the function $\Phi : \mathbb{R}_+ \times \mathbb{R}_+^* \to \mathbb{R}$:

$$\Phi(\omega,\tau) = \frac{|\phi_2(\omega)|^2}{|\phi_0(\omega,\tau)|^2}. \tag{2.36}$$

This leads to the following results:

Proposition 2.4.2: Construction of the crossing set Ω_2

Let $\Omega_2 \subset \mathbb{R}^2$ with $\tau \in \mathbb{R}_+^*$, denote the set of all pairs (ω,τ) such that (2.35) is satisfied. Then, for all $(\omega^*,\tau^*) \in \Omega_2$, the following inequality holds:

$$\frac{1}{25} \leq \Phi(\omega^*,\tau^*) \leq \frac{1}{9}. \tag{2.37}$$

Proof. We start by observing that equation (2.35) can be rewritten as:

$$\phi_0(\omega,\tau) = 4\phi_2 e^{-\boldsymbol{i}\omega} - \phi_2(\omega)e^{-2\boldsymbol{i}\omega}.$$

Applying the triangle inequality to this expression gives:

$$|\phi_0(\omega,\tau)| \leq 4\,|\phi_2(\omega\tau)| + |\phi_2(\omega\tau)| = 5\,|\phi_2(\omega\tau)|\,,$$

Similarly, applying the reverse triangle inequality gives:

$$|\phi_0(\omega,\tau)| \geq 4\,|\phi_2(\omega\tau)| - |\phi_2(\omega\tau)| = 3\,|\phi_2(\omega\tau)|\,.$$

Finally, squaring both sides of each inequality yields:

$$9\left|\phi_2(\omega)\right|^2 \leq \left|\phi_0(\omega,\tau)\right|^2 \leq 25\left|\phi_2(\omega)\right|^2,$$

which directly leads to inequality (2.37). $\square$

Proposition 2.4.3: Delay margin on the double delay case

Consider a properly posed closed-loop system with the characteristic function $\Delta_2(s;\tau)$defined by (2.19). The delay margin τ_{max} of the closed-loop system is given by:

$$\tau_{max} := \begin{cases} \min\limits_{(\omega,\tau)\in\Omega_2} \tau & \text{if} \quad \Omega_2 \neq \emptyset \\ +\infty & \text{otherwise} \end{cases}, \tag{2.38}$$

If $\Omega_2 \neq \emptyset$, the corresponding crossing occurs at a frequency ω^* such that $(\omega^*, \tau_{max}) \in \Omega_2$.

Proof. Equation (2.35) is equivalent to $\tau\Delta_2(\boldsymbol{i}\omega;\tau) = 0$. For sufficiently small τ, all the roots of Δ_2 lie in the left-half plane, as the system is properly posed, and, by continuity arguments, the smallest delay τ for which $(\omega,\tau) \in \Omega_2$ corresponds to the delay margin. This ends the proof. $\square$

Remark 6. *Although an explicit computation of the delay margin is not provided, Proposition 2.4.2 implies that τ_{max} can be determined by examining a specific interval.*

2.5 Illustrative examples

In this section, we present numerical examples to illustrate the various results discussed in this chapter.

Example 19 (Second order improperly-posed system)**.** *Consider a system represented by the following transfer function:*

$$H_{yu}(s) = \frac{-s}{s^2 - 5}, \tag{2.39}$$

which can be stabilized in closed-loop using a classical PD controller with control gains $(k_p, k_d) = (1.5, 1)$. These gains place the closed-loop characteristic roots at $s_{1,2} = -1 \pm 3\boldsymbol{i}$. Notably, the condition $k_d p_{n-1} = -1.5 < -1$ is satisfied, and the system's relative degree is one. According to Proposition 2.3.1, this implies the existence of a root with asymptotic behavior described by $s(\tau) = z^*/\tau$. The value of $z^*$is computed for both approximation cases using Corollary 2.3.1 and the QPmR algorithm (detailed in Appendix B, page 148). The results show that $z_1^* = 0.8742$ for the single-delay approximation and $z_2^* = 0.17525$ for the two-delay approximation. Table 2.1 summarizes the rightmost root of the closed-loop system for both cases, along with the stabilizing PD controller.

The behavior of the root as τ decreases within the interval $\tau \in (1/100, 1/200)$ is illustrated in Figure 2.7.

Table 2.1: **Different values of the spectral abscissa for the different implementations of the PD controller in closed-loop with the system described by** (2.39)**.**

Controller	Rightmost root	Delay parameter
$C_0(s)$	$s^* = -1 \pm 3\boldsymbol{i}$	–
$C_1(s)$	$s^* = 90.17 \approx z_1^*/\tau$	$\tau = 1/100$
$C_2(s)$	$s^* = 177.19 \approx z_2^*/\tau$	$\tau = 1/100$

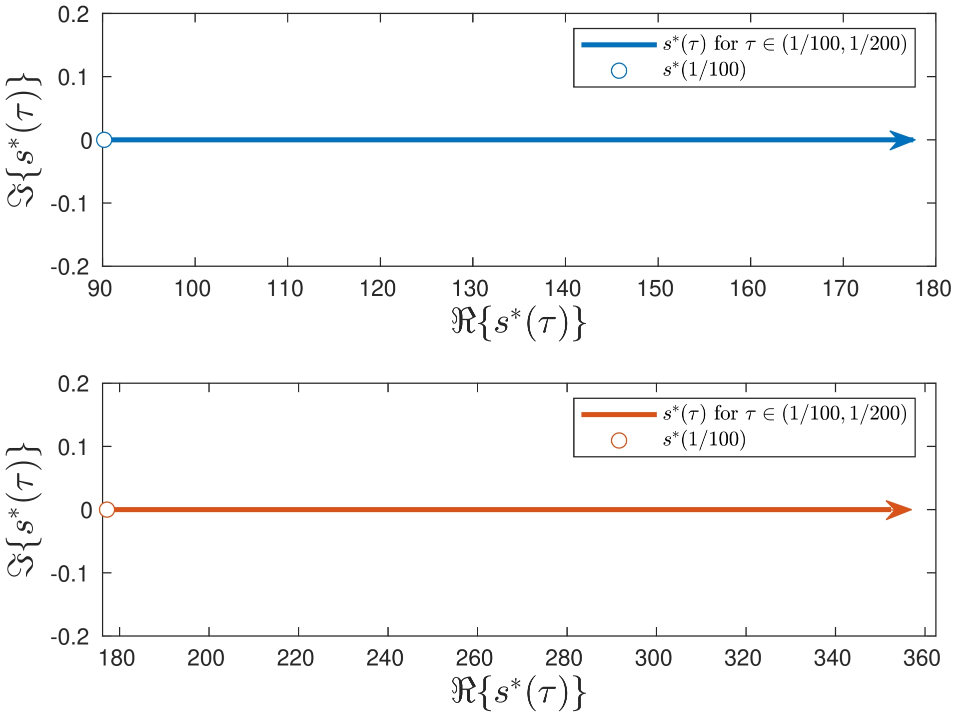

Figure 2.7: Evolution of the rightmost root of the closed-loop system with the one delay approximation (up) and the two delays approximation (down).

Example 20 (Third-order improperly-posed system)**.** *In this second example, we analyze a third-order system with transfer function representation:*

$$H_{yu}(s) = \frac{-5s^2}{s^3 + s^2 - s - 1}. \tag{2.40}$$

The system can be stabilized in closed-loop by selecting the control gains $(k_p, k_d) = (3, 2)$*, which result in the closed-loop characteristic roots located at* $s = \{-1.53, -0.012 \pm 0.269\boldsymbol{i}\}$*. Similar to the previous example, the values of* z_1^* *and* z_2^**, are computed and included in Table 2.2. For illustrative purposes, we consider a larger delay than in the previous example. It is important to note that the approximation* $s^*(\tau) = z^*/\tau$ *becomes less accurate for larger values of* τ*, as higher-order terms in the power series gain significance. To better characterize the root's behavior, higher-order terms of the power series would need to be computed using the Newton diagram method, considering the obtained* z^**. However, this procedure is beyond the scope of this thesis and is left for future work.*

Table 2.2: **Different values of the spectral abscissa for the different implementations of the PD controller in closed-loop with the system described by** (2.40)**.**

Controller	z^*	Rightmost root	Delay parameter
$C_0(s)$	–	$s^* = -0.012 \pm 0.269\boldsymbol{i}$	–
$C_1(s)$	$z_1^* = 9.99$	$s^* = 114.007 \approx z_1^*/\tau$	$\tau = 1/10$
$C_2(s)$	$z^* = 14.99$	$s^* = 164.006 \approx z_2^*/\tau$	$\tau = 1/10$

Example 21 (Delay independent stability on the properly-posed case)**.** *For the next example, consider the following transfer function:*

$$H_{yu}(s) = \frac{s+1}{s^2 - s + 1}. \tag{2.41}$$

Note that for this system, any $k_d > 0$ results in a properly-posed system. With this in mind, let the closed-loop control gains be $(k_p, k_d) = (3, 1)$. These gains result in closed-loop characteristic roots located at $s = (-3 \pm 23\boldsymbol{i})/4$. Since the system is properly-posed, the only factor to consider for the safe implementation of the controller is the value of the delay parameter τ. Let us consider the single-delay approximation of the derivative action, leading to the following closed-loop characteristic equation:

$$\Delta_1(s;\tau) = s^2 - s + 1 + (s+1)\left(3 + \frac{1 - e^{-\tau s}}{\tau}\right). \tag{2.42}$$

As already discussed, due to the continuity of characteristic roots with respect to system parameters and the properly-posed configuration, stability can only be lost if there exists a pair $(\omega, \tau) \in \mathbb{R}_+^2$ such that $\Delta_1(\boldsymbol{i}\omega;\tau) = 0$. Through algebraic manipulation, this condition leads to the following equation:

$$e^{-\boldsymbol{i}\omega} = 1 + \frac{(1 - \boldsymbol{i}\omega)(4 - \omega^2 + 2\boldsymbol{i}\omega)}{1 + \omega^2}.$$

Taking the square norm of both sides yields:

$$1 = \tau^2\omega^2 - 5\tau^2 + \frac{3(7\tau + 2)\tau}{\omega^2 + 1} + 2\tau + 1,$$

which is quadratic in τ with the following solutions:

$$\tau_1 = 0, \qquad \tau_2 = -\frac{2(\omega^2 + 4)}{16 - 4\omega^2 + \omega^4}.$$

Note that τ_1 is not of interest and, for τ_2, we need to determine whether there exist values of ω such that $\tau_2 > 0$. Observe that the numerator of τ_2 is always positive. Therefore, the denominator must be negative for $\tau_2 > 0$ due to the negative sign. However, the denominator reaches its minimum values at $\omega = \{0, \pm\sqrt{2}\}$, where it remains positive. Consequently, there are no positive values of τ for which a root crossing exists on the imaginary axis. This leads to

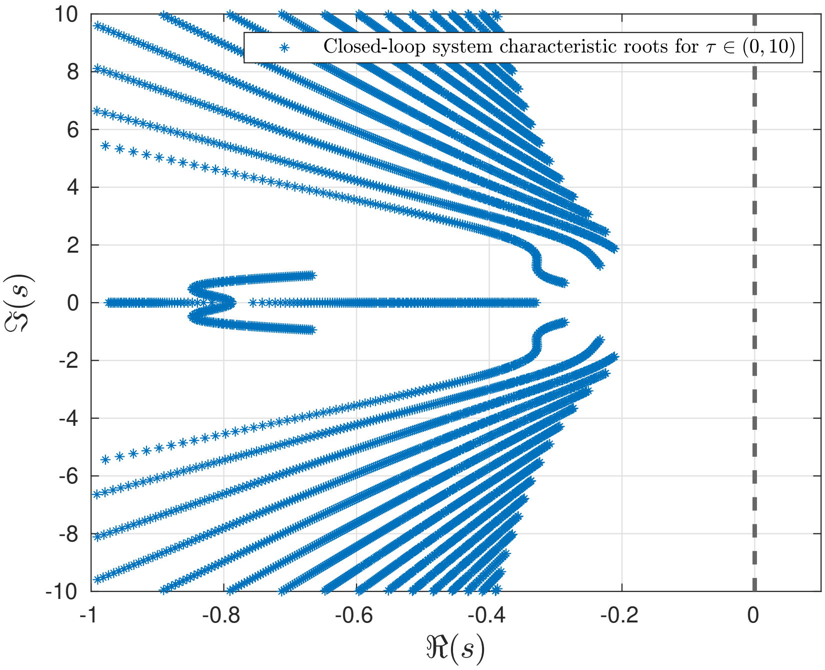

Figure 2.8: Closed-loop system roots evolution with the single delay approximation and $\tau \in (0, 10)$.

the conclusion that the closed-loop system maintains stability for any $\tau > 0$. *Note that, from Proposition 2.4.1, this is equivalent to* $\Omega = \emptyset$.

The evolution of the closed-loop characteristic roots for $\tau \in (0, 10)$ *is shown in Figure 2.8. As expected from the computations, no root crosses the imaginary axis, regardless of the value of the delay parameter.*

Example 22 (Stabilizing effects of the approximation)**.** *As mentioned in the first chapter, the idea of using delay as a control parameter is not new. Delays can, in fact, have a stabilizing effect and be employed as control parameters. With this in mind, consider the following transfer function:*

$$H_{yu}(s) = \frac{1}{s^4 - s^3 + s^2 + 25s - 100}, \tag{2.43}$$

which cannot be stabilized using a classical PD controller due to insufficient degrees of freedom. Let us now consider the control gains $(k_p, k_d) = (100.01, -24.8)$. *Using an ideal PD controller under these gains results in instability, with the closed-loop characteristic roots located at* $s = \{-0.51, -0.011, 0.76 \pm 1.09\boldsymbol{i}\}$. *The evolution of the rightmost roots of the closed-loop system, using the two-delay approximation, is shown in Figure 2.9. It can be observed that within the interval* $\tau \in (0.47, 0.58)$, *the closed-loop system becomes stable.*

Example 23 (Delay margin on the properly-posed case)**.** *Consider a second-order system with a transfer function defined as:*

$$H_{yu}(s) = \frac{K}{s^2 + as + b}, \tag{2.44}$$

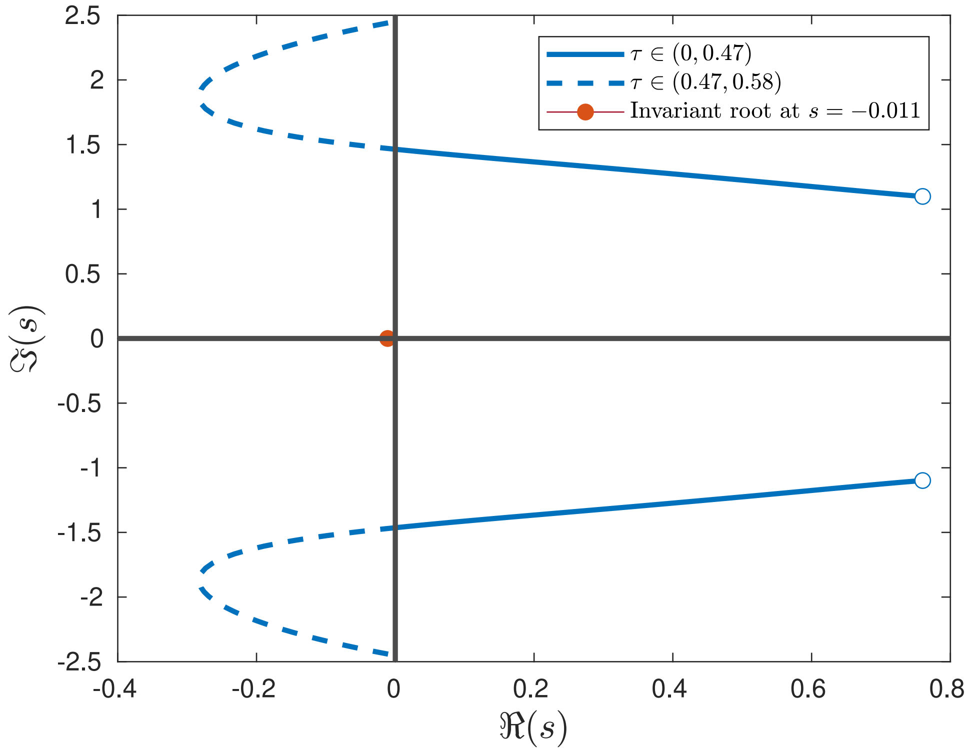

Figure 2.9: Effect of the delay on stability.

where $(a, b) \in \mathbb{R}^2$ are system's parameters, and $K \in \mathbb{R}^*$ is the open-loop gain. For this example, we set $K = 1$, $a = -1$ and $b = 1$. Let the controller gains be $(k_p, k_d) = (1, 2)$. Under these settings, the closed-loop characteristic roots become $s^* = (-1 \pm \sqrt{7})/2$. Next, we consider both implementations of the derivative action (single and double delay). The corresponding delay margin and crossing frequency for each approximation are summarized in Table 2.3. The root trajectories as the delay increases within the interval $(0, \tau_{max})$ are illustrated in Figures 2.10a and 2.11a for the respective approximations. Figures 2.10b and 2.11b illustrate how increasing the delay value impacts the closed-loop system's time-domain response to a step input. Notably, as the delay increases, the system exhibits more pronounced oscillatory behavior. Furthermore, as the delay approaches the respective delay margins τ_{max}, the system's response converges to a marginally stable behavior, as expected from a system with characteristic roots on the imaginary axis.

The delay margin for the single-delay approximation can be further validated using Proposition 2.4.1. Specifically, the delay as a function of the frequency ω is given by:

$$\tau(\omega) = \frac{4\left(\omega^2 - 2\right)}{\omega^4 - 3\omega^2 + 4}, \quad \omega^* = 2.27, \tag{2.45}$$

from which the delay margin is determined as $\tau_{max} = \tau(\omega^*) = 0.83$.

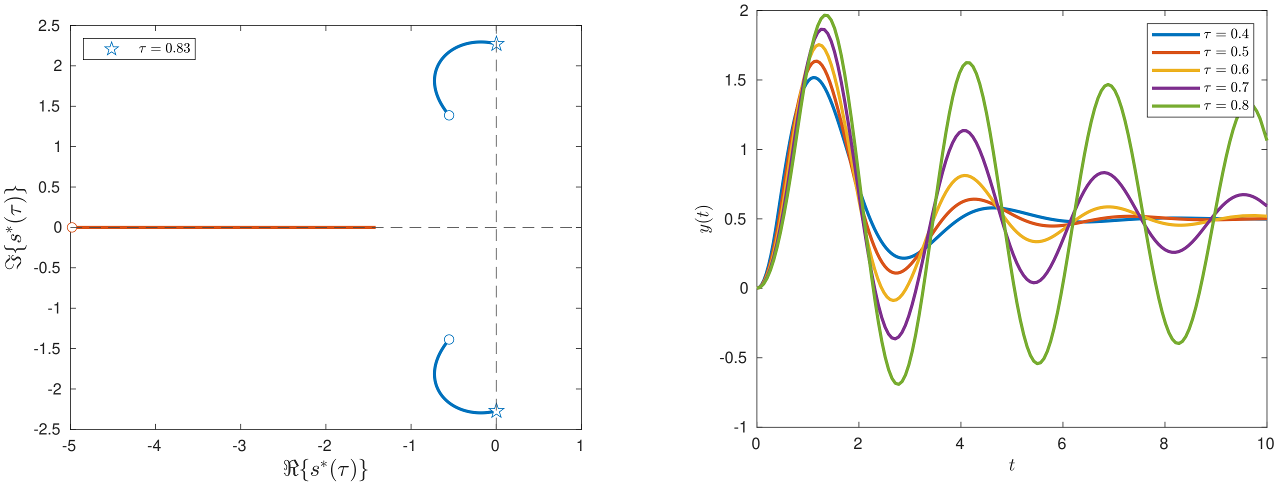

(a) Evolution of the closed-loop characteristic roots of system (2.44) in closed-loop with a PD controller with the single delay approximation and control gains $(k_p, k_d) = (1, 2)$.

(b) Time response of the closed-loop system to a step input with a single delay approximation as τ increases within the interval $(0.4, 0.8)$

Figure 2.10: Effect of the delay parameter on the time-domain response of the closed-loop system with the one delay approximation of the derivative action.

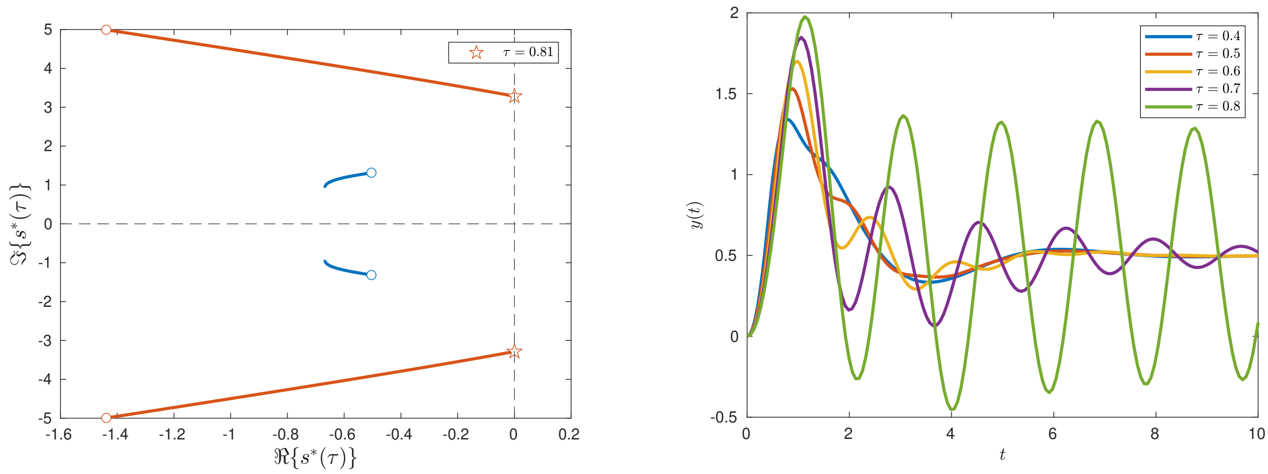

(a) Evolution of the closed-loop characteristic roots of system (2.44) in closed-loop with a PD controller with two delays approximation and control gains $(k_p, k_d) = (1, 2)$.

(b) Time response of the closed-loop system to a step input with a double delay approximation as τ increases within the interval $(0.4, 0.8)$

Figure 2.11: Effect of the delay parameter on the time-domain response of the closed-loop system with the two delays approximation of the derivative action.

Table 2.3: **Delay margin of the approximation with one and two delays in closed-loop with system (2.44).**

Controller	Delay margin τ_{max}	Crossing frequency ω^*
$C_1(s)$	$\tau_{max} = 0.83$	$\omega^* = 2.27$
$C_2(s)$	$\tau_{max} = 0.81$	$\omega^* = 3.28$

2.6 Effects of the approximation in PID controllers: Second-order systems case

In the following, we analyze the effect of incorporating a delay-difference approximation into the implementation of a classical PID controller. To this end, we consider systems described by the following second-order differential equation:

$$\ddot{y}(t) + a\dot{y}(t) + by(t) = cu(t), \tag{2.46}$$

where the triplet (a, b, c) represents the system parameters, with $(a, b, c) \in \mathbb{R}^2 \times \mathbb{R}_+$, and $u(t)$ is the system input. Second-order linear systems are of particular interest because they model various physical phenomena. The transfer function associated with this system is given by:

$$H_{yu}(s) = \frac{c}{s^2 + as + b}. \tag{2.47}$$

Next, we focus on the use of PID controllers for two main reasons. On the one hand, PID controllers are widely utilized in industry due to their simplicity in implementation and tuning. On the other hand, the system under consideration has a relative degree greater than one. As discussed earlier in this chapter, this condition is sufficient for the properly-posedness of the derivative action implementation. With these considerations, the classical PID controller is expressed as:

$$u(t) = -k_p y(t) - k_d \dot{y}(t) - k_i \int_0^t y(s)\, ds, \tag{2.48}$$

which, under the delay-difference approximation for the derivative action, becomes:

$$u_\tau(t) = -k_p y(t) - k_d \frac{y(t) - y(t-\tau)}{\tau} - k_i \int_0^t y(s)\, ds. \tag{2.49}$$

Note that the considered approximation uses a single delay term. In the Laplace domain, the controller in (2.48) is given by:

$$C_{PID}(s) = k_p + k_d s + \frac{k_i}{s}, \tag{2.50}$$

and the controller in (2.49) is expressed as:

$$C_\tau(s) = k_p + k_d \left(\frac{1 - e^{-\tau s}}{\tau} \right) + \frac{k_i}{s}. \tag{2.51}$$

The characteristic function of the closed-loop system with a pure derivative action is given by $\Delta : \mathbb{C} \times \mathbb{R}^3 \to \mathbb{C}$:

$$\Delta(s; \vec{k}) = s^3 + (k_d c + a)s^2 + (k_p c + b)s + k_i c, \tag{2.52}$$

where $\vec{k} = (k_p, k_i, k_d) \in \mathbb{R}^3$ represents the vector of control gains. After introducing the delay-difference approximation for the derivative action, the characteristic equation becomes $\Delta_\tau : \mathbb{C} \times \mathbb{R}^4 \to \mathbb{C}$:

$$\Delta_\tau(s; \vec{k}_\tau) = s^3 + as^2 + \left(b + \left(k_p + \frac{k_d}{\tau} \right) c \right) s + ck_i - cs\frac{k_d}{\tau} e^{-\tau s}, \tag{2.53}$$

where $\vec{k}_\tau = (\vec{k}, \tau) \in \mathbb{R}^3 \times \mathbb{R}_+$ includes the control gains $\vec{k}$ as defined earlier and the delay parameter $\tau > 0$ introduced by the approximation scheme.

2.6.1 Closed-loop stability regions

To ensure the exponential stability of the closed-loop system, the spectrum of the corresponding characteristic function must lie in $\mathbb{C}_-$. In other words, the spectral abscissa of the characteristic function must be negative.

In the following, we assume that k_i is chosen beforehand. In that spirit, for a classical implementation of PID control with a fixed $k_i > 0$ this condition is satisfied if the following inequalities hold:

$$k_d > -\frac{a}{c} \quad \wedge \quad k_p > \frac{ck_i - ab - bck_d}{ac + c^2 k_d}. \tag{2.54}$$

These two inequalities in (2.54) explicitly define the stable regions in the controller parameter space (k_p, k_d).

Next, based on the continuity property of the roots of the closed-loop system with respect to its parameters, any transition of a solution from the left-half plane (stability) to the right-half plane (instability), or vice versa, must involve a crossing through the imaginary axis. Consequently, when adopting the delay-difference approach, it becomes necessary to identify the corresponding stability crossing curves [1] that is, the set of all parameter pairs (k_p, k_d) for which there exists a characteristic root located on the imaginary axis. The following result provides a characterization of these stability crossing points:

[1]The concept of stability crossing curves is deeply discussed and exploited in Chapter 4. In the context of this Chapter, it is use only as a tool to compare the stability conditions of the system with and without the delay-difference approximation.

Proposition 2.6.1

Consider the system described by the transfer function given in (2.47), in closed-loop with the controller $u_\tau(t)$ with Laplace domain representation given by (2.51). For fixed $k_i > 0$ and $\tau > 0$, the stability crossing points are given by:

$$k_p(\omega) = \frac{\tan\left(\frac{\tau\omega}{2}\right)\left(a\omega^2 - ck_i\right) - b\omega + \omega^3}{c\omega}, \tag{2.55}$$

and

$$k_d(\omega) = \frac{\tau \csc(\tau\omega)\left(ck_i - a\omega^2\right)}{c\omega}. \tag{2.56}$$

Proof. The proof proceeds by observing that if a root lies on the imaginary axis, the following conditions must simultaneously hold:

$$\Re\{\Delta_\tau(\boldsymbol{i}\omega; \vec{k}_\tau)\} = 0,$$
$$\Im\{\Delta_\tau(\boldsymbol{i}\omega; \vec{k}_\tau)\} = 0.$$

Then, it suffices to solve for k_p and k_d. Thus, the proof is complete. □

Thanks to the $\mathcal{D}$-partition method (see, for instance, the Introduction, page 18), we know that the stability crossing points form a curve $\mathcal{K}$, representing the set of all such points. Furthermore, this curve divides the parameter space into disjoint regions, each characterized by a specific number of unstable roots. From the continuity of the characteristic roots with respect to the system parameters, we can conclude that a stable region, defined as a region with zero unstable roots, exists for sufficiently small delay values. With this in mind, in the following, we aim to compare the stable region obtained with the approximation for a given delay τ with the region for which (2.54) holds.

2.6.2 Effect of the delay-difference approximation on the stability region

In this section, we aim to exemplify how the stability region of the closed-loop system is affected by using the single-delay approximation. It is worth mentioning that if $\tau \to 0$, the stability region must converge to the region where the inequalities (2.54) hold. However, hardware limitations or specific implementation requirements may *impose* a certain lower bound on the delay parameter. This is not necessarily detrimental in terms of the stability of the closed-loop system. Indeed, while some stabilizing control gain pairs may become unstable, some unstable ones may now become stable, indicating that the selection of the delay parameter has to be done with some care. Let us consider the following example to exemplify what is being described here.

Example 24. *Consider the system with an open-loop transfer function given by:*

$$H_{yu}(s) = \frac{1}{s^2 + 4s + 4}. \tag{2.57}$$

Consider the inclusion of a PID controller in a closed-loop system to achieve specific performance objectives. Setting $k_i = 1$*, we can calculate the stability boundaries of the closed-loop system using both implementations, the classical implementation of the PID controller and the PID controller, with a delay-difference approximation. We assume a fixed delay parameter* $\tau = 1/2$ *for illustrative purposes. Figure 2.12 illustrates the differences in the stability boundaries with respect to the gains* k_p *and* k_d*. Interestingly, despite the relatively large delay used to approximate the derivative term, certain regions of the stable domain* expand *when the delay-difference approximation is employed. Conversely, other regions shrink, indicating that the delay parameter significantly influences the controller's stability.*

This observation highlights the importance of incorporating the delay parameter into the control design process to ensure a robust and reliable controller implementation.

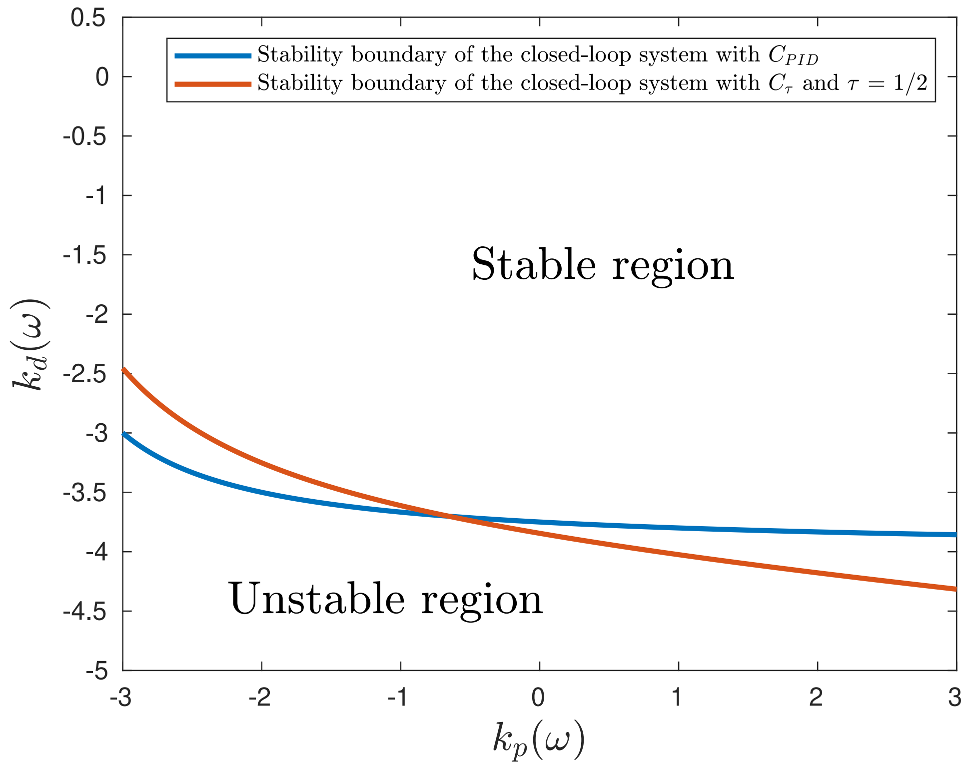

Figure 2.12: Stability boundary of the closed-loop system with the two different implementations of the PID controller.

2.6.3 Optimization of the spectral abscissa

We have already examined the effect of the approximation on the stability boundaries of the closed-loop system. The next question is: *For a given PID controller with specified gains* (k_p, k_i, k_d)*, , can the approximation improve the decay rate of the closed-loop system?* In this context, the decay rate of a stable solution in a linear system is determined by the rightmost characteristic root. Thus, the question can be rephrased as follows: *Is there a value of the delay parameter* τ *such that the rightmost root of the characteristic function* $\Delta_\tau(s; \vec{k}_\tau)$ *is located to the left* *of the rightmost root of* $\Delta_{PID}(s;\vec{k})$*?* While this scenario might seem counterintuitive, under certain conditions, it can indeed occur. Before analyzing this phenomenon, the following result provides a methodology for optimizing the decay rate in the delay-free implementation of the PID controller.

Proposition 2.6.2: Maximum exponential decay rate in the delay-free case

Consider the system described by the transfer function (2.47) in closed-loop with the controller (2.50), and assume that the integral gain $k_i^* \in \mathbb{R}$ is fixed. Let $-\sigma$ be the real part of the rightmost root of the closed-loop characteristic function. Then, the maximum value of σ that can be achieved with a stabilizing pair (k_p^*, k_d^*) is given by the maximum positive value such that the following system of inequalities has a real solution:

$$-3\sigma + a + ck_d > 0, \tag{2.58a}$$

$$\frac{8\sigma^3 - 8\sigma^2(a+ck_d) + 2\sigma\left((b+ck_p)+(a+ck_d)^2\right) - ab + ack_p + bck_d + c^2k_dk_p - ck_i}{3\sigma - (a+ck_d)} > 0, \tag{2.58b}$$

$$-\sigma^3 + \sigma^2(a+ck_d) - \sigma\,(b+ck_p) + ck_i > 0. \tag{2.58c}$$

Moreover, for $\sigma = \sigma^*$, where σ^* is the maximum value of σ such that the inequalities hold, the pair (k_p^*, k_d^*) is given by:

$$k_p^* = \frac{-b\sigma^* + ck_i + 2(\sigma^*)^3}{c\sigma^*}, \quad k_d^* = \frac{3\sigma^* - a}{c}. \tag{2.59}$$

Proof. The proof follows directly by applying the change of variable $s \to s-\sigma$ and analyzing the resulting characteristic equation $\Delta_{PID}(s-\sigma;\vec{k}) = 0$. Using the Routh-Hurwitz criterion, we determine the conditions under which the roots of this shifted equation remain in the left half of the complex plane and, in particular, the maximum shift such that there exist some pairs fulfilling the conditions. □

Proposition 2.6.2 follows a very simple mechanism, which consists of shifting the imaginary axis to the left and finding the maximum possible shift such that a stabilizing controller, with respect to the shifted axis, exists.

As mentioned, the interest is to improve the closed-loop system response, in the sense of *pushing* its spectral abscissa towards the left with the delay-difference approximation. The idea is, thus, the same as the one presented above for the delay-free case. The following result gives a sufficient condition such that the controller C_τ allows achieving a better decay rate than the controller C_{PID} under the assumption that both controllers have the same control gains.

Proposition 2.6.3: Necessary condition for the local minimum of the spectral abscissa

Consider the system described by the transfer function (2.47) in closed-loop with the delay-difference controller $C_\tau(s)$ given by (2.50). Assume that the following conditions hold:

(i)

$$\Re\left\{\frac{ck_d s\left(s\tau - e^{s\tau} + 1\right)}{\tau e^{s\tau}\beta + ck_d\tau(s\tau - 1)}\right\} = 0, \tag{2.60}$$

where $\beta = (\tau(s(2a + 3s) + b + ck_p) + ck_d)$.

(ii)

$$\Re\left\{\left.\frac{d^2 s}{d\tau^2}\right|_{s=s^*}\right\} > 0, \tag{2.61}$$

where s^* corresponds to a solution of (2.60).

Then, $\sigma = \Re\left(s^*\right)$ corresponds to a local minimum of the spectral abscissa.

Proof. Let $s(\tau)$ be implicitly defined by $\Delta_\tau(s; \vec{k}_\tau)$. We can easily compute the derivative $ds/d\tau$ using the implicit function theorem, leading to the expression on the left-hand side of equation (2.60). To identify critical points, we note that $ds/d\tau = 0$, which is a condition (i). To determine whether a critical point is a local minimum, we examine condition (ii). This ends the proof. □

We illustrate this result in Figure 2.13.

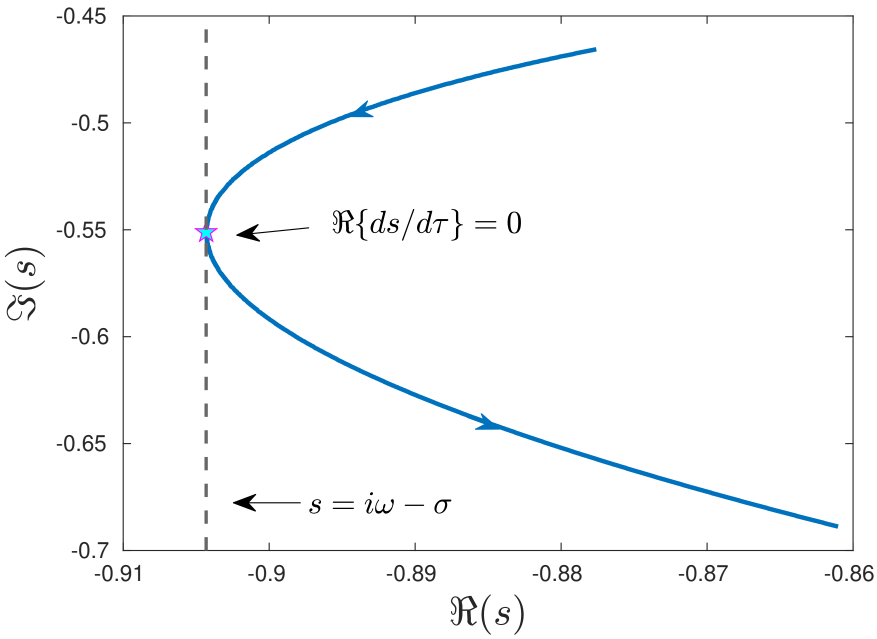

Figure 2.13: Local minima of the spectral abscissa.

2.6.4 Delay margin of the approximation on the PID controller

As with the case of a PD controller, it is important to determine how large the delay in the approximation can be before the stability of the closed-loop system with the PID controller is compromised. The following result provides a method to compute this stability margin.

Proposition 2.6.4: Delay Margin of the Closed-Loop System

Consider the dynamical system described by the transfer function (2.47). If the system is stable in closed-loop with $C_{PID}(s)$ for a triplet $(k_p, k_i, k_d) \in \mathbb{R}^3$ where $C_{PID}(s)$ is given by (2.50) then, it will remain stable if we replace $C_{PID}(s)$ by $C_\tau(s)$ given by (2.51) if $\tau \in (0, \widehat{\tau})$, where $\widehat{\tau}$ is given by

$$\widehat{\tau}(\omega) = \frac{2ck_d\omega^2\left(\omega^2 - b - ck_p\right)}{\omega^6 + \alpha_4\omega^4 + \alpha_2\omega^2 + c^2k_i^2}, \tag{2.62}$$

where $\alpha_4 := a^2 - 2(b + ck_p)$, $\alpha_2 := (b + ck_p)^2 - 2ack_i$, and the frequency ω is the smallest value satisfying

$$\tan^{-1}\left(\frac{b\tau\omega + ck_d\omega + ck_p\tau\omega - \tau\omega^3}{ck_i\tau - a\tau\omega^2}\right) + \tau\omega = \mathrm{Arg}\{-\boldsymbol{i}\omega ck_d\}. \tag{2.63}$$

Proof. From $\Delta_\tau(\boldsymbol{i}\omega; \vec{k}_\tau) = 0$ it follows that

$$e^{-\tau\boldsymbol{i}\omega} = -\boldsymbol{i}\frac{\tau}{ck_d\omega}\left((\boldsymbol{i}\omega)^3 + a(\boldsymbol{i}\omega)^2 + \left(b + k_pc + \frac{k_d}{\tau}c\right)\boldsymbol{i}\omega + ck_i\right).$$

Taking the Euclidean norm and the argument on both sides yields (2.62) and (2.63). This ends the proof. □

2.7 Applications

This section presents two application examples where the controller is implemented using the delay-difference approximation studied in this Chapter.

2.7.1 Study case: Angular positioning

The aim is to experimentally verify the delay margin of controllers $C_1(s)$ and $C_2(s)$ when controlling the angular position of a servo motor (see Figure 2.14) with transfer function representation given by:

$$H_{yu}(s) = \frac{\Theta(s)}{V(s)} = \frac{k}{s(Ts+1)}, \tag{2.64}$$

where the output we aim to control is the angular position of the motor $\Theta(s)[rad]$, and the input $V(s)[V]$. From Proposition 2.3.1, we can easily determine that the system is properly-posed, as it has a relative degree greater

Figure 2.14: QUBE servo 2. Figure retrieved from https://www.quanser.com/products/qube-servo-2/

than one. Therefore, we can consider the system in closed-loop with a PD controller, and we obtain the following characteristic function:

$$\Delta_i(s;\tau) = s(Ts+1) + kC_i(s), \quad i \in \{1,2\}, \tag{2.65}$$

where the plant parameters are given by $k = 23.65$ and $T = 0.345$ (such values were obtained via an identification process). Thanks to the presence of the pole at the origin, the system is naturally expected to present zero steady-state error when following a constant reference. This makes the choice of a PD controller intuitive. In particular, by taking $(k_p, k_d) = (1,1)$ we place the closed-loop characteristic roots at $s = \{-70.4, -0.97\}$. As both characteristic roots are over the real axis, the closed-loop system is expected to present no oscillations.

In Table 2.4, we summarize the corresponding delay margin of each approximation, as well as the frequency at which the crossing occurs. Note that these can be computed using Propositions 2.4.1 and 2.4.3.

Table 2.4: **Delay margin of the system** (2.64) **in closed-loop with both approximations.**

Controller	Delay margin τ_{max}	Crossing frequency ω^*
$C_1(s)$	$\tau_{max} = 0.076$	$\omega^* = 43.13$
$C_2(s)$	$\tau_{max} = 0.037$	$\omega^* = 86.17$

Next, we aim to validate these computations numerically and experimentally further. To this end, Figures 2.15 and 2.16 illustrate the temporal behavior of the system in closed-loop when a unit step input is applied as the reference. The following observations are particularly noteworthy:

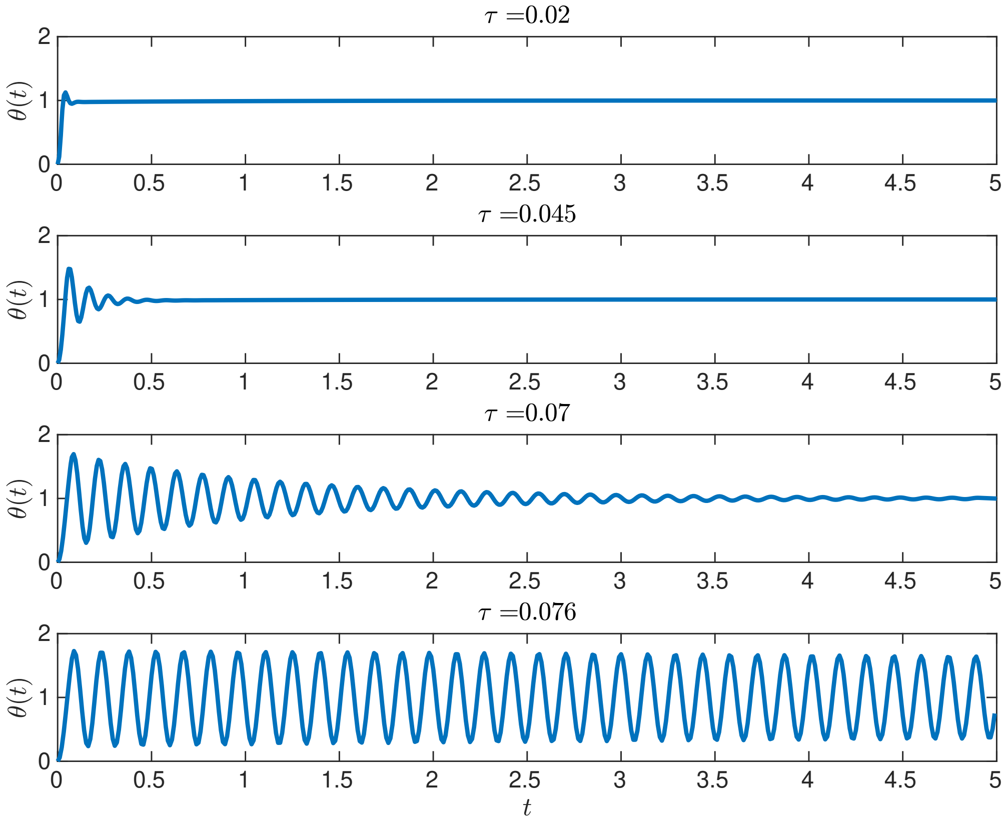

Figure 2.15: Numerical simulation of the QUBE servo 2 system in closed-loop with a PD controller with a single delay approximation of the derivative action.

1. For the corresponding delay margin in each case, setting $\tau = \tau_{max}$ results in an oscillatory response, as anticipated. This indicated that the computed delay margin is theoretically precise.

2. For smaller delay values, the system exhibits fewer oscillations. Notably, when the two-delay approximation is used with $\tau = 0.01$, the system shows no oscillations, consistent with the expected behavior derived from the location of the delay-free closed-loop characteristic roots.

3. The two-delay approximation has a delay margin of nearly half the delay margin observed with the single-delay approximation. This suggests that, while the single-delay approximation may be less accurate, it might be beneficial or even necessary in certain applications to consider a single-delay approximation.

The next question to address is whether the computed delay margin accurately characterizes the behavior of the physical plant. It is well understood that mathematical models inherently involve uncertainties and, at best, provide an approximation of the actual plant's behavior. In Figure 2.17, we present the system's output when a step reference of $\pi/4$ is applied as input.

There are two observations that are worth highlighting:

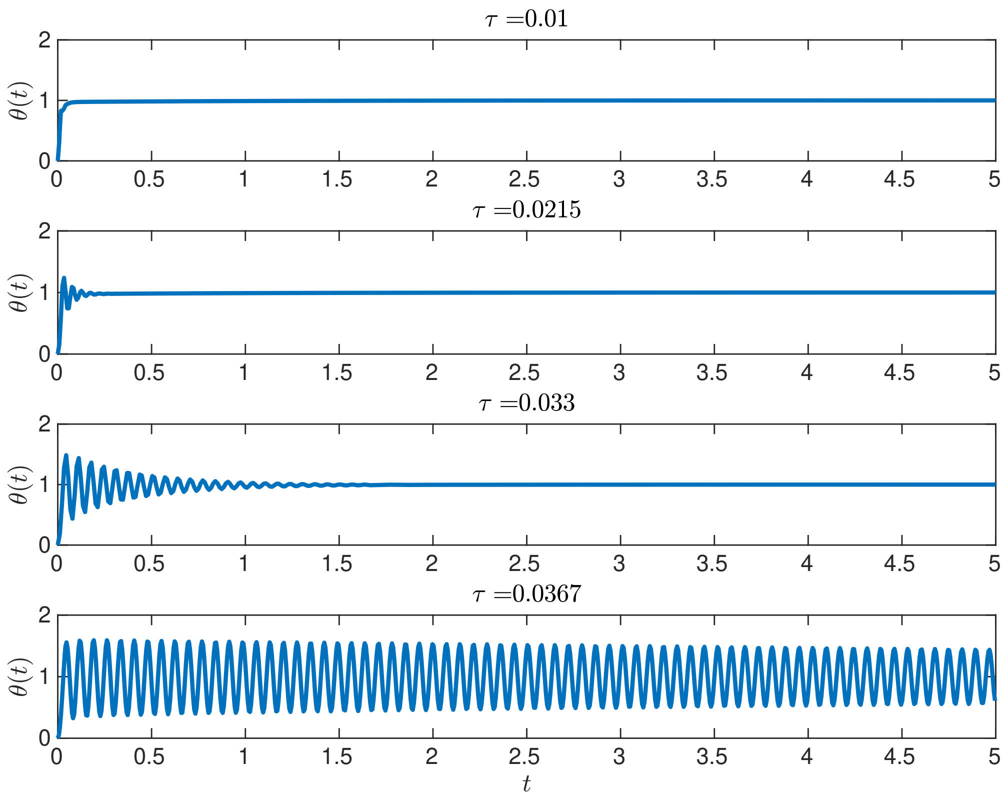

Figure 2.16: Numerical simulation of the QUBE servo 2 system in closed-loop with a PD controller with a double delay approximation of the derivative action.

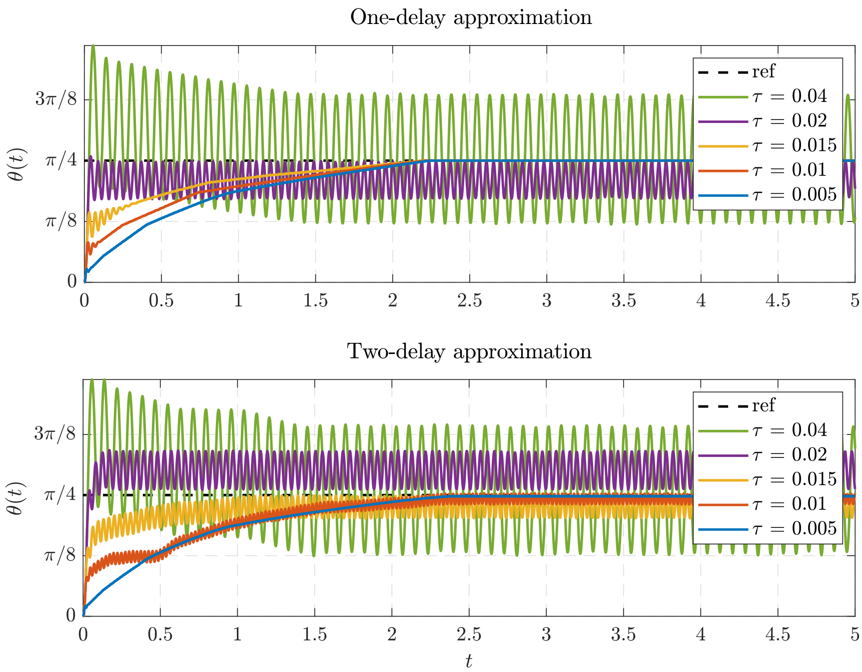

Figure 2.17: Control of the angular position of the QUBE servo 2 with a PD controller with approximations considering one and two delays, respectively.

1. The delay margin in both cases appears to be approximately $\tau = 0.04$, aligning with expectations for the two-delay approximation. However, this result does not hold for the one-delay approximation. Such discrepancies may arise due to uncertainties and simplifications in the mathematical model.

2. The system's actual response is slower than predicted by simulations. This discrepancy likely stems from the physical limitations of the motor. For instance, the model does not account for the motor's maximum achievable speed or the potential effects of friction. Moreover, the control output in the hardware is subject to saturation at $10V$, a constraint that was not considered in the simulation.

2.7.2 Study case: Chain of integrators

Consider a system that can be described by the following differential equation:

$$y^{(n)}(t) = u(t), \tag{2.66}$$

which correspond to a chain of n integrators. It is easy to note that such kind of systems can be easily stabilized using a control law of the following form:

$$u(t) = -\sum_{i=0}^{n-1} k_i y^{(i)}(t). \tag{2.67}$$

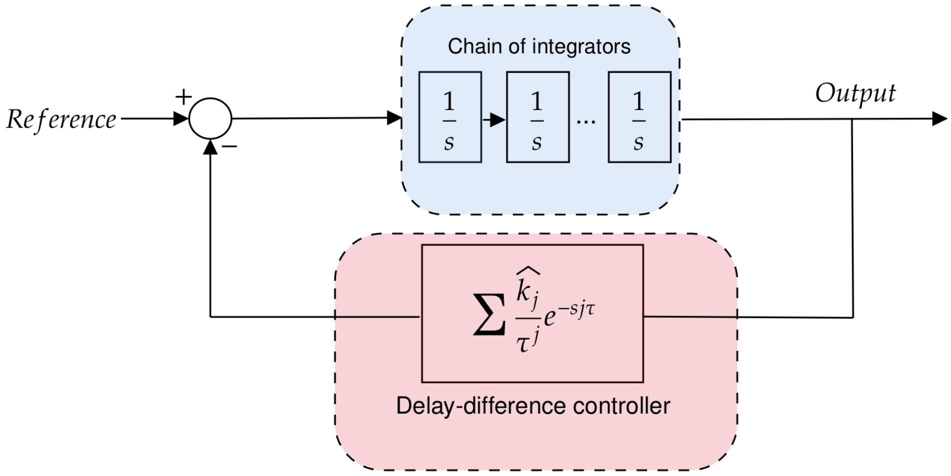

Figure 2.18: Transfer function representation of the closed-loop (2.66)-(2.69)

Under this approach, the closed-loop characteristic function $F : \mathbb{C} \to \mathbb{C}$ reads:

$$F(s) = s^n + \sum_{j=0}^{n-1} k_j s^j, \tag{2.68}$$

and one can place the n characteristic roots of the closed-loop system in any arbitrary location in the complex plane by choosing the appropriate gains k_j.

The main objective is to study the limitations of replacing each derivative term in the controller $u(t)$ by its corresponding delay difference approximation. In this case, we will only consider the approximation with one delay, such that we can replace the controller $u(t)$ with the following delay-based version of the controller:

$$u_\tau(t) = -\sum_{j=0}^{n-1} \sum_{m=0}^{j} (-1)^m \frac{k_j}{\tau^j} \binom{j}{m} y(t - m\tau). \tag{2.69}$$

After replacing the $n-1$ derivatives by the corresponding approximation, the closed-loop characteristic function $F_n : \mathbb{C} \to \mathbb{C}$ is given by:

$$F_n(s) = s^n + \sum_{j=0}^{n-1} \sum_{m=0}^{j} (-1)^m \frac{k_j}{\tau^j} \binom{j}{m} e^{-m\tau s}. \tag{2.70}$$

We aim to identify the interval $\mathcal{I} := (0, \tau_r)$ within which stability is preserved when the controller $u(t)$ is replaced by $u_\tau(t)$ for $\tau \in \mathcal{I}$. The proposed methodology builds on the direct method introduced by Walton and Marshall in 1987 (see also the introductory Chapter), with modifications to address delay-dependent coefficients. The closed-loop representation of system (2.66) with (2.69) can be expressed in transfer function form, as shown in Figure 2.18. It is important to note that, for $n \geq 2$, the system's relative degree exceeds one, thereby avoiding improperly-posed scenarios. When $n = 1$, the controller reduces to a proportional gain, ensuring no improperly-posedness issues arise in this case either.

To simplify the analysis, we introduce the change of variable $\tau = \frac{1}{p}$, and rewrite F_n as follows:

$$F_n(s) = P_0(s;p) + \sum_{j=1}^{n-1} P_j(p)e^{-js/p}. \tag{2.71}$$

With this structure, regardless of the value of n,the polynomials P_j for $j = \{1, 2, \dots, n-1\}$ depend only on the parameter p. Moreover, each polynomial, including P_0, always has degree $n-1$ in p. Next, as previously mentioned, we apply the direct method for stability. By noting that $F(\boldsymbol{i}\omega) = 0$ implies $F(-\boldsymbol{i}\omega) = 0$, we derive the following equation:

$$P_0(\boldsymbol{i}\omega;p)F_n(-\boldsymbol{i}\omega) - e^{\boldsymbol{i}\omega(n-1)/p}P_{n-1}(p)F_n(\boldsymbol{i}\omega) = 0, \tag{2.72}$$

which, as in the direct method, eliminates all terms involving $e^{\pm\boldsymbol{i}\omega(n-1)/p}$. After this manipulation, we can express:

$$F_{n-1}(\omega) = \widehat{P}_{0,1}(\omega;p) + \sum_{j=1}^{n-2} \widehat{P}_{j,1}(\omega;p)e^{\boldsymbol{i}j\omega/p}, \tag{2.73}$$

where $\widehat{P}_{j,k}$ epresents the polynomial obtained after the k-th iteration. This polynomial includes a term $P^2_{n-k}(p)$, resulting from the product of complex conjugates.

By iterating this process, similar to the direct method, the exponential terms are gradually eliminated. Eventually, we obtain a polynomial solely in (ω^2, p). The resulting polynomial has the following properties:

1. It contains only real coefficients.
2. It is of degree $n-1$ in p.
3. It is of degree n in ω^2.

With these ideas established, we present the following results:

Proposition 2.7.1: Stability crossings of the closed-loop system

Consider the characteristic function $F_n(s)$ given by (2.70) with $n \in \mathbb{N}^*$. Then, the pairs $(\tau, \omega) \in \mathbb{R}^2_+$ for which there exists a root of the form $s = \boldsymbol{i}\omega$ of $F_n(s)$, correspond to pairs for which the following holds:

$$\widehat{P}_{0,n-1}(\omega, p) + \widehat{P}_{1,n-1}(\omega, p) = 0, \tag{2.74}$$

$$\cos(\omega p(\omega)) = -\Re\left\{\frac{\widehat{P}_{0,n-2}(\omega; p(\omega))}{\widehat{P}_{1,n-2}(\omega; p(\omega))}\right\}, \tag{2.75}$$

$$\sin(\omega p(\omega)) = \Im\left\{\frac{\widehat{P}_{0,n-2}(\omega; p(\omega))}{\widehat{P}_{1,n-2}(\omega; p(\omega))}\right\}, \tag{2.76}$$

where $p(\omega)$ is the solution of (2.74) in p, and $\tau(\omega) = 1/p(\omega)$.

Proof. First, the need for Eq. (2.74) comes directly from the reduction process employed. Next, Eq. (2.75) and (2.76) can be obtained by noting that in the second to last iterations, one always obtains an equation of the form $P_0 + e^{-\boldsymbol{i}\omega p(\omega)} P_1 = 0$ and separating it on its real an imaginary part. □

Note that Proposition 2.7.1 characterizes the values of the delay parameter τ for which a root is located over the imaginary axis, but without giving any information on the interval $\mathcal{I}$. The following Corollary characterizes the given interval:

Corollary 2.7.1

Consider the characteristic function $F_n(s)$ given by (2.70) with $n \in \mathbb{N}^*$. Assume that $\tau \in (0, \tau_r)$, where τ_r corresponds to the smallest positive value of τ such that there exist $\omega \in \mathbb{R}_+$ for which the following holds:

$$\widehat{P}_{0,n-1}(\omega, p) + \widehat{P}_{1,n-1}(\omega, p) = 0,$$

$$\cos(\omega p(\omega)) = -\Re\left\{\frac{\widehat{P}_{0,n-2}(\omega; p(\omega))}{\widehat{P}_{1,n-2}(\omega; p(\omega))}\right\},$$

$$\sin(\omega p(\omega)) = \Im\left\{\frac{\widehat{P}_{0,n-2}(\omega; p(\omega))}{\widehat{P}_{1,n-2}(\omega; p(\omega))}\right\},$$

where $\tau = 1/p(\omega)$. Then, all the characteristic roots of $F_n(s)$ will be located at $\mathbb{C}_-$ for any $\tau \in (0, \tau_r) =: \mathcal{I}$.

Proof. By continuity arguments, it is clear that stability is preserved for any $\tau < \tau_r$. □

Remark 7. *It is important to note that Corollary 2.7.1 simply characterizes one interval of stability. However, as presented in the examples section, other stability intervals may exist.*

2.7.2.1 Numerical Example

Example 25. *Let us consider the simplest case for this first example, namely, a double integrator. Using the gains $k_1 = 10$ and $k_2 = 7$, the computed stability interval is $\mathcal{I} = (0, 0.5153)$, meaning the system remains stable for any $0 < \tau < 0.5153$. The question arises whether this interval is unique, i.e., whether any $\tau \notin \mathcal{I}$ necessarily leads to instability.*

Indeed, as shown in Figure 2.19, at $\tau = \tau_r = 0.5153$, the system loses stability. However, at $\tau = 2$, a characteristic root crosses from right to left, leading to a stable system over the interval $(2, 2.36)$.

This behavior can be further confirmed by examining the system's time-domain response to a unit step input, as illustrated in Figure 2.20. Specifically:

- *For $\tau < \tau_r$, the system stabilizes as expected.*
- *At $\tau = 1$, the system becomes unstable.*

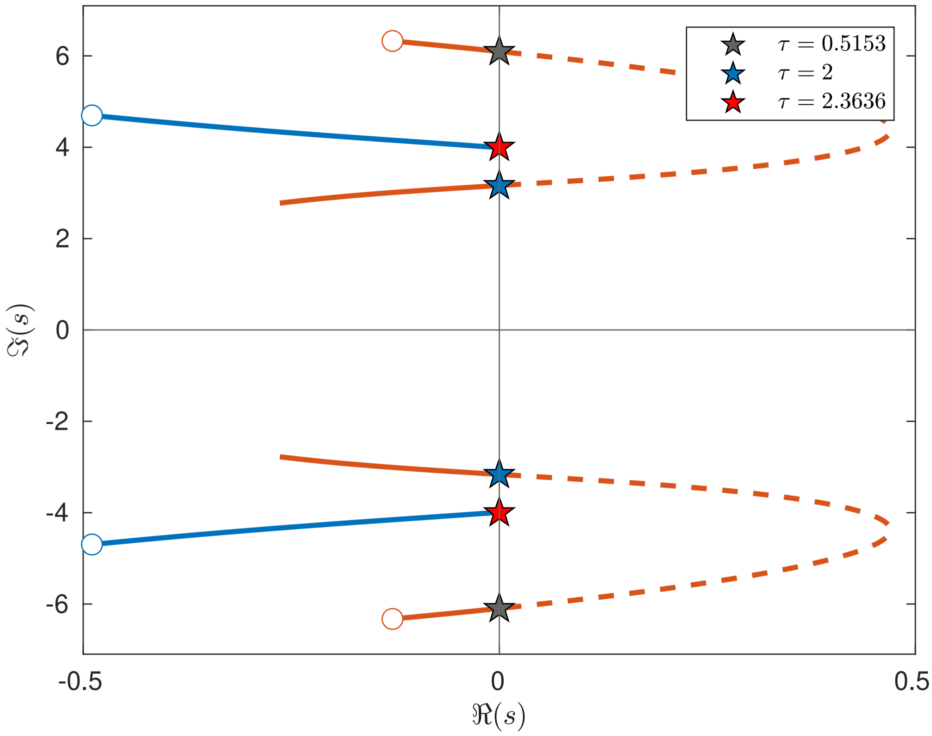

Figure 2.19: Evolution of the characteristic roots of $F_2(s)$ as $\tau \in (0, 2.36)$ increases.

- *For $\tau = 2.1$, within the second stability interval, the system stabilizes again, but with a slower response.*
- *Finally, for $\tau = 3 > 2.36$, the system destabilizes once more.*

While the system response within the second stability interval is notably slower compared to $\tau \in \mathcal{I}$, one advantage of this phenomenon is that the control gains become less critical as $1/\tau$ decreases.

2.8 Chapter summary and publications

This chapter characterizes the improperly-posedness of delay-difference approximations of the derivative action using one and two delays. Necessary and sufficient conditions for the properly-posedness of the closed-loop system are established, and a methodology to determine the delay margin in properly-posed cases is proposed. Numerical examples are provided to demonstrate the efficiency of the proposed methodology. Furthermore, the concept of utilizing the delay in the approximation scheme as a control parameter is demonstrated. This approach highlights how selecting an appropriate delay parameter can effectively stabilize the system, even in situations where the classical PD controller may not.

Additionally, the chapter includes a discussion on the impact of these approximations on PID controllers in which the specific case of second-order LTI SISO systems is considered. Two application cases are explored: (1) the

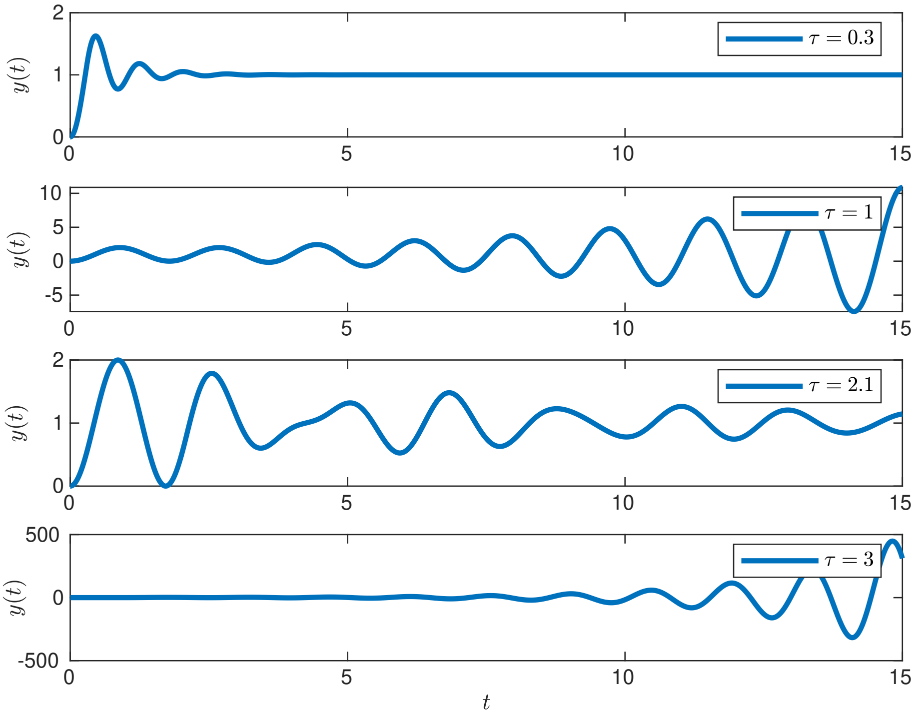

Figure 2.20: Time-domain response of the double integrator system for various values of τ.

stabilization of the angular positioning of a servo motor using approximations with one and two delays, where we specifically compare experimentally the performance as well as the delay-margin of the approximation, and (2) the analysis of the delay margin in the stabilization of a chain of integrators using a single-delay approximation.

The results presented in this chapter have led to the following publications:

- In Torres-García et al. (2022) (**Torres-García, D.**, Méndez-Barrios, F., Niculescu, S.-I., Martínez-González, A. (2022, November). Delay-difference approximation of pd-controllers. insights into improperly-posed closed-loop systems. In IFAC Workshop on Control of Complex Systems 2022, IFAC-PapersOnLine 55(40), 79–85.), we characterized the improperly-posed nature of the two- and three-point approximation schemes.

- In Torres-García[1] et al. (2024) (**Torres-García, D.**, Hernández-Gallardo J.-A., Méndez-Barrios, F., Niculescu, S.-I. (2024, March) Exploring Delay-Based Controllers. A Comparative Study for Stabilizing Angular Positioning. In: Cardona, M.N., Baca, J., Garcia, C., Carrera, I.G., Martinez, C. (eds) Advances in Automation and Robotics Research. LACAR 2023. Lecture Notes in Networks and Systems. (pp. 123-136).), we explored delay-based controllers, including PD controllers with both two- and three-point approximations, for controlling the angular position of a servo motor.

- In Torres-García et al. (2024) (**Torres-García, D.**, Méndez-Barrios, F., Niculescu, S.-I. (2024) Impact of Delay-Difference Approximation on PID Controllers: Stability and Performance Insights. 32nd Mediterranean

Conference on Control and Automation (MED), 616-621 IEEE.), we analyzed the impact of single-delay approximations on the stability and performance of PID controllers in closed-loop with a second-order scalar system.

- In Torres-García et al. (2024) (**Torres-García, D.**, Méndez-Barrios, C. F., and Niculescu, S. I. (2024, September). Insights into the Stabilization of a Chain of Integrators via Delay-Difference Approximations. In IFAC Workshop on Time Delay Systems 2024, IFAC-PapersOnLine, 58(27), 19-24.), we investigated the stabilization of a chain of integrators using delay-difference approximations of derivative actions.

Chapter 3

General case of the derivative action implementation via delay-difference operators

The kind of knowledge which is supported only by observations and is not yet proved must be carefully distinguished from the truth.

Leonhard Euler

Contents

3.1 Introduction

As seen in the previous chapter, one of the main tools used when implementing derivative actions is the finite difference method. Such a methodology can be extended to approximate the derivative using any number of *points* $\ell \in \mathbb{N}$. The interest in generalizing such an approximation comes from the fact that, depending on the application, one may require a more precise approximation. In this sense, there are two ways to achieve a better approximation. One is to take a *smaller* value of τ. The other option is to increase the number of points (or, equivalently, delays) used on the approximation scheme. However, it is unclear whether or not the properly-posedness conditions found for the case of one and two delays can be extended to a more general case.

3.2 General case of the delay difference approximation of PD-controllers

3.2.1 Problem formulation

Similarly to the previous chapter, we consider the class of LTI SISO systems described by:

$$\Sigma : \begin{cases} \dot{x}(t) = \boldsymbol{A}x(t) + \boldsymbol{B}u(t), \\ y(t) = \boldsymbol{C}x(t), \end{cases} \tag{3.1}$$

whose transfer function representation is given by:

$$H_{yu}(s) := \frac{P(s)}{Q(s)} \equiv \boldsymbol{C}(s\boldsymbol{I} - \boldsymbol{A})^{-1}\boldsymbol{B}, \tag{3.2}$$

where $Q(s)$ and $P(s)$ are polynomials in s of the form:

$$Q(s) := s^n + \sum_{j=0}^{n-1} q_j s^j, \quad P(s) := \sum_{j=0}^{m} p_j s^j, \quad q_j, p_j \in \mathbb{R}, \tag{3.3}$$

with $n := \deg(Q) > m := \deg(P)$.

We continue to consider PD controllers with the Laplace domain representation:

$$C_0(s) = k_p + k_d s. \tag{3.4}$$

However, unlike in the previous chapter, we generalize the derivative approximation by using ℓ past values of the output signal $y(t)$. Specifically, the derivative is approximated as:

$$\dot{y}(t) \approx \sum_{k=0}^{\ell} y(t_k) L_k'(t), \tag{3.5}$$

where $\ell \in \mathbb{N}$ represents the number of delays used, making it an $(\ell+1)$-point approximation. The delay $\tau \in \mathbb{R}_+$ is assumed strictly positive, with $t_k = t - k\tau$. Here, L_k denotes the k-th Lagrange interpolation polynomial for $y(t_k)$, defined as:

$$L_k(t) = \prod_{j=0,\, j\neq k}^{\ell} \frac{t - t_j}{t_k - t_j},$$

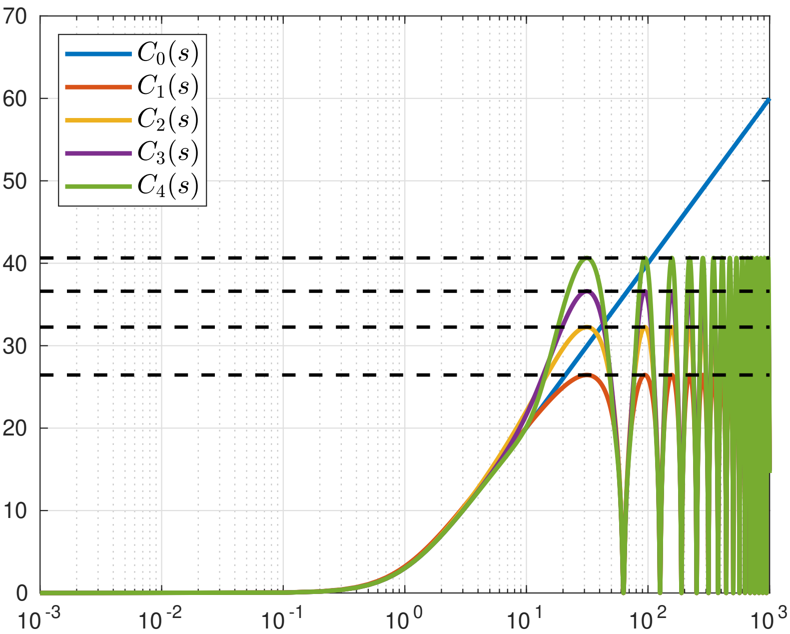

Figure 3.1: Change on the Bode diagram as we increase the number of delays on the approximation.

and its derivative is given by:

$$L'_k(t) = L_k(t) \sum_{j=0,\, j\neq k}^{\ell} \frac{1}{t - t_j}.$$

Applying the Laplace transform, the PD controller with this generalized approximation becomes:

$$C_\ell(s) := k_p + \frac{k_d}{\tau} \sum_{k=1}^{\ell} \frac{1}{k} (1 - e^{-\tau s})^k. \tag{3.6}$$

Using this controller, the characteristic function of the closed-loop system, $\Delta_\ell : \mathbb{C} \times \mathbb{R}_+ \to \mathbb{C}$, is expressed as:

$$\Delta_\ell(s;\tau) := Q(s) + \left(k_p + \frac{k_d}{\tau} \sum_{k=1}^{\ell} \frac{1}{k} (1 - e^{-\tau s})^k \right) P(s). \tag{3.7}$$

In the previous chapter, we highlighted two key advantages of using delay-difference approximations for implementing derivative actions: 1. Relying on past measurements of the output, instead of requiring direct measurements of its derivative, simplifies the controller implementation. 2. This approach attenuates the amplification of high-frequency noise.

However, the attenuation effect depends on the number of delays used. As shown in Figure 3.1, increasing the number of delays raises the upper limit of the magnitude, likely due to improved precision in the approximation. This observation underscores the importance of carefully selecting the type of approximation based on system requirements.

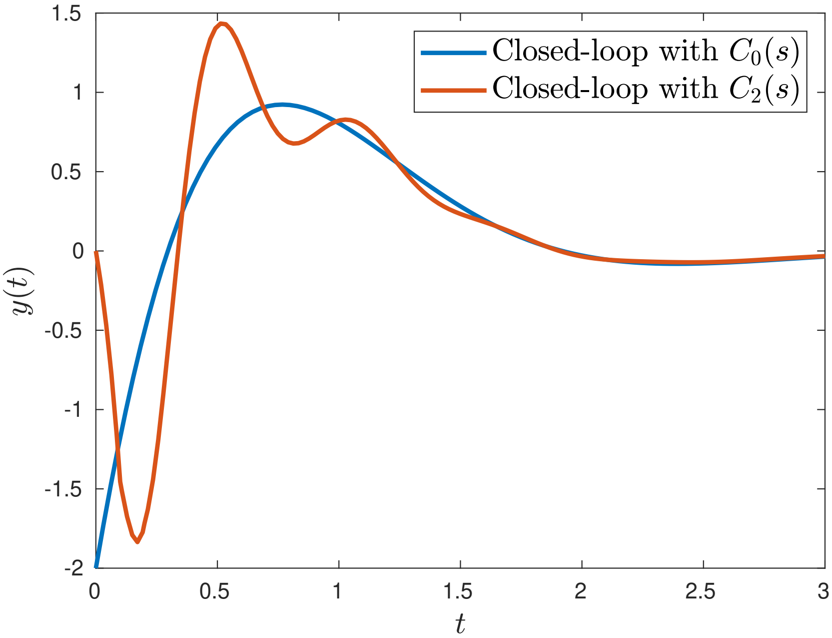

Figure 3.2: Step response of closed-loop system between $H_{yu}(s)$ and $C_0(s)$ and $C_2(s)$, respectively.

3.2.2 Motivating example

Intuitively, given that for the cases of one and two delays, the properly-posed intervals were the same, one might expect the same to happen in a more general scenario. This, however, is not the case. To illustrate such a problem, consider the following example:

Example 26. *Consider the system associated with the following transfer function:*

$$H_{yu}(s) = \frac{-s}{s^2 + 2}, \tag{3.8}$$

which can be stabilized by a PD controller. In particular, by choosing $(k_p, k_d) = (-1, 2/3)$ the closed-loop characteristic function has two roots, located at $s_{1,2} = -\frac{3}{2} \pm 1.9\boldsymbol{i}$. Let us next assume that we replace the PD-controller $C_0(s) = k_d s + k_p$ by:

$$C_2(s) = k_p + \frac{k_d}{2\tau}(3 - 4e^{-\tau s} + e^{-2\tau s}),$$

with $\tau = 0.1$. The system is properly-posed since $k_d p_{n-1} = -2/3 > -1$. However, after computing the right-most roots, one can verify that the closed-loop system between $H_{yu}(s)$ and $C_2(s)$ has the following characteristic roots: $\{-1.53 \pm 1.87\boldsymbol{i}, -2.98 \pm 10.42\boldsymbol{i}\}$. Naturally, we observe a pair of complex conjugate roots close to the delay-free ones. However, we can also observe that we now have an additional pair of complex conjugate roots at $s = -2.98 \pm 10.42\boldsymbol{i}$. We can observe the effect of such roots by observing the system response, depicted in Figure 3.2. One way to improve the approximation would be to consider a smaller value of τ. However, this is not always possible since the choice

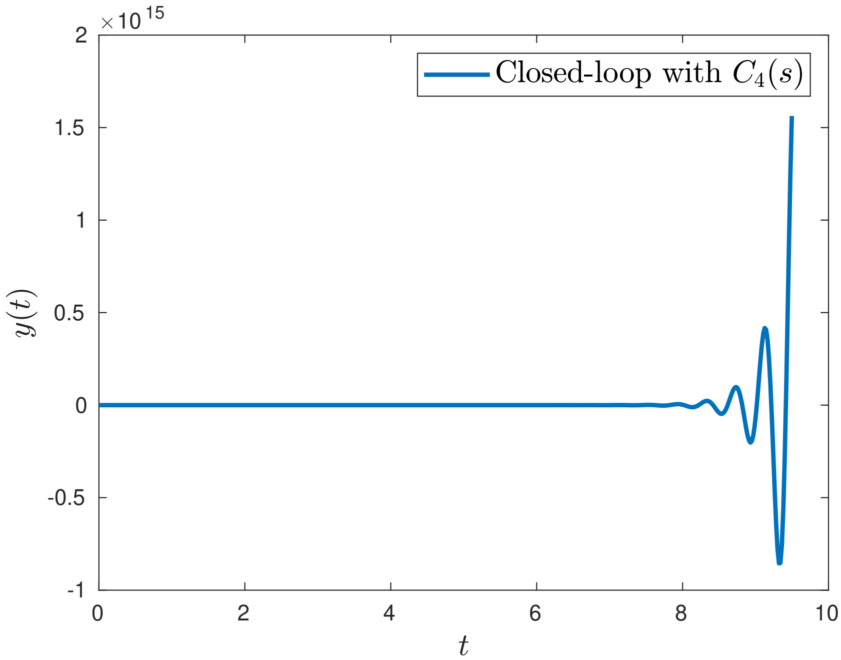

Figure 3.3: Step response of closed-loop system between $H_{yu}(s)$ and $C_4(s)$.

of delay may come from some hardware implementation constraints. In that spirit, we propose considering a better approximation, for example, one considering four delays. Under that approximation the controller $C_4(s)$ reads:

$$C_4(s) = k_p + \frac{k_d}{12\tau}(25 - 48e^{-\tau s} + 36e^{-2\tau s} - 16e^{-3\tau s} + 3e^{-4\tau s}).$$

Surprisingly, the inclusion of this approximation produces the following closed-loop characteristic roots: $\{-7.1 \pm 4.83\boldsymbol{i}, -1.501 \pm 1.93\boldsymbol{i}, 3.63 \pm 15.7\boldsymbol{i}\}$. *Under this new configuration, we have closed-loop characteristic roots closer to the delay-free ones. Nonetheless, now we also have a pair of complex conjugate roots on the right-half plane, which means the system is no longer stable. This means that, although the system in closed-loop with $C_2(s)$ is properly-posed, choosing $C_4(s)$ instead makes the system improperly posed. Figure 3.3 shows the system's behavior when a unit step is given as an input. This unexpected behavior motivates the results presented in the remaining part of this chapter.*

3.3 Improperly-posed case characterization

Although the approximation scheme considered in this chapter is more general, the concept of improperly-posedness remains consistent with that in Definition 2.3.1. Based on this definition, the problem of interest can be formulated as follows: identifying the structure of an unstable, unbounded solution of the characteristic function associated with an improperly-posed closed-loop system and determining the corresponding regions in the parameter space—comprising the gains, the delay, and the number of delays—where the closed-loop system exhibits improperly-posed behavior.

Similarly to the

Proposition 3.3.1: Root structure

Consider the system with transfer function (3.2) in closed-loop with the delay-based control scheme (3.6). Let $\ell \in \mathbb{N}$, and consider the closed-loop characteristic function Δ_ℓ given by (3.7). Then, when $\tau \to 0^+$ the quasipolynomial (3.7) has an unbounded root $s^* : \mathbb{R}_+ \to \mathbb{C}$ with the following structure:

$$s^*(\tau) = \frac{z^*}{\tau} + \varphi(\tau), \tag{3.9}$$

where $z^* \in \mathbb{C}^*$ and φ is a holomorphic function satisfying $\varphi(0) \neq 0$.

The proof can be found in Appendix A page 133.

Proposition 3.3.1 provides critical insights into the structure of specific solutions to the characteristic function. Building upon this framework, our next objective is to fully characterize these solutions by identifying z^* and determining its location in the complex plane. It is important to emphasize that the location of z^* (in $\mathbb{C}_+$ or $\mathbb{C}_-$) plays a decisive role in concluding whether the corresponding closed-loop system is improperly-posed or not.

3.3.1 Auxiliary quasipolynomial and its properties

To this point, we identified that there is a root $s^*(\tau)$ with singular behavior. However, as in Chapter 2 the aim is to determine the *location* of such a root in the complex plane for small values of τ. From the structure of $s^*(\tau)$ is it clear that the location of the root will depend on z^*. Therefore, we are interested in computing the constant z^*. From the Newton diagram method, we know that a root is close to z^*/τ, meaning that we can write $\Delta_\ell(z^*/\tau; \tau) \approx 0$. Next, we introduce the following auxiliary quasipolynomial $P_\ell^{aux} : \mathbb{C} \to \mathbb{C}$ defined as:

$$P_\ell^{aux}(w) = \lim_{\tau \to 0^+} \tau^n \Delta_\ell\left(w\tau^{-\beta}; \tau\right), \tag{3.10}$$

with $\beta = 1$ from the Newton polygon associated with Δ_ℓ.

Proposition 3.3.2: Obtention of the auxiliary quasipolynomial

The auxiliary quasipolynomial $P_\ell^{aux}(w)$ can be written as:

$$P_\ell^{aux}(w) := \begin{cases} w^n, & \text{if } m < n-1, \\ w^{n-1} f_\ell(w; k_d p_{n-1}), & \text{if } m = n-1, \end{cases} \tag{3.11}$$

where n and m denote the degrees of the denominator and numerator in (3.2), respectively, and p_{n-1} represents the leading coefficient of $P(s)$ in (3.2) when $m = n-1$. The parameter ℓ corresponds to the number of delays considered in the approximation and $f_\ell : \mathbb{C} \times \mathbb{R} \to \mathbb{C}$ is a complex analytic function defined as:

$$f_\ell(w; \alpha) := w + \alpha \sum_{k=1}^{\ell} \frac{(1 - e^{-w})^k}{k}. \tag{3.12}$$

Moreover, z^* is a non-trivial root of $P_\ell^{aux}(w)$.

The proof of 3.3.2 can be found on page 134.

Remark 8. *Note that $P_\ell^{aux}(w)$ always has n trivial roots, regardless of the specific values of n and m. Consequently, determining z^* reduces to identifying the non-trivial solutions of $f_\ell(w; \alpha) = 0$.*

Remark 9. *Similarly to what we found in Chapter 2, one sufficient condition for the properly-posedness of the closed-loop system is to have $m < n-1$, as it implies that $P_\ell^{aux}(w)$ do not have any non-trivial root.*

Remark 10. *Note that f_ℓ has an invariant root at the origin $w = 0$ for any ℓ and α.*

In the following, we aim to study the non-trivial roots of f_ℓ. For that, we have the following definitions

Definition 3.3.1: Frequency crossing set

Consider the function f_ℓ in (3.12) and a value $\alpha^* \in \mathbb{R}^*$. The *frequency crossing set* $\Omega_{\alpha^*} \subset \mathbb{R}_+^*$ is the set of all $\omega \in \mathbb{R}_+^*$ such that $f_\ell(\boldsymbol{i}\omega; \alpha^*) = 0$.

Definition 3.3.2: Critical pairs

We say that $\alpha \in \mathbb{R}^*$ is a *critical parameter* if there exists at least one real $\omega^* \in \Omega_{\alpha^*}$ satisfying $f_\ell(\boldsymbol{i}\omega^*; \alpha^*) = 0$. Similarly, a crossing frequency $\omega^* \in \Omega_{\alpha^*}$ is called a *critical value* if there exists $\alpha^* \in \mathbb{R}^*$ such that $f_\ell(\boldsymbol{i}\omega^*; \alpha^*) = 0$. Finally, the pair (α^*, ω^*) is called a critical pair.

From a parametric point of view, in Chapter 2 we concluded that the properly-posedness of the closed-loop system when $\ell = \{1, 2\}$ can be guaranteed if $\alpha > -1$. In that sense, our interest is to find similar conditions for a general case. With these ideas in mind, we have the following result:

Proposition 3.3.3: Properties of $f_\ell(w;\alpha)$

Let $\ell \in \mathbb{N}$, and consider the quasipolynomial $f_\ell(w;\alpha)$ given by (3.12). Then, the following properties hold:

(i) For a given $\alpha_0 \in \mathbb{R}^* \setminus \{-1\}$ the set $\mathcal{R}_\ell := \{r \in \mathbb{R}^* : f_\ell(r;\alpha_0) = 0\}$ has always $\operatorname{card}\{\mathcal{R}_\ell\} \le 2$.

(ii) For $\alpha_0 := -1$ the origin correspond to a root of multiplicity $\ell+1$ of $f_\ell(w)$.

(iii) There exists a sufficiently small value $0 < |\alpha| \ll 1$, such that all roots of $\widehat{f}_\ell(w;\alpha) := f_\ell(w;\alpha)/w$ lie in $\mathbb{C}_-$.

(iv) Let $\alpha = \alpha^* \in \mathbb{R}^* \backslash \{-1\}$ be a critical value. Then, the non-zero characteristic roots of the quasipolynomial f_ℓ located on the imaginary axis are simple.

For a detailed proof of 3.3.3, see page 135.

Proposition 3.3.3 highlights several key properties of f_ℓ, which will play a crucial role in determining whether the closed-loop system is properly or improperly posed. Notably, property (iii) establishes the existence of a properly-posed interval near the origin, although the precise boundaries of this interval remain to be determined.

Building on this discussion, we now introduce the sets $\mathcal{X}_\ell$ and $\mathcal{W}_\ell$ defined in the following way:

$$\mathcal{X}_\ell := \{\zeta^* \in [-1,1] : \varphi_\ell(\zeta^*) = 0\}, \tag{3.13}$$

and

$$\mathcal{W}_\ell := \left\{\omega \in \mathbb{R}^* : z = e^{i\omega} \text{ where } z \text{ satisfy } z^2 - 2\zeta^* z + 1 = 0, \text{ and } \zeta^* \in \mathcal{X}_\ell\right\}, \tag{3.14}$$

where φ_ℓ is a polynomial in ζ, with $\deg(\varphi_\ell) = \ell$ defined as:

$$\varphi_\ell(\zeta) := \sum_{k=1}^{\ell}\sum_{j=0}^{k} \frac{(-1)^j}{k}\binom{k}{j} T_j(\zeta), \tag{3.15}$$

where T_j corresponds to the $j-th$ Chebyshev polynomial of the first kind. Considering these definitions, the following result characterizes the critical pairs (α^*, ω^*).

Proposition 3.3.4: Critical pairs characterization

Let $\ell \in \mathbb{N}$, and consider the quasipolynomial $f_\ell(w;\alpha)$ given by (3.12). Then, $(\alpha^*, \omega^*) \in \mathbb{R}^* \times \mathbb{R}^*$ is a critical pair of $f_\ell(w;\alpha)$ if $\omega^* \in \mathcal{W}_\ell$ and α^* is given by:

$$\alpha^* := \frac{\omega^*}{\sin(\omega^*)\,\psi_\ell(\zeta^*)}, \tag{3.16}$$

where $\zeta^* \in \mathcal{X}_\ell$, and ψ_ℓ is a polynomial in ζ with $\deg(\psi) = \ell - 1$ defined by:

$$\psi_\ell(\zeta) := \sum_{k=1}^{\ell} \sum_{j=1}^{k} \frac{(-1)^j}{k} \binom{k}{j} U_{j-1}(\zeta),$$

where U_{j-1} is the $(j-1)-$th Chebyshev polynomial of the second kind.

The proof of Proposition 3.3.4 can be found on page 137.

Remark 11. *See the Introduction page 24 for more details on the Chebyshev polynomials of the first and second kind.*

Corollary 3.3.1

Let $\ell \in \mathbb{N}$, and consider the quasipolynomial $f_\ell(w;\alpha)$ given by (3.12). Then, all the roots of $f_\ell(w;\alpha)$ will lie in $\overline{\mathbb{C}}_-$ if $\alpha \in (\alpha_-, \alpha_+) \setminus \{0\}$, where α_- and α_+ are defined as

$$\alpha_+ := \min_{\zeta^* \in \mathcal{X}_\ell,\, \omega^* \in \mathcal{W}_\ell} \left\{ \alpha \in \mathbb{R}_+ : \alpha = \frac{\omega^*}{\sin(\omega^*)\,\psi_\ell(\zeta^*)} \right\} \text{ and } \alpha_- := \max_{\zeta^* \in \mathcal{X}_\ell,\, \omega^* \in \mathcal{W}_\ell} \left\{ \alpha \in \mathbb{R}_- : \alpha = \frac{\omega^*}{\sin(\omega^*)\,\psi_\ell(\zeta^*)} \right\}. \tag{3.17}$$

Proof. The proof follows straightforwardly from Proposition 3.3.3-(iii) and Proposition 3.3.4. ☐

3.3.2 Improperly-posedness detection

In the following, we identify two key properties that are fundamental to analyzing the properly-posedness of the closed-loop system:

1 Crossing directions of the critical roots: For a given critical pair (α^*, ω^*), this refers to determining the direction in which a root crosses the imaginary axis as $\alpha \in \mathbb{R}^*$ increases.

2 Stability index: For a given $\alpha \in \mathbb{R}^*$, this represents the number of roots of f_ℓ that lie in $\mathbb{C}_+$.

In this spirit, the use of the Implicit Function Theorem allows obtaining the following formula:

$$\operatorname{sign}\left(\Re\left[\frac{dw}{d\alpha}\right]^{-1}_{w=\boldsymbol{i}\omega^*,\alpha=\alpha^*}\right)=\operatorname{sign}\left(\Re\left[\frac{\alpha}{w(\alpha)}+\alpha^2\frac{e^{-w(\alpha)}}{w(\alpha)}\sum_{k=1}^{\ell}(1-e^{-w(\alpha)})^{k-1}\right]_{w=\boldsymbol{i}\omega^*,\alpha=\alpha^*}\right),$$

which indicates the sign of the derivative of w with respect to the parameter α, i.e., how is the root $w=\boldsymbol{i}\omega$ changing as α varies. With some simple computations, one can rewrite this equation in the following way:

$$\operatorname{sign}\left(\Re\left[\frac{dw}{d\alpha}\right]^{-1}_{w=\boldsymbol{i}\omega^*,\alpha=\alpha^*}\right)=\operatorname{sign}\left(-\Re\left[\sum_{k=1}^{\ell}\boldsymbol{i}^k 2^{k-1}e^{-\boldsymbol{i}\omega^*(k+1)/2}[\sin(\omega^*/2)]^{k-1}\right]\right). \tag{3.18}$$

It is worth noting that (3.18) no longer depend on the specific value of $\alpha=\alpha^*$, and instead rely only on the critical value ω and the number of delays ℓ. The following result allows for determining the direction in which a root crosses the imaginary axis:

Proposition 3.3.5: Crossing directions

Let $\ell\in\mathbb{N}$, and consider the auxiliary quasipolynomial $f_\ell(\cdot;\alpha)$ given by (3.12). Let $\alpha=\alpha^*\in\mathbb{R}^*\setminus\{-1\}$ be a critical parameter for the corresponding critical value ω^*. Then, for $\alpha>\alpha^*$ sufficiently close to α^*, the root $w\left(\alpha\right)$ will *cross* towards stability (from $\mathbb{C}_+$ to $\mathbb{C}_-$) if the following inequality holds:

$$\Re\left[\frac{dw}{d\alpha}\right]^{-1}_{w=\boldsymbol{i}\omega^*,\alpha=\alpha^*}<0.$$

The crossing will be towards instability (from $\mathbb{C}_-$ to $\mathbb{C}_+$) if the inequality is reversed.

Proof. From Proposition 3.3.3, property-(*iv*) any root of the form $w=\boldsymbol{i}\omega$ is simple. As a consequence, the Implicit Function Theorem (see Theorem 0.2.1 at page 14) is valid, and it is easy to observe that it suffices to examine in which direction the real part of the root is moving. □

Proposition 3.3.5 lets us identify the direction in which a root crosses the imaginary axis. Next, we need a methodology to *count* the number of roots on $\mathbb{C}_+$. To this end, let us introduce the following stability indicator function $\mathcal{I}:(-1,+\infty)^*\times\mathbb{R}^*\to\{0,\pm1\}$:

$$\mathcal{I}(\alpha^*):=\operatorname{sign}\left(\Re\left[\frac{dw}{d\alpha}\right]^{-1}_{w=\boldsymbol{i}\omega^*,\alpha=\alpha^*}\right). \tag{3.19}$$

The aim is to count the number of roots crossing from one side to the other. One advantage that we have is Property-(*iii*) in Proposition 3.3.3, since it indicated that for $|\alpha|$ sufficiently close to zero, the number of roots on $\mathbb{C}_+$ is zero. With these ideas in mind, we have the following result:

Proposition 3.3.6: Stability index computation

Let $\ell, N \in \mathbb{N}$, and consider the auxiliary quasipolynomial $f_\ell(\cdot;\alpha)$ given by (3.12). For a given $(\alpha^*, \ell) \in (-1,+\infty)^* \times \mathbb{N}$, let α_h, $h \in \{1,\ldots,N\}$ be the solutions of Proposition 3.3.4, such that the following order relations hold:

$$-1 < \alpha_1 < \alpha_2 < \ldots < \alpha_{N-1} < \alpha^* \leq \alpha_N.$$

Then, the number of roots located in $\mathbb{C}_+$ is given by:

$$n^{(\ell,\alpha_0)} = (1+\operatorname{sign}(\alpha^*)) \sum_{i=j+1}^{N-1} \mathcal{I}(\alpha_i) - (1-\operatorname{sign}(\alpha^*)) \sum_{i=N}^{j} \mathcal{I}(\alpha_i), \tag{3.20}$$

where $j \in \mathbb{N}$ is chosen by considering that it satisfies $\alpha_j = \alpha_-$, with α_- given by Corollary 3.3.1.

Proof. From Proposition 3.3.3, Property-(iii), we know that, regardless of the number of delays, there exists an interval $\alpha \in (\alpha_-, \alpha_+)^*$ such that f_ℓ/w is stable. In other words, f_ℓ has no roots in $\mathbb{C}_-$. By continuity with respect to α, roots can only transition from the left-half plane to the right-half plane by crossing the imaginary axis.

Furthermore, from Proposition 3.3.3, Property-(iv), any root on the imaginary axis is simple, meaning each crossing corresponds to a pair of complex-conjugate roots. Additionally, the same result implies that real crossings can only occur at $\alpha^* \in \{0,-1\}$. Since $\alpha^* > -1$, these observations collectively conclude the proof. □

With the notations and results above, we now state the main results in terms of the improperly-posedness characterization:

Theorem 3.3.1: Improperly-posedness characterization

Given a system Σ with corresponding transfer function H_{yu} given by (3.2) subjected to a PD controller with the derivative action approximated via a delay-difference approximation and frequency-domain representation (3.6), the following properties hold:

(i) If the relative degree is greater than one ($n > m+1$), then the closed-loop system is always properly-posed independently of the number of delays in the delay-difference approximation scheme.

(ii) If the relative degree of the system equals one ($n \equiv m+1$), then there exists an open interval $(\gamma_1, \gamma_2) =: I_\ell \subset \mathbb{R}$, such that the closed-loop system is properly-posed if the gain "k_d" satisfies the condition $\gamma_1 < k_d p_{n-1} < \gamma_2$, where p_{n-1} corresponds to the leading coefficient of P. Furthermore, as the number of delays ℓ increases, the diameter of the interval I_ℓ decreases.

The proof can be found in Appendix A page 138. Additionally, see Appendix B page 151 for a Python function

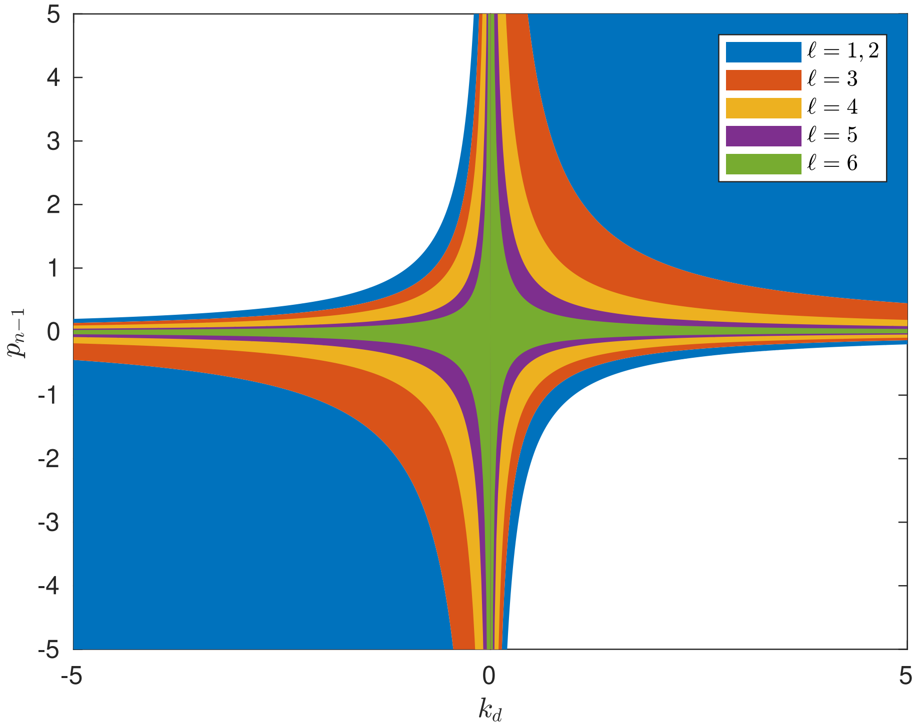

Figure 3.4: Change on the improperly-posed region as function of k_d and p_{n-1} for different values of ℓ.

that allows detecting the corresponding crossings of f_ℓ as well as the direction of the crossing, for a given ℓ[1]. In Figure 3.4, the evolution of the properly-posed intervals is illustrated as a function of the control gain k_d and the parameter p_{n-1}. The figure demonstrates how the region shrinks as the number of delays incorporated into the approximation increases. Furthermore, Table 3.1 provides the corresponding f_ℓ for each approximation, for $\ell \in \{1, 2, \dots, 6\}$. While the rate at which the diameter of the interval I_ℓ decreases is not explicitly characterized, it can be observed that the constraints on k_d become significantly more restrictive as ℓ increases, given that p_{n-1} is a fixed system parameter.

Table 3.1: **Properly-posed interval for different values of ℓ.**

ℓ	I_ℓ	$f_\ell(w;\alpha)$	Color in Figure 3.4
1	$I_1 = (-1, +\infty)$	$w + \alpha\left(1 - e^{-w}\right)$	
2	$I_2 = (-1, +\infty)$	$w + \alpha\left(\frac{3-4e^{-w}+e^{-2w}}{2}\right)$	
3	$I_3 = (-0.68, 2.56)$	$w + \alpha\left(\frac{11-18e^{-w}+9^{-2w}-2e^{-3w}}{6}\right)$	
4	$I_4 = (-0.405, 0.92)$	$w + \alpha\left(\frac{25-48e^{-w}+36^{-2w}-16e^{-3w}+3e^{-4w}}{12}\right)$	
5	$I_5 = (-0.238, 0.430)$	$w + \alpha\left(\frac{137-300e^{-w}+300^{-2w}-200e^{-3w}+75e^{-4w}-12e^{-5w}}{60}\right)$	
6	$I_6 = (-0.138, 0.2189)$	$w + \alpha\left(\frac{147-360e^{-w}+450^{-2w}-400e^{-3w}+225e^{-4w}-72e^{-5w}+10e^{-6w}}{60}\right)$	

[1]For simplicity, in the Python function we use n instead of ℓ to refer to the number of delays considered.

3.4 Numerical examples

Example 27 (Low-order system with low-order approximation)**.** *Consider the system with the following transfer function representation:*

$$H_{yu}(s) = \frac{s}{s^2+5}, \tag{3.21}$$

and assume it is in a closed-loop configuration with a PD controller with a three-delay approximation. Under this approximation, the properly-posed interval is $I_3 = (-0.68, 2.56)$*. For illustrative examples, let us consider* $k_p = 1$ *and* $k_d = -4/5$*. With such control gains, the delay-free closed-loop characteristic equation has roots at* $s = \frac{5}{2}\left(-1 \pm \boldsymbol{i}\sqrt{3}\right)$*. Using Proposition 3.3.4, we can verify that, for* $\alpha = -0.68$*, a root of* $f_3(w;\alpha)$ *crosses at* $\omega = 1.32$*. Next, by computing the roots of* $f_3(w;-0.8)$ *with the help of the QPmR algorithm, we can verify that there is a root at* $w = 0.109 \pm \boldsymbol{i}1.085$*. This suggests that the closed-loop characteristic function* $\Delta_3(s;\tau)$ *would have a root of the form:*

$$s(\tau) = \frac{0.109 \pm 1.085\boldsymbol{i}}{\tau} + \mathcal{O}(1).$$

Consider $\tau = 1/1000$*; this would suggest a root around* $s \approx 109 \pm 1085\boldsymbol{i}$*. We can corroborate such an approximation numerically. Indeed, we find a root at* $s = 110.81 \pm 1086.7\boldsymbol{i}$*. Note that the system is closed-loop stable with the ideal derivative, and we are considering an approximation with a "small" value of the delay and three delays (or four points), which, intuitively, should correspond to a very good approximation, yet stability is not preserved. One observation that is worth noting is that the crossing may occur at frequencies* $\omega \neq 0$*. Thus, the singular behavior will push the roots to the right and, additionally, increase the oscillations. The time-domain response of the system to a unit step input with* $\tau = 1/1000$ *is depicted for the approximations with two (up) and three (down) delays in Figure 3.5.*

Example 28 (High-order system with four-delays approximation)**.** *Consider the system described by the following transfer function:*

$$H_{yu}(s) = \frac{s^4}{s^5+s^4+24s^3+34s^2+23s+6}, \tag{3.22}$$

which is unstable in open-loop configuration. We consider the system in closed-loop with a PD controller with gains given by $(k_p, k_d) = (4, 1)$*, which stabilizes the system placing the roots of the closed-loop characteristic function at* $s = -0.55 \pm 0.51\boldsymbol{i}$*,* $s = -0.41 \pm 3.04\boldsymbol{i}$ *and* $s = -0.54$*. Let us consider an approximation of four delays to implement the derivative action. In this case, the improperly-posed interval corresponds to* $I_4 = (-0.405, 0.92)$ *thus, with* $k_d p_{n-1} = 1$*, the considered configuration is improperly-posed. In particular,* $f_4(w, 1)$ *has an unstable root at* $w = 0.019 \pm 4.4\boldsymbol{i}$*. Similarly to the previous example, this implies the existence of a root close to* $s = (0.019 \pm 4.4\boldsymbol{i})/\tau$*. If we consider* $\tau = 1/100$*, we can compute the characteristic roots of the closed-loop characteristic function, which include an unstable root given by* $s = 1.45 \pm 441\boldsymbol{i}$*. It is worth noting that the approximation of the roots is* "less

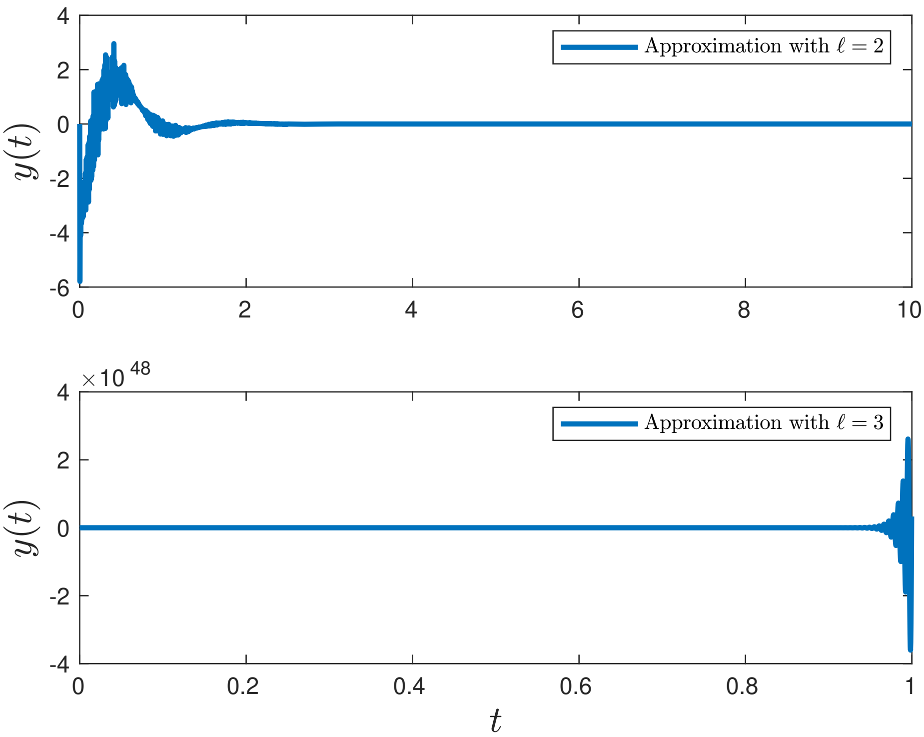

Figure 3.5: Time-domain response to a unit step input of system represented by the transfer function (3.21) with the two and three delays approximation and $\tau = 1/1000$.

precise" *than in the previous example. This is a direct effect of considering a larger value of the delay, as the Newton diagram method characterized the behavior as* $\tau \to 0$. *Figure 3.6 depicts the behavior of the unstable root* $s(\tau)$ *as the value of* τ *approaches zero.*

Example 29 (High-order system with high-order approximation). *Consider a system with transfer function representation given by:*

$$H_{yu}(s) = \frac{s^5 + 1}{s^6 + 2s^5 + 39s^4 + 77s^3 + 86s^2 + 55s + 10}, \tag{3.23}$$

which is open-loop unstable and can be stabilized by considering a classic PD controller with proportional gain given by $k_p = 8$ *and derivative gain given by* $k_d = 2$. *Considering an approximation with six delays, the closed-loop system is improperly-posed as* $I_6 = (-0.138, 0.2189)$. *Moreover, in this case, there are multiple unstable roots as more crossings occur. Table 3.2 summarizes the result of applying Propositions 3.3.4 and 3.3.6 to* $f_6(w; \alpha)$. *Note that more crossings occur, but Table 3.2 only includes those for* $0 < k_d p_{n-1} < 2$, *as those are the ones affecting the stability of the considered closed-loop system. We can observe that five different complex conjugate unstable roots appear for the chosen delay parameter* τ.

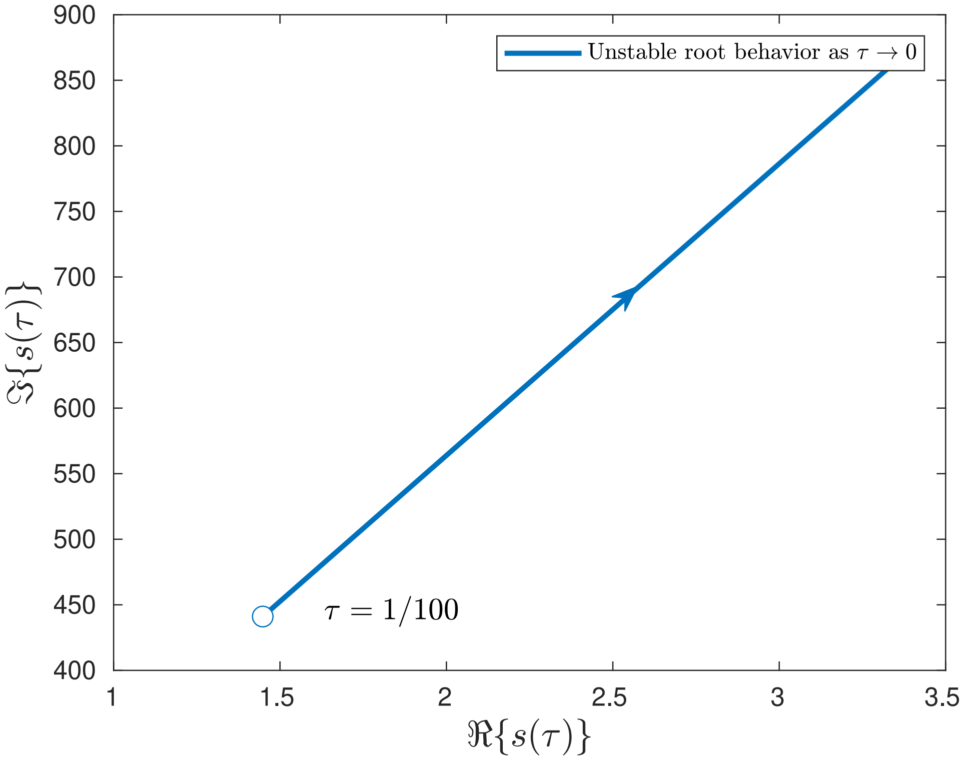

Figure 3.6: Behavior of the unstable root as $\tau \to 0$.

Table 3.2: **Roots crossing** $f_6(w;\alpha)$**.**

α^*	ω^*	Crossing direction	Unstable roots
$\frac{40(\pi-c_2)}{c_1} = 0.21$	$c_3 - 2\pi$	1	1
$\frac{40(4\pi-c_2)}{c_1} = 0.57$	$c_3 - 4\pi$	1	2
$\frac{40(3\pi-c_2)}{c_1} = 0.93$	$c_3 - 6\pi$	1	3
$\frac{40(4\pi-c_2)}{c_1} = 1.29$	$c_3 - 8\pi$	1	4
$\frac{40(5\pi-c_2)}{c_1} = 1.69$	$c_3 - 10\pi$	1	5

$$c_1 := 7\sqrt{336\sqrt{14}+1263}; \quad c_2 := \tan^{-1}\left(\sqrt{\tfrac{3}{13}\left(4\sqrt{14}+17\right)}\right); \quad c_3 := 2\tan^{-1}\left(\sqrt{\tfrac{1}{13}\left(12\sqrt{14}+51\right)}\right).$$

3.5 Some comments on the delay margin

Similarly to the cases presented in Chapter 2, in the properly-posed case, an upper bound exists such that the closed-loop system preserves stability. In particular, such an upper bound, which we refer to as the delay margin of the approximation, can be computed similarly to that of the Direct Method. However, in the general case where $\ell \in \mathbb{N}$ can be chosen arbitrarily, such methodology leads to an enormous computational effort and non-unique solutions.

3.6 Chapter summary and publications

In this chapter, we extended the results from Chapter 2 by generalizing the analysis to systems with multiple delays. Specifically, we examined how increasing the number of delays affects the properly-posedness of the closed-loop system. Interestingly, rather than simplifying the design, the inclusion of additional delays imposes stricter constraints on the system parameters to ensure properly-posedness.

It is worth noting that while the analysis of time-delay systems with delay-dependent parameters and the study of safety implementations of delay-difference approximations are not new, the generalization to systems with an arbitrary yet commensurate number of delays introduces a novel contribution to the literature. Furthermore, the methods employed here do not rely on geometric tools, unlike those in the work of Beretta and Kuang (2002). However, it remains an open question whether these ideas can be readily extended to the noncommensurate case.

Additionally, we briefly addressed the problem of determining the delay margin in this more general setting, offering preliminary ideas for its computation. However, a complete characterization of this problem is deferred to future work.

The results presented in this chapter are summarized in the following publications:

- In Torres-García et al. (2023) (**Torres-García, D.**, Méndez-Barrios, F., Niculescu, S.-I. (2023, June). Some Remarks on the Implementation of a Derivative Action via a Delay-Difference Approximation. ECC 2023 - European Control Conference, European Control Association.), we introduced initial ideas on generalizing the characterization of improperly-posed approximations involving ℓ delays.

- In Méndez-Barrios et al. (2024) (Méndez-Barrios, C.-F., **Torres-García, J.-D.**, and Niculescu, S.-I. (2024), Delay-difference approximations of PD-controllers. Improperly-posed systems in multiple delays case, International Journal of Robust and Nonlinear Control. 34(10), 6431-6454.), we provided a comprehensive characterization of the improperly-posed nature of delay-difference approximations involving an arbitrary number of delays.

Chapter 4

PI controllers for LTI SISO time-delay systems

All the effects of nature are only the mathematical consequences of a small number of immutable laws.

Pierre-Simon Laplace

Contents

4.1 Introduction

As discussed in previous chapters, derivative actions introduce various limitations when designing PID-like controllers. Notably, derivatives in the control scheme amplify high-frequency noise. Moreover, as thoroughly analyzed in

Chapters 3 and 4, such an operator is *improperly posed*, complicating their practical implementation.

This chapter focuses on employing PI controllers in closed-loop configurations with second-order LTI SISO systems that exhibit input/output channel delays and non-minimum phase (NMP) behavior. The latter refers to systems with unstable zeros. As we will explore in this chapter, both unstable zeros and time delays present significant analytical challenges and are frequently encountered in practical applications.

It is worth mentioning that the use of PID controllers to stabilize systems with time delays is not new. In fact, since the 1970s, there have been numerous contributions addressing this problem and providing guidelines for properly tuning control parameters. In particular, works such as Datta et al. (1999), Silva et al. (2007), and Oliveira et al. (2009) offer methodologies for synthesizing stabilizing controllers for linear systems with time delays.

The primary objective in this chapter is to determine the control gains (k_p, k_i) that, when a system can be stabilized using a PI controller, maximize the decay rate or, equivalently, minimize the spectral abscissa of the closed-loop system. This problem has been addressed previously for specific cases. In Ramírez et al. (2015), a particular case of optimizing the spectral abscissa of minimum-phase second-order systems using Proportional-Integral-Retarded (PIR) controllers is presented. Similarly, Torres-García et al. (2022) adopts a similar approach to optimize the spectral abscissa of a first-order system with delay. More recently, Michiels et al. (2024) provided a numerical characterization of the spectral abscissa for second-order systems, analyzing different configurations of the right-most root in the optimal case. On this chapter, we present an extension of the mentioned results to systems that have NMP behavior.

4.2 Stability analysis of non-minimum phase systems

In this chapter, we consider a continuous Linear Time-Invariant (LTI) Single-Input/Single-Output (SISO) dynamical system of the form:

$$\Sigma : \begin{cases} \dot{x}(t) = \boldsymbol{A}x(t) + \boldsymbol{B}u(t-h), \\ y(t) = \boldsymbol{C}x(t), \end{cases} \tag{4.1}$$

including a delay $h > 0$ in the input channel. The transfer function of the system is written as:

$$H_{yu}(s;h) := \frac{P(s)}{Q(s)}e^{-hs} \equiv \boldsymbol{C}(s\boldsymbol{I} - \boldsymbol{A})^{-1}\boldsymbol{B}e^{-hs}, \tag{4.2}$$

and we focus on the case of NMP second-order systems. This consideration is motivated by the wide array of systems that can be modeled by this dynamics, such as power electronics converters (see, for example, Sree and Chidambaram (2006); Zhao and Gao (2010); Chen et al. (2010); Begum et al. (2017); Pandey et al. (2017)). Under this consideration, the polynomials Q and P read:

$$Q(s) = s^2 + as + b, \quad a, b \in \mathbb{R}, \tag{4.3}$$

and

$$P(s) = k(s - z), \quad k \in \mathbb{R}^*, z \in \mathbb{R}_+. \tag{4.4}$$

In this case, the NMP behavior of the systems comes from $z > 0$. The control scheme is considered to be a classical PI controller, which in the Laplace domain reads:

$$C(s) = k_p + \frac{k_i}{s}. \tag{4.5}$$

As discussed in the previous chapters, the interest in this kind of low-order controller comes from its industrial popularity. Such popularity can be attributed to both the ease of implementation and the many results and developments on PID-like controllers. In particular, PI controllers have the advantage of assuring zero steady-state error when the reference is a step function, and several results have proven that, even though time-delay systems are infinite-dimensional systems, PI controllers are an effective solution for control problems involving delays.

Under the above considerations, the characteristic function of the closed-loop system $\Delta : \mathbb{C} \times \mathbb{R}^2 \times \mathbb{R}_+ \to \mathbb{C}$ is given by:

$$\Delta(s; k_p, k_i, h) := s^3 + as^2 + bs + ke^{-hs}\,(s - z)\,(k_p s + k_i). \tag{4.6}$$

Here, it is worth recalling the definition of the spectral-abscissa:

Definition 4.2.1: Spectral abscissa

For a closed-loop system with given characteristic function Δ, the spectral abscissa function $\rho : \mathcal{F}(\mathbb{C};\mathbb{C}) \to \mathbb{R}$:

$$\rho(\Delta) = \max\left\{\Re(s_0) : s_0 \in \mathbb{C}, \Delta(s_0; k_p, k_i, h) = 0\right\}$$

In the remaining of this section, the problem we aim to solve can be stated as follows:

Problem 1. *For a second-order NMP LTI SISO system with transfer function given by* (4.2) *in closed-loop with a PI controller given by* (4.5)*, find the gains* $(k_p^\star, k_i^\star) \in \mathbb{R}^2$ *such that the spectral abscissa of the closed-loop system achieves its minimal value.*

4.3 Delay free case

Before analyzing the system in the presence of the delay, we might want to observe the effect of unstable zeroes in closed-loop systems. Assume that $h = 0$ and, for simplicity and without any loss of generality $k = 1$, leading to the following characteristic function:

$$\tilde{\Delta}(s; k_p, k_i) := \Delta(s; k_p, k_i, h = 0) = s^3 + (a + k_p)s^2 + (b + k_i - k_p z)s - k_i z. \tag{4.7}$$

In this case, $\tilde{\Delta}$ will have three different roots. The stability condition for the closed-loop system can then be obtained using the classical Routh-Hurwitz criterion, which leads to the following:

$$a + k_p > 0 \wedge k_p < \frac{b}{z} \wedge \frac{(a + k_p)(k_p z - b)}{a + k_p + z} < k_i \wedge k_i < 0. \tag{4.8}$$

Among the effects of the unstable zeroes, we can note different things. First, the gain k_i has to be negative (or, for the general case, $\mathrm{sign}(k_i) = -\mathrm{sign}(k)$). Next, the given region is close and finite. Note that, in the absence of zeroes, we can only stabilize systems with $a > 0$ and, in that scenario, we would only need $k_i > 0$ and $k_p > \frac{k_i - ab}{a}$, which corresponds to an open region that extends indefinitely.

4.4 Geometry of the stability region

From the continuity properties of the characteristic roots of the closed-loop system with respect to the system parameters, it is known that for any root to cross from $\mathbb{C}_-$ to $\mathbb{C}_+$ (or vice-versa), a crossing may occur through the imaginary axis $\boldsymbol{i}\mathbb{R}$. Thanks to this property, as presented in the first Chapter, the $\mathcal{D}$-partition method allows us to decompose the parameter space in disjoint regions, which are characterized by having the same number of unstable roots. In particular, whenever a region corresponds to zero unstable roots or, in other words, to stability, we will refer to such a region as $\mathcal{S}$. In this spirit, the first characteristic about $\mathcal{S}$ that is easy to note is described in the following result:

Proposition 4.4.1

Let $\Delta(s; k_p, k_i, h)$ be the closed-loop characteristic function given by (4.6). Then, $\mathrm{sign}(k_i) = -\mathrm{sign}(k)$ is a necessary condition for the stability of the closed-loop system.

Proof. We begin by observing that for $s = 0$ and $z > 0$, the following relation holds:

$$\mathrm{sign}(\Delta(0; k_p, k_i, h)) = -\mathrm{sign}(kk_i). \tag{4.9}$$

Additionally, for some sufficiently large $s = r^* >> 0$, it is clear that $\Delta(r^*; k_p, k_i, h) > 0$. Now, consider the case where $\mathrm{sign}(k_i) = \mathrm{sign}(k)$. Under this assumption, we have $\Delta(0; k_p, k_i, h) < 0$. Since $\Delta(s; k_p, k_i, h)$ is continuous for $s \in \mathbb{R}_+$, the Intermediate Value Theorem guarantees the existence of at least one root $r \in (0, r^*)$. This observation ends the proof. □

For the remainder of this chapter, we will assume $k = 1$, unless stated otherwise, without any loss of generality.

4.4.1 Crossing curves characterization

Next, we define the set of all frequencies where there exists a crossing in the following way:

Definition 4.4.1: Frequency crossing set

The frequency crossing set $\Omega \subset \mathbb{R}$ is the set of all ω such that, for a given h, there exist at least one pair of control gains $(k_p, k_i) \in \mathbb{R}^2$ such that

$$\Delta(\boldsymbol{i}\omega; k_p, k_i, h) = 0. \tag{4.10}$$

Note that $\Delta(\boldsymbol{i}\omega; k_p, k_i, h) = 0$ implies $\Delta(-\boldsymbol{i}\omega; k_p, k_i, h) = 0$. For this reason, in the remaining part of this section, we only consider positive frequencies, that is, $\Omega \subset \mathbb{R}_+^*$. Next, we define in the following way the set of pairs (k_p, k_i) for which the exits a crossing frequency:

Definition 4.4.2: Stability crossing curves

The stability crossing curve $\mathcal{K}$ is the set of all pairs $[k_p, k_i]^T \in \mathbb{R}^2$ for which there exist $\omega \in \Omega$. Furthermore, any point $\vec{k} \in \mathcal{K}$ is referred to as a *crossing point*.

Finally, to characterize the *crossing points* that compose the curve $\mathcal{K}$ we have the following result:

Proposition 4.4.2: Crossing points characterization

Consider the system described by the transfer function (4.2) in closed-loop with the PI controller (4.5). Then, the crossing points $\vec{k} = (k_p(\omega), k_i(\omega)) \in \mathbb{R}^2$ are given by:

$$k_p(\omega) = \frac{\omega \sin(h\omega)\alpha_1 + \cos(h\omega)\alpha_2}{\omega^2 + z^2}, \tag{4.11}$$

$$k_i(\omega) = \frac{\omega\left(\sin(h\omega)\alpha_3 + \omega\cos(h\omega)\alpha_4\right)}{\omega^2 + z^2}, \tag{4.12}$$

where $\alpha_1 = \left(\omega^2 - az - b\right)$, $\alpha_2 = \left(bz - \omega^2(a+z)\right)$, $\alpha_3 = \left(\omega^2(a+z) - bz\right)$ and $\alpha_4 = \left(\omega^2 - az - b\right)$. Furthermore, if $\omega = 0$, we have $k_i = 0$.

Proof. The proof follows directly from observing that if $\Delta(\boldsymbol{i}\omega; k_p, k_i, h) = 0$ then the following conditions must simultaneously hold:

$$\Re\left\{\Delta(\boldsymbol{i}\omega; k_p, k_i, h)\right\} = 0 \quad \wedge \quad \Im\left\{\Delta(\boldsymbol{i}\omega; k_p, k_i, h)\right\} = 0.$$

Solving these equations for k_p and k_i yields the expressions in (4.11) and (4.12). For $\omega = 0$, the condition is obtained directly by noting that $\Delta(0; \cdot, \cdot, \cdot) = -zk_i$, which completes the proof. □

Naturally, with the crossing points already characterized, it is easy to *construct* the curve $\mathcal{K}$ in the following way:

Corollary 4.4.1

Consider the system described by the transfer function $H_{yu}(s;h)$ given by (4.2) in closed-loop with the PI controller in (4.5), then the stability crossing curve $\mathcal{K} = \mathcal{K}_\omega \cup \mathcal{K}_0$ is given by:

$$\mathcal{K}_\omega := \left\{ \vec{k} \in \mathbb{R}^2 : \vec{k} := (k_p(\omega), k_i(\omega)), \forall \omega \in \Omega \right\},$$
$$\mathcal{K}_0 := \left\{ \vec{k} \in \mathbb{R}^2 : \vec{k} := (k_p, 0),\ k_p \in \mathbb{R} \right\}.$$

Appendix B page 152 presents a Matlab function that allows plotting the given region in a given interval.

Next, the interest is to identify the direction the roots cross, that is, from $\mathbb{C}_+$ to $\mathbb{C}_-$, or vice-versa, as a pair of parameters cross the given curve $\mathcal{K}$. Before tackling this problem, a useful idea is to define a *direction* in the curve. In this spirit, we refer to the *positive* direction of the curve as the direction that corresponds to increasing ω. Moreover, we refer to the region located to the left when moving in the positive direction as the region on the left. Similarly, we also define the region on the right. This concepts are exemplified in Figure 4.1. The following results

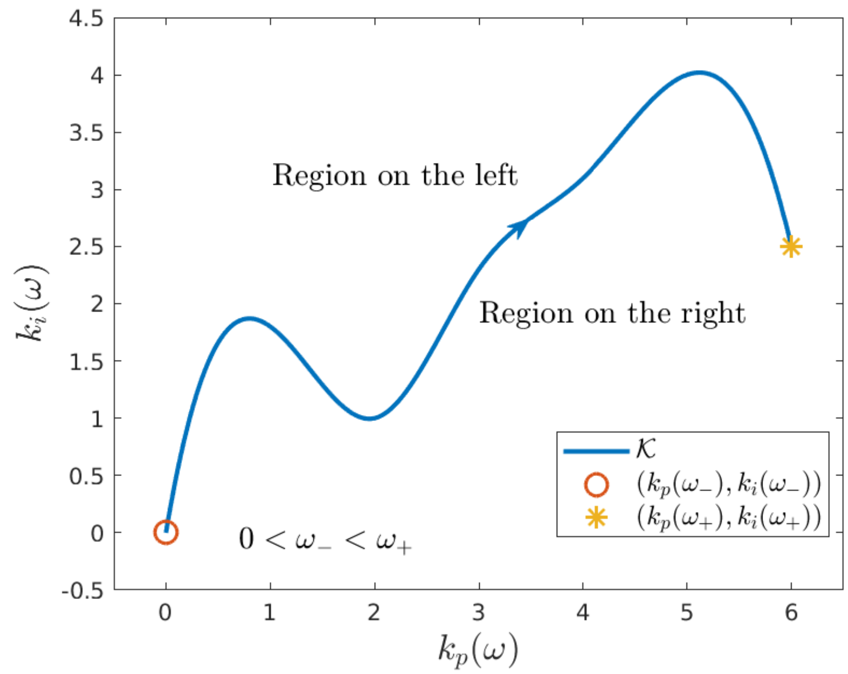

Figure 4.1: Positive direction of the curve $\mathcal{K}$.

characterize the relationship between crossing the curve $\mathcal{K}$ at $\omega \neq 0$ and crossing the imaginary axis:

Proposition 4.4.3: Crossing directions

Consider the system described by the transfer function $H_{yu}(s;h)$ in (4.2) in closed-loop with the PI controller (4.5). Then, a pair of characteristic roots cross the imaginary axis from $\mathbb{C}_+$ to $\mathbb{C}_-$ ($\mathbb{C}_-$ to $\mathbb{C}_+$) if $\vec{k}$ traverses the stability crossing curve $\mathcal{K}$ from left to right (right to left) with respect to the positive direction of the curve.

The proof of Proposition 4.4.3 can be found in Appendix A.

It is clear that a crossing can also occur through $\mathcal{K}_0$. In this case, the crossing will not always imply the same crossing direction in the complex plane, as described in the following result:

Proposition 4.4.4: Crossing at $\omega = 0$

Consider the system described by the transfer function $H_{yu}(s;h)$ in (4.2) in closed-loop with the PI controller (4.5). Then, a real characteristic root crosses from $\mathbb{C}_+$ to $\mathbb{C}_-$ ($\mathbb{C}_-$ to $\mathbb{C}_+$) if $\vec{k}$ traverses the stability crossing curve $\mathcal{K}_0$ from up to down at any crossing point located to the right (left) of $\vec{k}_0$ given by:

$$\vec{k}_0 = \begin{bmatrix} k_{p0} \\ k_{i0} \end{bmatrix} = \begin{bmatrix} b/z \\ 0 \end{bmatrix}.$$

The proof can be found in Appendix A.

Before continuing, we illustrate graphically the idea of the crossing directions in Figure 4.2.

Here, it is important to mention that there are systems of the form (4.1) that cannot be stabilized using a PI controller. With this idea in mind, the following result guarantees that if the stable region $\mathcal{S}$ exists, this region is also the only stable region.

Proposition 4.4.5: Uniqueness of the stability region

Consider the system described by the transfer function $H_{yu}(s;h)$ in (4.2) in closed-loop with the PI controller (4.5) with characteristic function $\Delta(s; k_p, k_i, h)$ given by (4.6). Then, if a region exists inside the control parameter space (k_p, k_i) such that all the characteristic roots are located inside $\mathbb{C}_-$, then such a region is unique.

The proof can be found in Appendix A.

4.4.2 Stability index computation

As previously discussed, each disjoint region in the parameter space corresponds to a specific number of unstable roots. Identifying the number of unstable roots, $n \in \mathbb{N}$ associated with a given region is of interest. We refer to n as

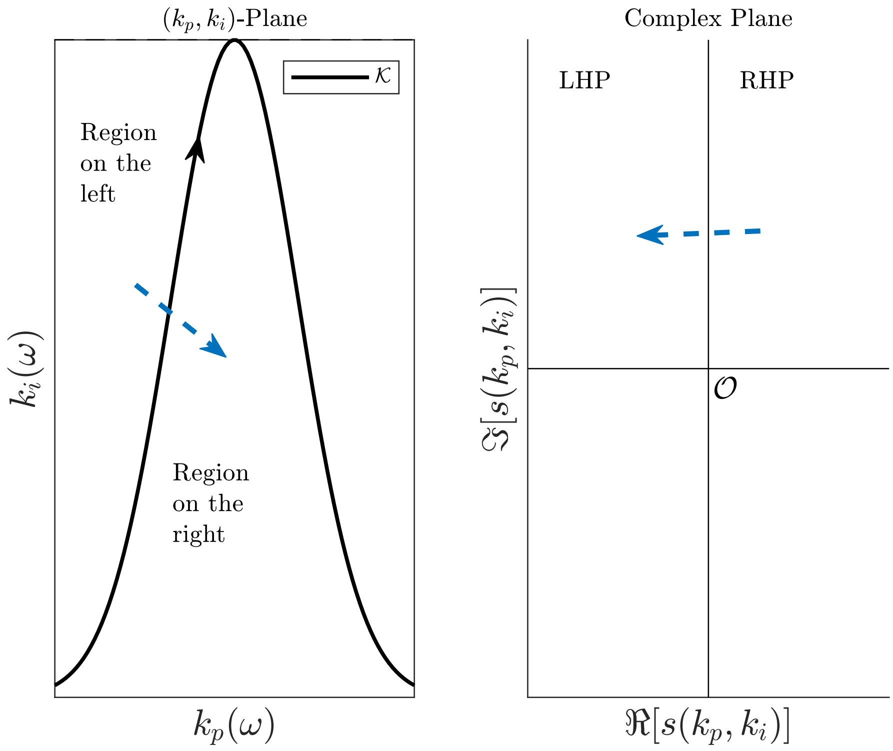

Figure 4.2: Crossing directions. On the left, we observe a crossing from the region on the left to the positive direction, and on the right, we observe a root crossing from $\mathbb{C}_+$ to $\mathbb{C}_-$.

the stability index of that region.

To address this problem, let n_0 represent the number of unstable roots associated with the origin $\mathcal{O}$, i.e., the number of unstable roots when $\vec{k} = [0, 0]^T$. Note that $n_0 \in \{0, 1, 2\}$, determined by the unstable roots of $Q(s)$.

Next, consider the line segment $\overline{\mathcal{O}\vec{k}^*}$ connecting $\mathcal{O}$ and $\vec{k}^*$. This segment intersects the stability crossing curve $\mathcal{K}_\omega$ whenever $\vec{k} = \varepsilon\vec{k}^*$ with $\varepsilon \in (0, 1)$,meaning the crossing point vector is parallel to $\vec{k}^*$. The line containing $\overline{\mathcal{O}\vec{k}^*}$ is given by $k_i = (k_i^*/k_p^*)k_p$. The corresponding $\omega = \omega^* \in \Omega$ for which the intersection occurs must satisfy the equation:

$$k_p^* k_i(\omega^*) - k_i^* k_p(\omega^*) = 0, \tag{4.13}$$

and we will refer to the set of all ω^* for which (4.13) holds as $\Omega^* \subseteq \Omega$. To analyze these intersections, we introduce the indicator function $\mathcal{I} : \mathbb{R} \times \mathbb{R}^2 \times \Omega^* \to \{0, \pm 1\}$:

$$\mathcal{I}(\varepsilon, k_p^*, k_i^*, \omega^*) := \begin{cases} \text{sign}\,(\delta)\,, & \text{if } \varepsilon \in (0, 1) \\ 0, & \text{if } \varepsilon \notin (0, 1), \end{cases} \tag{4.14}$$

where:

$$\delta = \left.\frac{ds}{dk_i}\right|_{s=\boldsymbol{i}\omega^*, k_p=\varepsilon k_p^*, k_i=\varepsilon k_i^*},$$

where ds/dk_i is determined via the implicit function theorem.

Three cases arise:

The crossing curve $\mathcal{K}_\omega$ starts at the origin $\mathcal{O}$ If $b = 0$ since at $\omega = 0$ the crossing points are given by:

$$k_i(0) = 0 \quad \wedge \quad k_p(0) = \frac{b}{z}.$$

Therefore, in this case $n_0 = 1$ if $a < 0$ and $n_0 = 0$ otherwise.

The crossing curve $\mathcal{K}_\omega$ passes through the origin $\mathcal{O}$ at $\omega \neq 0$ If $a = 0$ and $b > 0$, since the crossing points read:

$$k_p(\omega) = \frac{\left(b - \omega^2\right)\left(z\cos(h\omega) - \omega\sin(h\omega)\right)}{\omega^2 + z^2},$$

and

$$k_i(\omega) = \frac{\omega\left(\omega^2 - b\right)\left(\omega\cos(h\omega) + z\sin(h\omega)\right)}{\omega^2 + z^2},$$

therefore $k_p(\omega) = k_i(\omega) = 0$ at $\omega = \sqrt{b}$.

The crossing curve $\mathcal{K}_\omega$ never touches the origin $\mathcal{O}$ In thise case, n equals the number of unstable roots of $Q(s)$.

With this analysis, we establish the following result.

Proposition 4.4.6: Stability index computation

Let $\vec{k}^* := [k_p^*, k_i^*] \notin \mathcal{K}$ be an arbitrary pair in the parameter plane (k_p, k_i). For any such $\vec{k}^*$, , the number of unstable characteristic roots, n, is given by:

$$n = n_0 + 2\sum_{\omega\in\Omega^*} \mathcal{I}(\varepsilon, k_p^*, k_i^*, \omega) + \eta_0, \tag{4.15}$$

where η_0 corresponds to the sign of the direction of the crossing of the root crossing through the origin.

Proof. Consider the characteristic quasipolynomial Δ. For $k_p = 0$ and $k_i = 0$, the characteristic roots correspond to those of $Q(s)$, plus the corresponding crossing at $\omega = 0$, which direction can be identified with Proposition 4.4.4. By continuity, the number of unstable roots of the closed-loop characteristic quasipolynomial remains constant unless a crossing occurs on the stability crossing curve $\mathcal{K}$.

Since $\mathcal{K}$ lies along the horizontal axis of the parameter plane (k_p, k_i), any crossings as we traverse the line segment

$\overrightarrow{\mathcal{O}k^*}$ must occur through $\mathcal{K}_\omega$. According to the $\mathcal{D}$-departition theory, these crossings correspond to complex conjugate root crossings of the characteristic quasipolynomial.

The indicator function $\mathcal{I}$ determines the direction of each crossing based on the sign of the derivative of the characteristic root with respect to k_i. Thus, $\mathcal{I}$ accurately captures the net change in the number of unstable roots as the parameter values traverse $\overrightarrow{\mathcal{O}k^*}$. This observation ends the proof. $\square$

4.4.3 Optimization of the spectral abscissa

Before continuing, we introduce the concept of σ-stability:

Definition 4.4.3: σ-stability

Let $\sigma \in \mathbb{R}_+^*$ be a strictly positive real number. Then the closed-loop system (4.2)-(4.5) is said to be $\sigma-$stable if its spectral abscissa $\rho(\Delta)$ verifies the inequality $\rho(\Delta) \leq -\sigma$.

This definition states that we can study the stability of a closed-loop system with respect to a given vertical axis $-\sigma + \boldsymbol{i}\mathbb{R}$. In the following, the objective is to find the maximum value of σ such that there exists at least one pair $(k_p^\star, k_i^\star)$ that σ-stabilizes the system. But, before establishing the main results of this section, allow us to introduce the concept of a *self-intersection*:

Definition 4.4.4: Self-intersection

We say that the stability crossing curve $\mathcal{K}$ presents a self-intersection if there exist a pair $(\omega_-, \omega_+) \in \mathbb{R}_+^2$ such that $\omega_- < \omega_+$ and:

$$k_p(\omega_-) \equiv k_p(\omega_+) \quad \wedge \quad k_i(\omega_-) \equiv k_i(\omega_+), \tag{4.16}$$

where $k_p(\cdot)$ and $k_i(\cdot)$ are crossing points given by (4.11) and (4.12), respectively.

Note that one intuitive way to study the σ-stability of a closed-loop system is by considering the change of variable $s \to s - \sigma$. That is, the optimal spectral abscissa corresponds to the maximum value of σ such that, under the proposed change of variable, there exists a stability region $\mathcal{S}$. We illustrate the effect of the change of variable in Figure 4.3.

With these ideas in mind, inspired by a geometrical observation, we divide the optimization of the spectral abscissa into the following three cases:

Case I. The optimal spectral abscissa corresponds to a triple real root, which arises only in cases where the stability frontier does not present self-intersections.

Case II. The optimal spectral abscissa corresponds to a double complex conjugate root.

Case III. The optimal spectral abscissa corresponds to a complex conjugate root plus a simple real root.

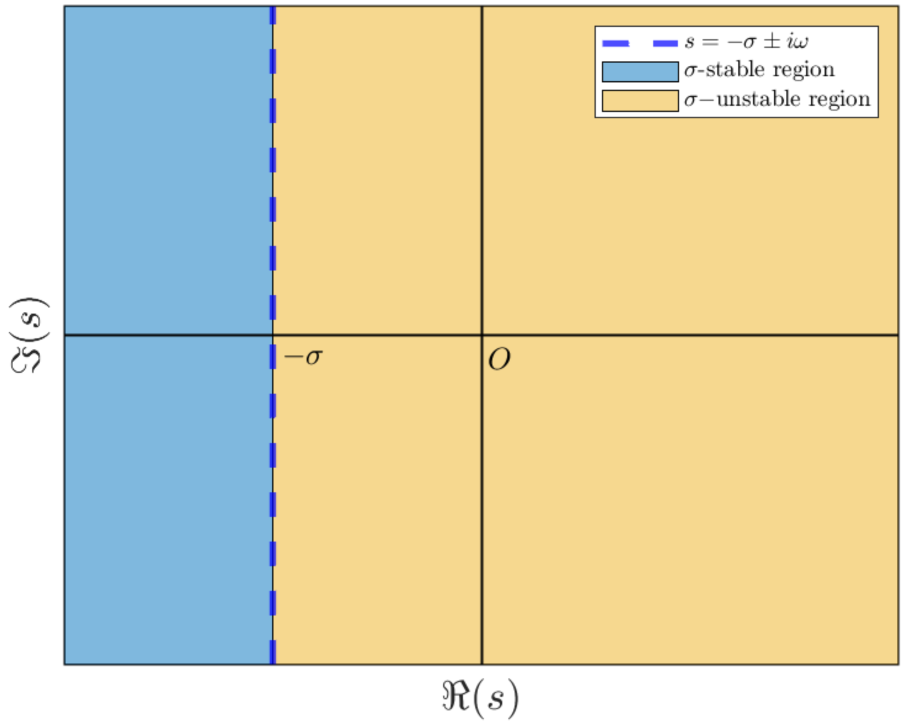

Figure 4.3: σ-stable region in the complex plane.

We illustrate the corresponding cases in Figure 4.4.

We first consider where the stability crossing curves do not self-intersect, for which we have the following result:

Theorem 4.4.1: Optimal σ in the self-intersection free case

Consider the system described by the transfer function $H_{yu}(s;h)$ in (4.2) in closed-loop with the PI controller (4.5), and assume that the corresponding crossing curve $\mathcal{K}$ does not have self-intersections, then the spectral abscissa $\rho(\Delta)$ achieves its minimum value $\widehat{\sigma}$ at the smallest real positive root of the following fifth-order polynomial:

$$p(\sigma) := \sigma^5 + a_4\sigma^4 + a_3\sigma^3 + a_2\sigma^2 + a_1\sigma + a_0, \tag{4.17}$$

where:

$$a_4 = 2z - a - \frac{4}{h}, \quad a_3 = z(z-2a) + b + \frac{2}{h^2} - \frac{2(a-5z)}{h}, \quad a_2 = \frac{z\left(-hz(ah+6) + 6ah + 2bh^2 + 6\right)}{h^2},$$
$$a_1 = \frac{z(2z(2ah+3) + bh(hz-2))}{h^2}, \quad a_0 = -\frac{2z(az+bhz+b)}{h^2}.$$

Moreover, the point corresponds to a triple real root.

The proof of Theorem 4.4.1 is presented in the Appendix A. Note that Theorem 4.4.1 only gives us information on the minimal value the spectral abscissa can achieve using a PI controller. The following result allows us to compute

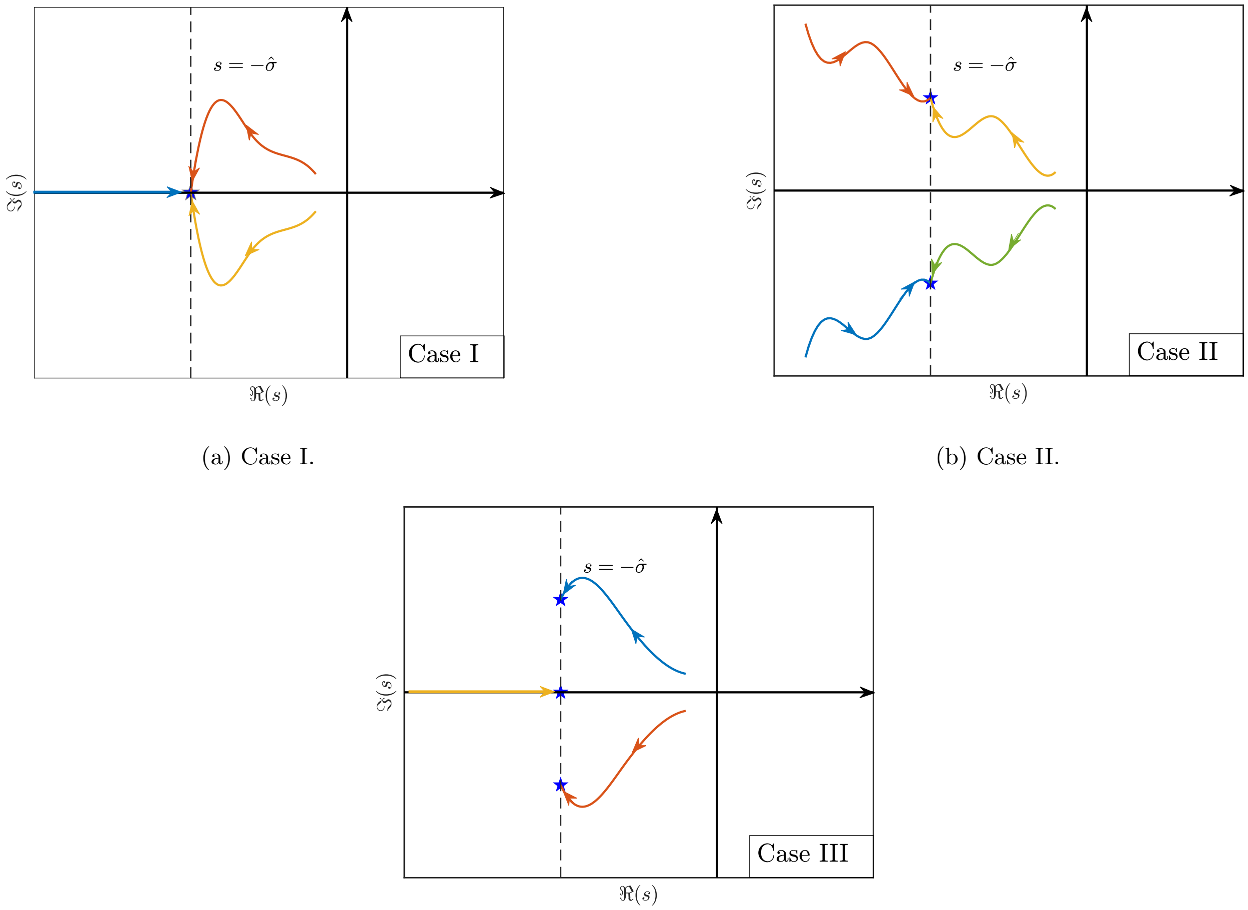

(a) Case I.

(b) Case II.

(c) Case III.

Figure 4.4: Different configurations of the optimal spectral abscissa.

the control gains that achieve such a decay rate:

Corollary 4.4.2: Optimal gains in the self-intersection free case

Consider the system described by the transfer function $H_{yu}(s;h)$ in (4.2) in closed-loop with the PI controller in (4.5), and assume that the corresponding curve $\mathcal{K}$ does not have self-intersections, then optimal control gains $(\widehat{k}_p, \widehat{k}_i) \in \mathbb{R}^2$ that place the spectral abscissa $\rho(\Delta)$ as far left as possible are given by:

$$\widehat{k}_p = \frac{\left(-h\widehat{\sigma}^4 + c_1\widehat{\sigma}^3 - c_2\widehat{\sigma}^2 - c_3\widehat{\sigma} + bz\right)}{e^{h\widehat{\sigma}}(\widehat{\sigma}+z)^2}, \tag{4.18}$$

where

$$c_1 = ah - hz + 2, \quad c_2 = -z(ah+3) + a + bh, \quad c_3 = z(2a+bh),$$

and

$$\widehat{k}_i = \frac{\widehat{\sigma}^2(\widehat{\sigma}(c_4 + c_5 z + \widehat{\sigma}) - az - b(h(\widehat{\sigma}+z)+1))}{e^{h\widehat{\sigma}}(\widehat{\sigma}+z)^2}, \tag{4.19}$$

where

$$c_4 = h\widehat{\sigma}(a - \widehat{\sigma}), \quad c_5 = ah - h\widehat{\sigma} + 2.$$

Proof. The proof is straightforward by solving the system of equations (A.31)-(A.33) for k_p and k_i (see the proof of Theorem 4.4.1 in the Appendix A). □

Next, in the presence of self-intersections in the stability crossing curves, we propose an algorithm to identify the optimal gains. The algorithm starts by considering an interval of σ values and an interval of crossing frequencies. The results rely on the fact that, for the maximum value of σ, if the crossing curve presents self-intersections, the region σ must be composed of either one crossing frequency $\omega \neq 0$ or by two, one of them being $\omega = 0$. The algorithm proceeds as follows:

Initialization Define an increasing sequence (σ_j) and a set of crossing frequencies Ω_{ω_j} for each given σ_j. For each pair (σ_j, ω), construct the σ-stability crossing curve $\mathcal{K}_{\sigma_j,\omega}$.

Region Verification Verify the existence of a σ-stable region $\mathcal{S}_{\sigma_j}$. If such a region exists:

1. Compute the cardinality of the region $\mathcal{S}_{\sigma_j}$.
2. Determine the cardinality of the intersections between the curve for $\omega \neq 0$ and the line corresponding to $\omega = 0$.

Case identification If card $\left\{\mathcal{S}_{\sigma_j}\right\} = 1$, the region has collapsed to a point. Identify the case of collapse:

Case II No intersections are present, indicating a double complex root.

Case I One intersection exists, indicating that the line corresponding to $\omega = 0$ (a real root) is part of the collapse.

Determine the maximum σ The value σ_j at which the region collapses is denoted as $\widehat{\sigma}$. If no collapse occurs within the initial sequence, extend the sequence and reinitialize the procedure.

The formalized steps of the algorithm are presented in Algorithm 2.

Algorithm 2: Optimization of the spectral abscissa.

Data: $\mathcal{S}$: stable region of (4.6);
Γ: interval (σ_0, σ_ℓ), with $\sigma_0 := \sigma^{(-)}$ and $\sigma_\ell := \sigma^{(+)}$;
$\mathcal{K}_{\sigma_j,\omega}$: sets parameterized by $\omega \in \Omega_{\sigma_j} := [\underline{\omega}_{\sigma_j}, \overline{\omega}_{\sigma_j}]$.
Assumptions: $\mathcal{S} \neq \emptyset$
Result: Optimal spectral abscissa $\widehat{\sigma}$.
Initialization:
$j \leftarrow 0$; $\Gamma \leftarrow (\sigma_0, \sigma_\ell)$; $flag \leftarrow 1$;
while $flag = 1$ **do**
  Compute $N_j^{(s)} \leftarrow \text{card}\left\{\mathcal{S}_{\sigma_j}\right\}$; Compute $N_j^{(k)} \leftarrow \text{card}\left\{\mathcal{K}_{\omega,\sigma_j} \cap \mathcal{K}_{0,\sigma_j}\right\}$;
  if $N_j^{(s)} = 1$ *and* $N_j^{(k)} = 0$ **then**
    $\widehat{\sigma} \leftarrow \sigma_j$; Case $\leftarrow$ Case II; $flag \leftarrow 0$;
  else
    if $N_j^{(s)} = 1$ *and* $N_j^{(k)} = 1$ **then**
      $\widehat{\sigma} \leftarrow \sigma_j$; Case $\leftarrow$ Case III; $flag \leftarrow 0$;
  Increment $j \leftarrow j + 1$;
  if $j > \ell$ **then**
    Update Γ and restart from $j \leftarrow 0$;
return $\widehat{\sigma}$

4.5 Fragility of PI controllers

Next, now that we have a tool to achieve the minimum possible spectral abscissa, we present the fragility of the controller. The problem of *fragility* can be thought of in the following way: *"how large of a deviation can a system tolerate for the parameters"*. Formally, the question to this answer reduces to solving the following problem:

Problem 2. *For a second-order NMP LTI SISO system with transfer function given by* (4.2) *in closed-loop with a PI controller given by* (4.5)*, with given stabilizing control gains* $(k_p^*, k_i^*) \in \mathbb{R}^2$*, find the maximum controller parameter deviation* d*, such that the closed-loop system preserves stability as long as the following inequality holds:*

$$\sqrt{(k_p - k_p^*)^2 + (k_i - k_i^*)^2} < d. \tag{4.20}$$

In order to solve this problem, allow us to introduce the following function $\gamma : \mathbb{R}_+ \to \mathbb{R}_+$:

$$\gamma(\omega) := \begin{cases} \sqrt{(k_p(\omega) - k_p^*)^2 + (k_i(\omega) - k_i^*)^2} & \text{if } \omega \in \mathbb{R}_+^* \\ |k_i^*| & \text{if } \omega = 0, \end{cases} \tag{4.21}$$

With this in mind, we have the following result:

Proposition 4.5.1: Fragility of the PI controller

Let $\vec{k}^*$ be a stabilizing controller. Then the maximum controller parameter deviation d, such that the closed-loop system preserves stability, is given by:

$$d = \min_{\omega \in \Omega_c \bigcup \{0\}} \{\gamma(\omega)\}, \tag{4.22}$$

where $\Omega_c \subseteq \mathbb{R}_+$ is the set of roots of the function $f : \Omega \to \mathbb{R}_+$ given by:

$$f(\omega) = \left\langle \vec{k}(\omega) - \vec{k}^*, \frac{d\vec{k}}{d\omega} \right\rangle. \tag{4.23}$$

Proof. By assumption, $\vec{k}^*$ is a stabilizing controller, meaning $\vec{k} \in \mathcal{S}$. Hence, the only possible way for $\vec{k}^*$ to lose stability is by crossing the boundary of $\mathcal{S}$, which is naturally in $\mathcal{K}$. We know that $\mathcal{K}$ is composed of $\mathcal{K}_\omega$ and $\mathcal{K}_0$. For any $\vec{k}^*$ with $k_i \neq 0$, it is evident that the Euclidean distance to $\mathcal{K}_0$ is given by $\gamma(0)$. This follows from the fact that $\mathcal{K}_0$ represents the set of controllers for which the system's characteristic equation has a root at zero frequency, which corresponds to the horizontal axis. The minimal distance from $\vec{k}^*$ to $\mathcal{K}_\omega$ is determined by the points where the vector $\vec{k}(\omega) - \vec{k}^*$ is perpendicular to the tangent to the crossing curve $\mathcal{K}_\omega$. In mathematical terms, this condition is satisfied whenever $f(\omega) = 0$, where $f(\omega)$ is a function that measures the perpendicularity condition. It is important to recall that the tangent to the crossing curve $\mathcal{K}_\omega$ is well-defined for all $\omega \neq 0$. This ensures that the calculation of the minimal distance is valid for any $\omega > 0$. Therefore, for any $\omega \neq 0$, the distance from $\vec{k}^*$ to $\mathcal{K}_\omega$ is given by $\gamma(\omega)$. This completes the proof. □

4.6 Closed-loop system's delay margin

The problem of finding the delay margin of the closed-loop system follows a very similar spirit to that of the *"fragility"*. Similarly to the delay-difference approximation presented in previous chapters, the delay margin is a measure of *"how large of a delay can the closed-loop system tolerate"*. In that sense, note that we have been considering that the delay parameter $h \in \mathbb{R}_+$ is known and constant. However, it is clear that, as with any other parameter, some uncertainty might be produced by the identification process. Therefore, it is natural to ask how much the delay parameter can vary before losing stability for a pair of stabilizing gains $\vec{k}^* = (k_p^*, k_i^*)$. With this in mind, we have the following definition:

Definition 4.6.1: Delay margin of the closed-loop system

Consider the closed-loop characteristic function $\Delta(s; k_p, k_i, h)$ and its spectral-abscissa $\rho(\Delta)$. Assume that the controller $C(s)$ with gains $\vec{k}^* = (k_p^*, k_i^*)$ is a stabilizing controller. Then the *delay margin* of the closed-loop system is defined by

$$h_{max} := \sup\{\beta \in \mathbb{R}_+ : \rho(\Delta) < 0 \quad \forall h \in [h^*, \beta)\},$$

where h^* is the corresponding delay parameter of the system.

Consider the function $F : \mathbb{R}^3 \times \mathbb{R}_+ \to \mathbb{R}$ given by:

$$F(\omega, k_p, k_i, h) := a^2\omega^4 + \left(\omega^3 - b\omega\right)^2 - \left(\omega^2 + z^2\right)\left(k_i^2 + k_p^2\omega^2\right). \tag{4.24}$$

We also introduce the set $\Xi \subset \mathbb{R} \times \mathbb{R}_+$ as the set of all pairs (ω^*, h^*) such that, for a given pair (k_p^*, k_i^*) the following system of equations hold:

$$F(\omega^*, k_p^*, k_i^*, h^*) = 0, \tag{4.25}$$

$$h^*\omega^* = \arg\left\{\frac{\omega^*(\omega^*(\omega^* - \boldsymbol{i}a) - b)}{(z - \boldsymbol{i}\omega^*)(k_p^*\omega^* - \boldsymbol{i}k_i^*)}\right\}. \tag{4.26}$$

We have the following result:

Proposition 4.6.1: Delay margin of the closed-loop system

Consider the system described by the transfer function $H_{yu}(s; h)$ in (4.2) in closed-loop with the PI controller $C(s)$ in (4.5), and let $\vec{k}$ be a stabilizing pair. Then, the delay margin h_{max} of the closed-loop system is given by:

$$h_{max} := \min_{(\omega, h) \in \Xi} h. \tag{4.27}$$

Moreover, for $h = h_{max}$ a characteristic root crosses from $\mathbb{C}_-$ to $\mathbb{C}_+$ at $\omega = \omega^*$, where ω^* correspond to the given pair $(\omega^*, h_{max}) \in \Xi$.

Proof. First, it is clear that if $\Delta(\boldsymbol{i}\omega; k_p, k_i, h) = 0$, the following must hold:

$$(\boldsymbol{i}\omega)^3 + a(\boldsymbol{i}\omega)^2 + b\boldsymbol{i}\omega = e^{-h\boldsymbol{i}\omega}((\boldsymbol{i}\omega) - z)(k_i + k_p(\boldsymbol{i}\omega)),$$

which leads directly to (4.25) and (4.26). Next, since the closed-loop system is assumed to be stable and by the

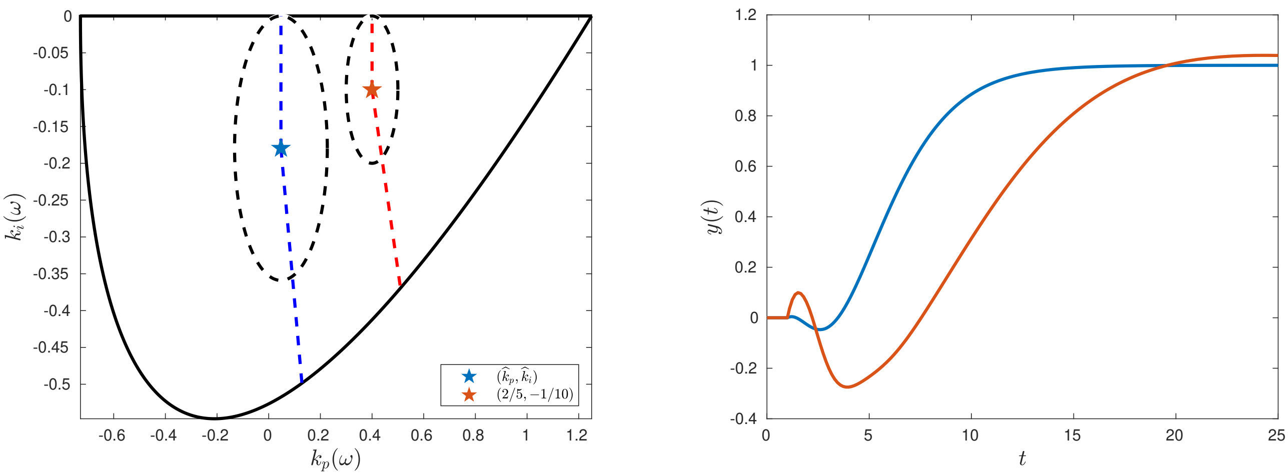

(a) Stability region and selected gains location for the system described by transfer function (4.28).

(b) Closed-loop system's response to a unit step input.

Figure 4.5: Control gains comparison.

continuity property of the characteristic roots w.r.t. the delay parameter h, the only possible way to lose stability is by crossing the imaginary axis. Moreover, by the same arguments, the smallest h for which there exists such a crossing must be from $\mathbb{C}_-$ to $\mathbb{C}_+$. This last observation ends the proof. $\square$

4.7 Numerical examples

Example 30 (Open-loop stable system)**.** *Let us consider the system described by the following transfer function:*

$$H_{yu}(s;h) = \frac{s-1}{s^2+s+\frac{5}{4}} e^{-s}, \tag{4.28}$$

which is stable in open-loop, with its poles located at $s = -1/2 \pm \boldsymbol{i}$. Using Theorem 4.4.1, we determine that the minimum achievable value of the spectral abscissa is $\rho(\Delta) = -0.666425$. From the expressions provided in Corollary 4.4.2, the control gains that achieve this optimal spectral abscissa are $\widehat{k}_p = 0.0473484$ and $\widehat{k}_i = -0.179506$.

We also compare an alternative stabilizing controller with gains $k_p = 2/5$ and $k_i = -1/10$. The locations of both sets of gains within the stability region are illustrated in Figure 4.5a. The corresponding closed-loop time responses for each controller are shown in Figure 4.5b. Additionally, Table 4.1 summarizes the key characteristics of both controllers, including their respective delay margins, which were computed using Proposition 4.6.1.

It is noteworthy that while the optimal controller achieves a faster response and is less fragile, the alternative controller has a larger delay margin. This observation highlights the trade-offs involved in control design and underscores that the choice of control gains should depend on the specific requirements of the application at hand.

Table 4.1: **Different controllers performance for system described by transfer function** (4.28).

$\vec{k}$	$\rho(\Delta)$	$d = \min(\gamma(\omega))$	h_{max}
$(\widehat{k_p}, \widehat{k_i}) = (0.0473484, -0.179506)$	-0.6664	0.179	8.639
$(k_p, k_i) = (2/5, -1/10)$	-0.1795	0.100	12.81

Example 31 (Open-loop oscillator)**.** *Consider the oscillator described by the following transfer function:*

$$H_{yu}(s; h) = \frac{s - 1/3}{s^2 + 4} e^{-s/2}, \tag{4.29}$$

with a pair of imaginary poles located at $s = 2\boldsymbol{i}$. Using Algorithm 2, we first identify that the configuration of the optimal spectral abscissa corresponds to a double complex conjugate root, i.e., Case II. Secondly, the optimal gains that achieve this configuration are determined as $\widehat{k}_p = 0.2591$ and $\widehat{k}_i = -2.0463$. These gains position the closed-loop spectral abscissa at $\rho(\Delta) = -1.23$, corresponding to a double root at $s = -1.23 \pm 0.75\boldsymbol{i}$. As in the previous example, we also consider an arbitrarily stabilizing controller with gains $k_p = 2$ and $k_i = -2$. The system responses for both controllers are shown in Figure 4.6b, while their respective locations in the stability region are depicted in Figure 4.6a. It is easy to observe from the figures that the optimal controller not only outperforms the arbitrary controller in terms of system response but also exhibits a larger margin of stability. This indicates that the optimal controller is less fragile to perturbations.

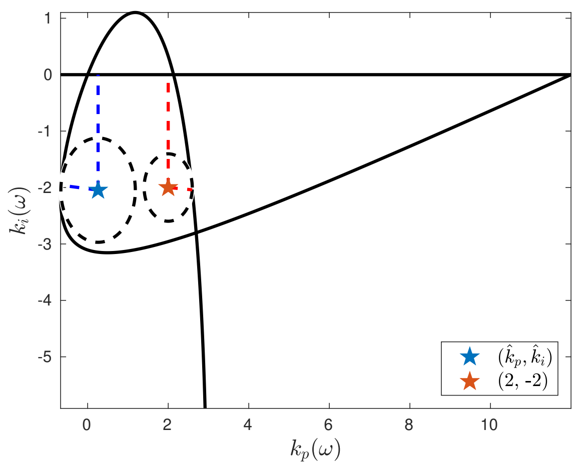

(a) Stability region and selected gains location for the oscillator with transfer function (4.29).

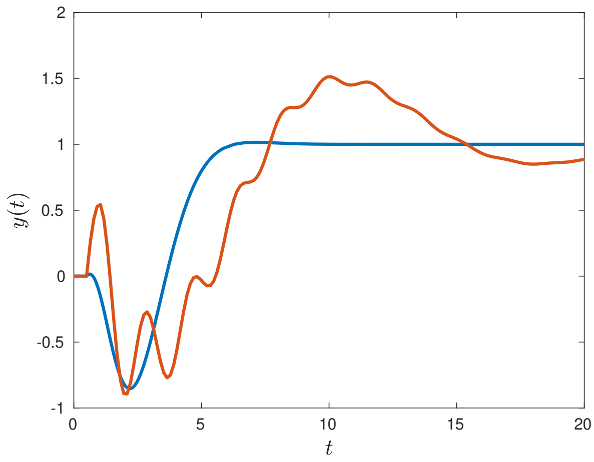

(b) Closed-loop system's response to a unit step input.

Figure 4.6: Control gains comparison for the oscillator in (4.29).

Example 32 (Open-loop unstable system)**.** *Consider the unstable system described by the following transfer function:*

$$H_{yu}(s; h) = \frac{s - 2}{s^2 - \frac{s}{2} + \frac{13}{4}} e^{-2s}. \tag{4.30}$$

The system presents two unstable poles located at $s = \left(1 \pm \sqrt{51}\boldsymbol{i}\right)/4$. *Using Algorithm 2 we can determine that, on the one hand, the optimal minimal spectral abscissa corresponds to* $\rho(\Delta) = -\widehat{\sigma} = -0.1818$ *and, on the other hand, that the corresponding case is Case III. The corresponding gains are* $(\widehat{k_p}, \widehat{k_i}) = (-0.425, -0.272)$*, placing the right-most characteristic roots at* $s = \{-0.1818, -0.1818 \pm 2\boldsymbol{i}\}$*, and depicted inside the stable region in Figure 4.30, where we can also observe the distance to the stability crossing curve which corresponds to* $d = 0.114$. *Additionally, Figure 4.7b shows the response of the closed-loop system to a unit step input.*

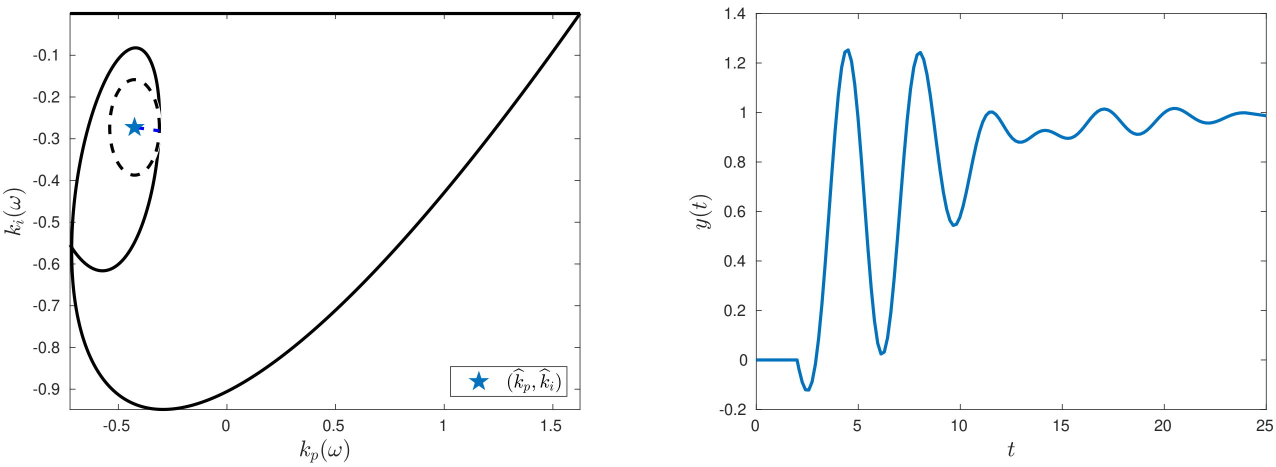

(a) Stability region and optimal gains location for the unstable system described by the transfer function (4.30).

(b) Closed-loop system's response to a unit step input.

Figure 4.7: System described by transfer function (4.30) in closed-loop with the optimal PI controller.

In this configuration, one thing worth noting is what is happening to the stability region at the optimal point. We depict such a region in Figure 4.8, where we also indicate the location of the optimal gains.

4.8 Applications: the DC-DC boost converter

Consider the standard DC-DC Boost Converter, which consists of a voltage source E, a switching component M, an inductor L, a capacitor C, and a load resistor R, as illustrated in Figure 4.9. PI controllers are often considered an ideal solution for controlling such circuits due to two main reasons (for a detailed discussion on the control of DC-DC boost converters using PI controllers, see Alvarez-Ramirez et al. (2001); Mamizadeh et al. (2018); Warrier et al. (2024); Hernández-Gallardo et al. (2024)).

Firstly, electrical systems are frequently subjected to high-frequency noise. As a result, derivative controllers are typically avoided in these applications. Secondly, a common requirement in the control design for this type of circuit is the elimination of steady-state error, which makes the inclusion of integral action essential.

Despite the system being stable in open-loop operation, the design of a closed-loop control strategy remains necessary to achieve the desired performance.

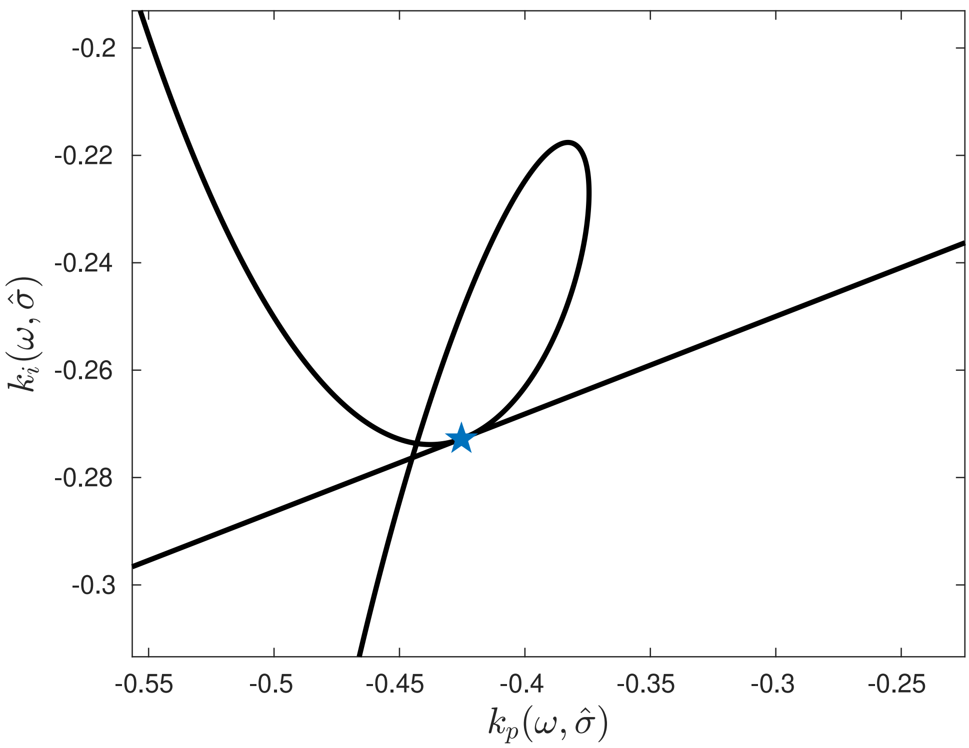

Figure 4.8: $\widehat{\sigma}$-stable region corresponding to a single point, which is the intersection between both parts composing the curve $\mathcal{K}$ when $s \to s - \widehat{\sigma}$.

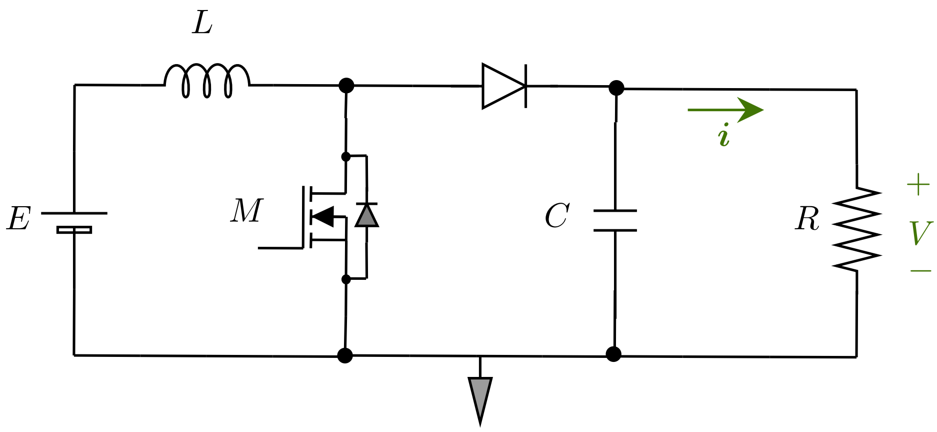

Figure 4.9: DC-DC Boost converter.

With the above discussion in mind, the following transfer function describes the output voltage due to the duty cycle:

$$H_{yu}(s) = -\frac{K\omega_0^2(zs-1)}{s^2 + \dfrac{\omega_0}{Q}s + \omega_0^2}e^{-hs}. \tag{4.31}$$

The parameter $K \in \mathbb{R}_+^*$ represents the DC gain, $\omega_0 \in \mathbb{R}_+^*$ is the natural frequency, and the unstable zero is located at $s = 1/z$. Additionally, h denotes the input delay, and Q is the quality factor. These parameters are considered as follows:

$$K = \frac{E}{\eta^2}, \quad \omega_0 = \frac{\eta}{\sqrt{LC}}, \quad z = \frac{L}{\eta^2 R},$$
$$Q = \eta R \sqrt{\frac{C}{L}}\ , h = 8 \times 10^{-3}.$$

We start by noting that in this case, the open-loop gain of the system is negative, and as a consequence, we expect $k_i > 0$ in the given stable region. Since the stability crossing curves do not present self-intersections, we can find the minimal spectral abscissa, as well as the corresponding optimal gains, with the help of Theorem 4.4.1 and Corollary 4.4.2. The result indicates that the minimal spectral abscissa is $\rho(\Delta) = -216.8$, achieved with the gains $k_p = 2.7 \times 10^{-3}$ and $k_i = 1.21$.

Figures 4.10a and 4.10b illustrate the stability region of the circuit and the closed-loop response to a unit step input, respectively. Two key observations can be made:

1. The system exhibits a very fast response, taking less than 50 milliseconds to reach the reference. This situation is natural, as the system corresponds to an electrical one.

2. The distance to instability is notably small, quantified as $d = 0.017$. It is important to note that, in our analysis, the parameters are dimensionless. However, in practical applications, these parameters correspond to physical components. Consequently, the acceptable tolerance for something as the fragility will depend on the specific application and the type of device being considered.

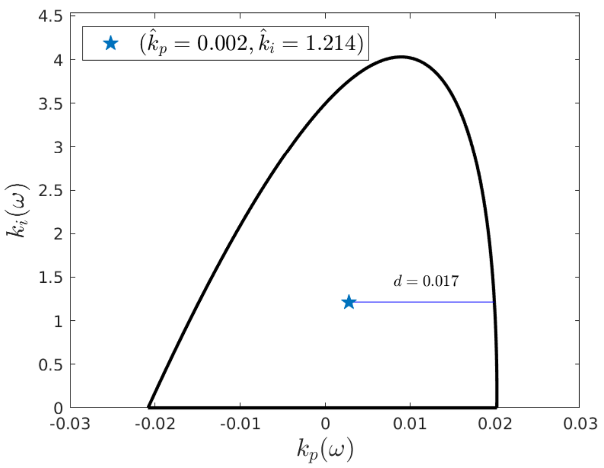

(a) Stability region and optimal gains location for the circuit in Figure 4.9, with transfer function representation given in (4.31)

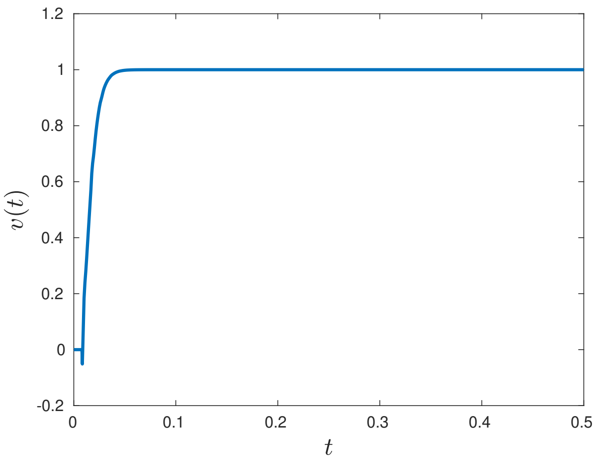

(b) Closed-loop system's response to a unit step input.

Figure 4.10: Optimization of the spectral abscissa of the system describing the circuit in Figure 4.9.

4.9 Chapter summary and publications

In this chapter, we presented a systematic approach for optimizing the performance of a second-order non-minimum phase LTI SISO system with respect to its spectral abscissa and, consequently, its decay rate. Although this problem has been addressed in prior works, the incorporation of non-minimum phase behavior, along with the consideration of the general case, that being second-order systems that are stable, marginally stable, or even unstable in open-loop, marks a significant advancement in the optimization of the spectral abscissa in the general case. The findings are organized into two parts:

Triple Real Root Case We provide an analytical solution to determine the exact values of (k_p, k_i) that optimize the spectral abscissa. This result is derived assuming that the stability crossing curve does not exhibit self-intersections.

Self-Intersecting Stability Curve Case When the stability crossing curve has self-intersections, two distinct scenarios can arise. For this situation, we propose an algorithm that computes the optimal gains (k_p, k_i) while distinguishing between the two possible configurations.

The significance and practical applicability of these results were demonstrated using a physical system example: a DC-DC boost converter.

The following articles were published as a result of the work presented in this chapter:

- In Torres-García et al. (2024) (**Torres-García, D.**, Méndez-Barrios, F., Niculescu, S.-I., Hernández-Gómez, M. (2024)PI Control for Optimal Spectral Abscissa in General Non-Minimum Phase Systems with Time Delay. 2024 10th International Conference on Control, Decision and Information Technologies (CoDIT), 1358-1363 IEEE.), we introduced the geometrical intuition behind minimizing the spectral abscissa of a second-order non-minimum phase system in closed-loop with a PI controller and presented the first version of the corresponding algorithm.

- In Torres-García et al. (2024) (**Torres-García, D**, Méndez-Barrios, F., Niculescu, S.-I. Stabilization of second-order non-minimum phase system with delay via PI controllers. Spectral abscissa optimization. IEEE Access.), we expanded on the minimization of the spectral abscissa, providing additional proofs to guarantee that, whenever the system can be stabilized with a PI controller, the stable region is unique.

Conclusions and perspectives

Sometimes it is the people no one imagines anything of who do the things that no one can imagine.

Alan Turing

Conclusions

This thesis addresses two primary issues, which were thoroughly analyzed. Firstly, the characterization of improperly-posed problems arising from the discretization of the derivative operator is examined. This topic holds significant practical relevance, as implementing derivative action in control strategies often requires a discretization process. The results provide a clear methodology to identify properly and improperly-posed cases, which can guide the selection of the most appropriate discretization method based on specific application requirements and hardware-software constraints.

Secondly, the thesis presents an analysis of non-minimum phase linear systems with delay. To address this challenge, we propose stabilizing such systems using PI controllers. A key contribution of this work is the development of a methodology to determine control gains that minimize the spectral abscissa of the closed-loop system, thereby ensuring stability and improved performance.

Perspectives

Several open problems remain, and the following naturally extend the results presented in this thesis:

1. **Analysis of alternative discretization schemes for the derivative operator**. In particular, investigating the case of non-commensurate delays. Instead of using a discretization of the form:

$$C(s) = \sum_{j=1}^{\ell} k_j(\tau) e^{-j\tau s}, \tag{4.32}$$

consider the impact of varying the step sizes between points, leading to a controller of the form:

$$C(s) = \sum_{j=1}^{\ell} k_j(\vec{\tau}) e^{-\tau_j s}, \tag{4.33}$$

where $\vec{\tau} = \{\tau_0, \tau_1, \ldots, \tau_\ell\}$, and each delay τ_j is chosen independently.

2. **Computation of higher-order terms in the Puiseux series of the singular solution**. Deriving higher-order terms would provide deeper insights into the solution's behavior, particularly for larger delay values.

3. **Extension of the Newton diagram method to multiple variables**. Extending this method is essential for analyzing the non-commensurate case of the approximation correctly. This extension would enable a more rigorous study of systems with non-uniform delay distributions.

4. **Investigation of self-intersections in the stability crossing curve.** As discussed in Chapter 4, one critical challenge in identifying optimal parameters—based on the spectral abscissa—is the occurrence of self-intersections in the stability crossing curve. Determining the conditions that lead to such intersections, as well as localizing the self-intersection points, remains an open problem. Addressing this issue may require tools from algebraic geometry and would significantly enhance the applicability of geometric methods, such as those presented in Chapter 4.

5. **Extension of the optimization of the spectral abscissa to more general systems**. Optimizing the spectral abscissa in a broader context remains an open problem, as the spectral abscissa is generally a non-smooth function. While some numerical results are available for certain classes of systems, a comprehensive characterization and optimization methodology has yet to be established in the open literature.

Appendix A

Proofs of main results

A.1 Proofs from Chapter 2

Proof of Proposition 2.3.1

Proof. First, note that for $\tau \to 0$, the root is close to z^*/τ. From this observation, we have $\Delta_j(z^*/\tau;\tau)$. Since $n > m$, this means that we can avoid having terms in $1/\tau$ by multiplying by τ^n, which leads to rewriting the characteristic function in the following way: $\tilde{\Delta}_j(s;\tau) = \tau^n \Delta_j(\tau s;\tau)$. This leads to the following expressions:

$$\tilde{\Delta}_1(s;\tau) = \tau^n Q\left(\frac{s}{\tau}\right) + \tau^n P\left(\frac{s}{\tau}\right)\left(k_p + k_d\left(\frac{1-e^{-s}}{\tau}\right)\right), \tag{A.1}$$

$$\tilde{\Delta}_2(s;\tau) = \tau^n Q\left(\frac{s}{\tau}\right) + \tau^n P\left(\frac{s}{\tau}\right)\left(k_p + k_d\left(\frac{1-e^{-s}}{\tau}\right)\left(\frac{3-e^{-s}}{2}\right)\right). \tag{A.2}$$

Next, following the Newton diagram method, we need to find the coefficients of the roots with the given form $s^*(\tau) = z^*/\tau$. Such coefficients are given by the non-zero solutions of the following equation:

$$f_j(w) = \lim_{\tau\to 0} \tilde{\Delta}_j(w;\tau) = 0. \tag{A.3}$$

Such limits can be separated as follows:

$$\lim_{\tau\to 0} \tilde{\Delta}_1(w;\tau) = \lim_{\tau\to 0} \tau^n Q\left(\frac{w}{\tau}\right) + k_p \lim_{\tau\to 0} \tau^n P\left(\frac{w}{\tau}\right) + k_d \lim_{\tau\to 0} (1-e^{-w})\tau^{n-1} P\left(\frac{w}{\tau}\right),$$

$$\lim_{\tau\to 0} \tilde{\Delta}_2(w;\tau) = \lim_{\tau\to 0} \tau^n Q\left(\frac{w}{\tau}\right) + k_p \lim_{\tau\to 0} \tau^n P\left(\frac{w}{\tau}\right) + k_d \lim_{\tau\to 0} \left(\frac{3-e^{-w}}{2}\right)(1-e^{-w})\tau^{n-1} P\left(\frac{w}{\tau}\right).$$

It is easy to note that, if $n > m+1$, $\lim_{\tau\to 0} \tau^n P(w/\tau) = 0$, which lead to the following:

$$\lim_{\tau\to 0} \tilde{\Delta}_j(w;\tau) = \lim_{\tau\to 0} \tau^n Q\left(\frac{w}{\tau}\right) = w^n, \quad \forall j \in \{1,2\}.$$

In such a case, all solutions of $f(w) = 0$ are trivial and are not considered for the Newton diagram method. Next, let $n = m+1$. In this case, note that we have:

$$\lim_{\tau\to 0} \tau^{n-1} P\left(\frac{w}{\tau}\right) = p_{n-1} w^{n-1},$$

which means that f_j can be written in the following way:

$$\begin{aligned} f_1(w) &= w^{n-1}(w + k_d p_{n-1}(1 - e^{-w})), \\ f_2(w) &= w^{n-1}\left(w + k_d p_{n-1}(1 - e^{-\omega})\left(\frac{3 - e^{-w}}{2}\right)\right). \end{aligned}$$

Note that both f_1 and f_2 have $n-1$ trivial roots; thus, to find z^*, we need to find the other roots of both quasipolynomials. Let $k_d p_{n-1} = \alpha$, then we have:

$$\bar{f}_1(w) = w + \alpha(1 - e^{-w}) = 0, \tag{A.4}$$

$$\bar{f}_2(w) = w + \alpha(1 - e^{-w})\left(\frac{3 - e^{-w}}{2}\right) = 0. \tag{A.5}$$

From the structure of the solution $s^*(\tau)$, we can see that the system is properly-posed if (A.4) and (A.5) have no solutions with positive real parts. Let us first tackle (A.4). We already mentioned that $w = 0$ is a solution, and we can easily observe that $\lim_{s\to\infty} w + \alpha(1 - e^{-\tau w}) = +\infty$. Next, let us take the first derivative of $\bar{f}_1$ that is $\bar{f}_1'(w) = 1 + \alpha e^{-w}$. Note that if the derivative is negative, that would imply that there exists some solution $r \in \mathbb{R}_+$. This would only happen if $\alpha < -1/e^{-w}$. Since the maximum of $1/e^{-w}$ is at 0, this leads directly to $\alpha < -1$. Therefore, if $\alpha < -1$, $\bar{f}_1$ has a real positive root. We can take the exact same approach for $\bar{f}_2$:

$$\bar{f}_2'(w) = 1 + \frac{\alpha}{2}(4e^{-w} - 2e^{-2w}) < 0 \implies \alpha < \frac{-1}{2e^{-w} - e^{-2w}}. \tag{A.6}$$

In this case the maximum of $2e^{-w} - e^{-2w}$ is also at 0, thus we have $\alpha < -1$. In both cases, we observe that $\alpha < -1$ implies the existence of a real positive solution, meaning that the characteristic root $s^*(\tau)$ will be located in the right-half plane, making the system improperly posed. Next, we want to prove that if $\alpha > -1$, it implies that the system is properly-posed. That means that, if $\alpha > -1$, there does not exist $w = \sigma + \boldsymbol{i}\omega$ with $\sigma > 0$ and $\omega \neq 0$, such that $\bar{f}_j(\sigma+\boldsymbol{i}\omega)=0$. First, let us consider $\bar{f}_1$. If $w=\sigma+\boldsymbol{i}\omega$ is a root of $\bar{f}_1$ the following must hold:

$$\Re\{\bar{f}_1(\sigma+\boldsymbol{i}\omega)\}=\sigma+\alpha(1-e^{-\sigma}\cos(\omega))=0, \tag{A.7}$$

$$\Im\{\bar{f}_1(\sigma+\boldsymbol{i}\omega)\}=\omega+\alpha e^{-\sigma}\sin(\omega)=0. \tag{A.8}$$

It is easy to observe that if $\alpha\geq 0$, (A.7) will always be positive. Therefore, no roots in $\mathbb{C}_+$ will exist. Next, for $\alpha\in(-1,0)$ it is easy to observe that (A.8) is a strictly increasing function that nullifies at $\omega=0$, thus, for $\alpha\in(-1,0)$ it is never zero for $\omega\neq 0$. Finally, for $\bar{f}_2$ we have:

$$\Re\{\bar{f}_2(\sigma+\boldsymbol{i}\omega)\}=\sigma+\frac{1}{2}\alpha\left(3+e^{-2\sigma}\cos(2\omega)-4e^{-\sigma}\cos(\omega)\right), \tag{A.9}$$

$$\Im\{\bar{f}_2(\sigma+\boldsymbol{i}\omega)\}=\omega-\alpha\sin(\omega)\left(e^{-2\sigma}\cos(\omega)-2e^{-\sigma}\right) \tag{A.10}$$

Similarly, the real part is always positive for $\alpha\geq 0$, and no root with a positive real part will exist. For $\alpha\in(-1,0)$, we consider the following:

$$\begin{aligned}\frac{d(\Im\{\bar{f}_2(\sigma+\boldsymbol{i}\omega))\}}{d\omega}&=1+\alpha e^{-2\sigma}\left(2e^{\sigma}\cos(\omega)-\cos(2\omega)\right)\\&=1+\alpha\left(2e^{-\sigma}\cos(\omega)-e^{-2\sigma}\cos(2\omega)\right)\\&=1+\alpha(2e^{-\sigma}\cos(\omega)+e^{-2\sigma}(1-2\cos^2(\omega)))\\&=1+\alpha(2e^{-\sigma}\cos(\omega)(1-e^{-\sigma}\cos(\omega))+e^{-2\sigma}),\end{aligned}$$

which is always positive for $\alpha\in(-1,0)$, which means the function is strictly increasing, and the only root is $\omega=0$. With this last observation, we can conclude that $\alpha>-1$ implies that $z^*<0$ and, therefore, that the system is properly-posed. This ends the proof. □

A.2 Proofs from Chapter 3

Proof of Proposition 3.3.1

Proof. To simplify the problem, let us define $\tilde{\Delta}(s;\tau):=\tau\Delta_\ell(s;\tau)$ and consider the following power series expansion:

$$e^{-\tau s}=1-s\tau+\frac{s^2\tau^2}{2!}+\mathcal{O}(\tau^3). \tag{A.11}$$

Without loss of generality, note that this power series is expanded around $\tau=0$. Since Δ and $\tilde{\Delta}$ share the same roots, characterizing the solutions of $\tilde{\Delta}$ is equivalent to characterizing those of Δ.

As a second step, we construct the corresponding Newton's Polygon of $\tilde{\Delta}$. To achieve this, $\tilde{\Delta}$ can be expressed as:

$$\tilde{\Delta}(s;\tau) = \tau Q(s) + \tau k_p P(s) + k_d P(s) \sum_{k=1}^{\ell} \frac{1}{k}(1-e^{-\tau s})^k. \tag{A.12}$$

Here, $\deg Q > \deg P$. By definition, neither Q nor P depends on τ, and neither they are equal to zero. Regardless of the degrees of Q and P, there will always be a part of Newton's diagram with a slope of 0 at its beginning. This is evident from the term $\tau Q(s) + \tau k_p P(s)$, which expands as:

$$q_n s^n \tau + q_{n-1} s^{n-1} \tau + \cdots + q_0 \tau + k_p p_m s^m + \cdots + k_p p_0 \tau,$$

where $n > m$. Such terms generate a horizontal line in Newton's diagram with a length of at least $n - m$.

To construct the second part of the diagram, consider the quasi-polynomial term:

$$k_d P(s) \sum_{k=1}^{\ell} \frac{1}{k}(1-e^{-\tau s})^k.$$

Substituting the series expansion from (A.11) into (A.12), we obtain:

$$k_d P(s) \sum_{k=1}^{\ell} \frac{1}{k}(s\tau - \frac{s^2\tau^2}{2} + \cdots)^k.$$

This results in a polynomial in $s\tau$. Since $P(s)$ depends only on s, the product expands as:

$$P(s)(a_1 s\tau + a_2 s^2\tau^2 + \cdots) = (p_m s^m + \cdots + p_0)a_1 s\tau + (p_m s^m + \cdots + p_0)a_2 s^2\tau^2 + \cdots .$$

For each term, the rightmost point on the Newton diagram corresponds to $s^{m+i}\tau^i$ with $i \in \mathbb{N}$. Regardless of the coefficients a_i, these terms always produce a line with a slope $\beta = 1$, starting at $i = n$ and extending to the right. This observation completes the proof. □

Proof of Proposition 3.3.2

Proof. First, note that

$$\tau^n \Delta_\ell(w\tau^{-1};\tau) = \tau^n Q(w\tau^{-1}) + P(w\tau^{-1}) \left(\tau^n k_p + \tau^{n-1} k_d \sum_{k=1}^{\ell} \frac{1}{k} \left(1 - e^{-w}\right)^k \right).$$

Next, we divide the analysis into two cases.

Case 1: $m < n-1$ Under this assumption, we compute the following limits:

$$\begin{aligned}
\lim_{\tau\to 0^+} \tau^n Q(w\tau^{-1}) &= \lim_{\tau\to 0^+} \left(w^n + q_{n-1}w^{n-1}\tau + \cdots + q_0\tau^n\right) = w^n,\\
\lim_{\tau\to 0^+} \tau^n k_p P(w\tau^{-1}) &= \lim_{\tau\to 0^+} k_p \left(p_m w^m \tau^{n-m} + p_{m-1}w^{m-1}\tau^{n-m+1} + \cdots + p_0\tau^n\right) = 0,\\
\lim_{\tau\to 0^+} \tau^{n-1} k_d P(w\tau^{-1}) \sum_{k=1}^{\ell} \frac{1}{k}\left(1-e^{-w}\right)^k &= \sum_{k=1}^{\ell} \frac{1}{k}\left(1-e^{-w}\right)^k \lim_{\tau\to 0^+} k_d \left(p_m w^m \tau^{n-1-m} + \cdots + p_0\tau^{n-1}\right) = 0.
\end{aligned}$$

From these results, we conclude that when $m < n-1$, $P_\ell^{aux}(w) = w^n$.

Case 2: $m = n-1$ In this case, we compute:

$$\begin{aligned}
\lim_{\tau\to 0^+} \tau^n Q(w\tau^{-1}) &= \lim_{\tau\to 0^+} \left(w^n + q_{n-1}w^{n-1}\tau + \cdots + q_0\tau^n\right) = w^n,\\
\lim_{\tau\to 0^+} \tau^n k_p P(w\tau^{-1}) &= \lim_{\tau\to 0^+} k_p \left(p_m w^m \tau^{n-m} + p_{m-1}w^{m-1}\tau^{n-m+1} + \cdots + p_0\tau^n\right) = 0,\\
\lim_{\tau\to 0^+} \tau^{n-1} k_d P(w\tau^{-1}) \sum_{k=1}^{\ell} \frac{1}{k}\left(1-e^{-w}\right)^k &= \sum_{k=1}^{\ell} \frac{1}{k}\left(1-e^{-w}\right)^k \lim_{\tau\to 0^+} k_d \left(p_{n-1} w^{n-1} + \cdots + p_0\tau^{n-1}\right)\\
&= k_d p_{n-1} w^{n-1} \sum_{k=1}^{\ell} \frac{1}{k}\left(1-e^{-w}\right)^k.
\end{aligned}$$

Thus, we find:

$$P_\ell^{aux}(w) = w^n + k_d p_{n-1} w^{n-1} \sum_{k=1}^{\ell} \frac{1}{k}\left(1-e^{-w}\right)^k = w^{n-1}\left(w + k_d p_{n-1} \sum_{k=1}^{\ell} \frac{1}{k}\left(1-e^{-w}\right)^k\right),$$

which corresponds to $w^{n-1} f_\ell(w; k_d p_{n-1})$.

Finally, by the Newton diagram method, the root z^* is determined as a non-trivial solution of $P_\ell^{aux}(w) = 0$.

□

Proof of Proposition 3.3.3

Proof. The proof of each property is presented individually:

(i) Let $\alpha_0 \in \mathbb{R}^*$ and $\alpha_0 \neq -1$. Next, consider the derivative of f_ℓ:

$$\begin{aligned}
f_\ell'(r;\alpha_0) := \left.\frac{d}{dw} f_\ell(w;\alpha_0)\right|_{w=r} &= 1 + \alpha_0(1-\rho)\sum_{k=1}^{\ell} \rho^{k-1} \equiv 1 + \alpha_0\left(\sum_{k=1}^{\ell}\rho^{k-1} - \sum_{k=1}^{\ell}\rho^k\right),\\
\implies f_\ell'(r;\alpha_0) &= 1 + \alpha_0(1-\rho^\ell), \qquad \text{(A.13)}
\end{aligned}$$

where $\rho := 1 - e^{-r}$ and $r \in \mathbb{R}^*$. From (A.13), it is evident that f_ℓ' can have a maximum of two solutions in $\mathbb{R}$, implying that card $\{\mathcal{R}_\ell\} \leq 2$, which ends the proof of (i).

(*ii*) it is evident that $w = 0$ is a root of f_ℓ for any $\ell \in \mathbb{N}$. In addition, we have the following:

$$f'_\ell(w;\alpha_0) = 1 + \alpha_0 e^{-w} \sum_{k=0}^{\ell-1} \left(1 - e^{-w}\right)^k. \tag{A.14}$$

Next, we introduce the change of variable $z := 1 - e^{-w}$, which results in:

$$f'_\ell(z;\alpha_0) = 1 + \alpha_0 \left(1 - z\right) \sum_{k=0}^{\ell-1} z^k \equiv (1 + \alpha_0) - \alpha_0 z^\ell. \tag{A.15}$$

Now, the change of variable suggests that $w = 0$ is a root of f'_ℓ if and only if $z = 0$ is a root of (A.15). Therefore, the proof of (*ii*) is complete by noticing that for $\alpha_0 = -1$, $z = 0$ is a root of f'_ℓ of multiplicity ℓ.

(*iii*) Let us define $\varphi : \mathbb{C} \to \mathbb{C}$ by $\varphi(w) := \frac{1-e^{-w}}{w}$, which is analytic and bounded in $\overline{\mathbb{C}_+}$. Moreover, it has the following limits:

$$\lim_{w\to 0} \varphi(w) = 1 \quad \wedge \quad \lim_{|w|\to\infty} \varphi(w) = 0.$$

Next, show the boundedness of φ in $\overline{\mathbb{C}_+}$, consider $|w| > 1$. It is easy to observe that, under such a consideration, the following holds:

$$\left|\frac{1 - e^{-w}}{w}\right| \leq \frac{1 + |e^{-w}|}{|w|} \leq e^{-\Re\{w\}} + 1.$$

Next, consider $w \in B_1$, where $B_1 \subset \mathbb{C}$ is a closed ball of radius one in the complex plane. From the analyticity of φ and the compactness of the ball B_1, by the Heine–Cantor Theorem, we can conclude that φ is bounded for $w \in B_1$. Next, from its definition we see that $\widehat{f}_\ell$ is analytic in $\mathbb{C}$ and, furthermore, it can be expressed as:

$$\widehat{f}_\ell(w;\alpha) = 1 + \alpha\varphi(w) \sum_{k=1}^{\ell} \frac{(1 - e^{-w})^{k-1}}{k}.$$

Next, we introduce $M := \sum_{k=1}^{\ell} 2^{k-1}/k$, and consider the following inequality:

$$\left|\sum_{k=1}^{\ell} \frac{(1 - e^{-w})^{k-1}}{k}\right| \leq M.$$

Hence, by choosing α_0 such that $M\,|\alpha_0| < 1$, the following holds:

$$|\alpha_0|\,|\varphi(w)| \left|\sum_{k=1}^{\ell} \frac{(1 - e^{-w})^{k-1}}{k}\right| < 1,$$

which allows concluding that $\widehat{f}_\ell(w;\alpha) \neq 0$, $\forall w \in \overline{\mathbb{C}_+}$ and all $|\alpha| \leq |\alpha_0|$, which ends the proof.

(iv) The proof follows straightforwardly by noticing that the equations:

$$f_\ell\left(\boldsymbol{i}\omega;\alpha\right)=0 \quad\wedge\quad \left.\frac{d}{ds}f_\ell\left(w;\alpha\right)\right|_{w=\boldsymbol{i}\omega}=0,$$

are incompatible for all $\omega\in\mathbb{R}$ and all $\alpha\in\mathbb{R}^*$.

□

Proof of Proposition 3.3.4

Proof. It is easy to observe that if for $w=\omega\in\mathbb{R}$ the following must hold:

$$f_\ell\left(\boldsymbol{i}\omega;\alpha\right)=0 \quad\Leftrightarrow\quad f_\ell\left(-\boldsymbol{i}\omega;\alpha\right)=0. \tag{A.16}$$

Therefore, if $w=\boldsymbol{i}\omega$ is a critical root, the following equations must be simultaneously satisfied:

$$\begin{aligned} f_\ell\left(\boldsymbol{i}\omega;\alpha\right)+f_\ell\left(-\boldsymbol{i}\omega;\alpha\right) &= 0, & \text{(A.17)}\\ f_\ell\left(\boldsymbol{i}\omega;\alpha\right)-f_\ell\left(-\boldsymbol{i}\omega;\alpha\right) &= 0. & \text{(A.18)}\end{aligned}$$

From (A.17) we have the following:

$$\begin{aligned} f_\ell\left(\boldsymbol{i}\omega;\alpha\right)+f_\ell\left(-\boldsymbol{i}\omega;\alpha\right) &= \left(\boldsymbol{i}\omega+\alpha\sum_{k=1}^{\ell}\frac{(1-e^{-\boldsymbol{i}\omega})^k}{k}\right)+\left(-\boldsymbol{i}\omega+\alpha\sum_{k=1}^{\ell}\frac{(1-e^{\boldsymbol{i}\omega})^k}{k}\right),\\ &= \alpha\sum_{k=1}^{\ell}\left(\frac{\left(1-e^{-\boldsymbol{i}\omega}\right)^k+\left(1-e^{\boldsymbol{i}\omega}\right)^k}{k}\right). \end{aligned} \tag{A.19}$$

Which means that, for a critical root $w=\boldsymbol{i}\omega$, the following equation holds:

$$\sum_{k=1}^{\ell}\frac{\left(1-e^{-\boldsymbol{i}\omega}\right)^k+\left(1-e^{\boldsymbol{i}\omega}\right)^k}{k}=0. \tag{A.20}$$

Next, we introduce the change of variable $z:=e^{-\boldsymbol{i}w}$. With this change of variable, (A.20) rewrites as:

$$\sum_{k=1}^{\ell}\frac{(1-z)^k+\left(1-z^{-1}\right)^k}{k}=0. \tag{A.21}$$

It is clear to see that (A.21) is a reciprocal polynomial and, since $|z|=1$, (A.21) can be written in terms of Chebyshev polynomials of the first kind. To this end, consider $\zeta:=\frac{1}{2}\left(z+z^{-1}\right)$, which allows rewriting equation (A.20) as:

$$\sum_{k=1}^{\ell}\sum_{j=0}^{k}\frac{(-1)^j}{k}\binom{k}{j}T_j\left(\zeta\right)=0. \tag{A.22}$$

Since the solutions of (A.22) are given by the set $\mathcal{X}_\ell$, it follows that all critical roots $w = \pm \boldsymbol{i}\omega$ are given by the elements of $\mathcal{W}_\ell$, as stated. Next, in order to compute the critical values of α, α^*, consider $\omega^* \in \mathcal{W}_\ell$ and its associate value z^*, which from (A.18) yields:

$$\begin{aligned} f_\ell(\boldsymbol{i}\omega^*;\alpha) - f_\ell(-\boldsymbol{i}\omega^*;\alpha) &= \left(\boldsymbol{i}\omega^* + \alpha\sum_{k=1}^{\ell}\frac{(1-e^{-\boldsymbol{i}\omega^*})^k}{k}\right) - \left(-\boldsymbol{i}\omega^* + \alpha\sum_{k=1}^{\ell}\frac{(1-e^{\boldsymbol{i}\omega^*})^k}{k}\right), \\ &= \boldsymbol{i}2\omega^* + \alpha\sum_{k=1}^{\ell}\left(\frac{(1-z^*)^k - \left(1-\frac{1}{z^*}\right)^k}{k}\right), \\ &= \boldsymbol{i}2\omega^* + \alpha\left(z^* - (z^*)^{-1}\right)\sum_{k=1}^{\ell}\sum_{j=1}^{k}\frac{(-1)^j}{k}\binom{k}{j}U_{j-1}(\zeta^*). \end{aligned} \tag{A.23}$$

Finally, considering the definition of ψ_ℓ and noting that $z^* - (z^*)^{-1} = \boldsymbol{i}2\sin(\omega^*)$, solving for α in (A.23) reveals that α^* is given by (3.16), which concludes the proof. □

Proof of Theorem 3.3.1

Proof. (i) can be directly verified using Corollary 3.3.1 and the Newton diagram method. For (ii), the system is properly posed if and only if all nontrivial solutions of the auxiliary quasipolynomial $P_\ell^{aux}(w)$, defined in (3.11), lie in $\mathbb{C}_-$. Since trivial solutions are not relevant, we focus on the quasipolynomial $f_\ell(w;\alpha)$ introduced in (3.12). Utilizing Proposition 3.3.3, Property-(*ii*), and Proposition 3.3.4, we can explicitly determine at least one interval for the parameter α where condition (ii) is satisfied.

□

A.3 Proofs from Chapter 4

Proof of Proposition 4.4.3

Proof. The proof proceeds constructively. Consider the characteristic equation.

$$\Delta(s;k_p,k_i,h) = 0$$

. Introduce the change of variable $s \to s - \sigma$, where $\sigma \in \mathbb{R}$. Under this transformation, two distinct crossing curves emerge:

1. $\mathcal{K}_\omega$, obtained by fixing $\sigma = \sigma^* \in \mathbb{R}_+$, and letting $\omega \in \mathbb{R}_+$ vary.

2. $\mathcal{K}_\sigma$, obtained by fixing $\omega^* \in \mathbb{R}_+$, and letting $\sigma \in \mathbb{R}$ vary.

The tangents to these curves at any point are expressed as follows:

1. For $\mathcal{K}_\omega$:

$$\vec{t} = (dk_p/d\omega, dk_i/d\omega)^T$$

2. For $\mathcal{K}_\sigma$:

$$\vec{t_\sigma} = (dk_p/d\sigma, dk_i/d\sigma)^T$$

At their intersection, consider the normal vector $\vec{n_t} = (-dk_i/d\omega, dk_p/d\omega)$ oriented to the left relative to the positive direction of $\mathcal{K}_\omega$. The inner product of $\vec{n_t}$ and $\vec{t_\sigma}$ is given by:

$$\langle \vec{n_t}, \vec{t_\sigma} \rangle = \frac{dk_p}{d\omega}\frac{dk_i}{d\sigma} - \frac{dk_i}{d\omega}\frac{dk_p}{d\sigma}.$$

For the crossing to occur in a consistent direction, the sign of this inner product, $\text{sign}(\langle \vec{n_t}, \vec{t_\sigma} \rangle)$ must remain constant. We next obtain the given tangents for each of the curves. First, differentiate $\Delta(\boldsymbol{i}\omega - \sigma^*; k_p, k_i, h) = 0$ with respect to ω:

$$\boldsymbol{i}\frac{\partial \Delta}{\partial \omega} + \frac{\partial \Delta}{\partial k_p}\frac{dk_p}{d\omega} + \frac{\partial \Delta}{\partial k_i}\frac{dk_i}{d\omega} = 0,$$

and introduce the following notations:

$$R_0 + \boldsymbol{i}I_0 = \boldsymbol{i}\frac{\partial \Delta}{\partial \omega}, \tag{A.24}$$

$$R_1 + \boldsymbol{i}I_1 = -\frac{\partial \Delta}{\partial k_p}, \tag{A.25}$$

$$R_2 + \boldsymbol{i}I_2 = -\frac{\partial \Delta}{\partial k_i}. \tag{A.26}$$

This leads to the linear system:

$$\begin{pmatrix} R_1 & R_2 \\ I_1 & I_2 \end{pmatrix} \begin{pmatrix} \frac{dk_p}{d\omega} \\ \frac{dk_i}{d\omega} \end{pmatrix} = \begin{pmatrix} R_0 \\ I_0 \end{pmatrix},$$

Provided that $R_1 I_2 - R_2 I_1 \neq 0$, the tangent vector can be expressed as:

$$\vec{t} = \frac{1}{R_1 I_2 - R_2 I_1} \begin{pmatrix} R_0 I_2 - R_2 I_0 \\ R_1 I_0 - I_1 R_0 \end{pmatrix}.$$

Similarly, differentiate $\Delta(\boldsymbol{i}\omega^* - \sigma; k_p, k_i, h) = 0$ with respect to σ:

$$\boldsymbol{i}\frac{\partial \Delta}{\partial \sigma} + \frac{\partial \Delta}{\partial k_p}\frac{dk_p}{d\sigma} + \frac{\partial \Delta}{\partial k_i}\frac{dk_i}{d\sigma} = 0,$$

Using the same notations for R_1, R_2, I_1 and I_2, and defining $R_\sigma + \boldsymbol{i} I_\sigma = \boldsymbol{i}\frac{\partial \delta}{\partial \sigma}$, we find:

$$R_\sigma = -I_0 \tag{A.27}$$

$$I_\sigma = R_0 \tag{A.28}$$

The tangent vector $\vec{t_\sigma}$ is given by:

$$\vec{t_\sigma} = \frac{1}{R_1 I_2 - R_2 I_1} \begin{pmatrix} R_0 R_1 + I_0 I_1 \\ -R_0 R_2 - I_0 I_2 \end{pmatrix},$$

provided that $R_1 I_2 - R_2 I_1 \neq 0$.

Next, using the definitions of$\vec{n_t}$ and $\vec{t_\sigma}$, the inner product is given by:

$$\langle \vec{n_t}, \vec{t_\sigma} \rangle = \frac{R_0^2 + I_0^2}{R_1 I_2 - R_2 I_1},$$

Thus:

$$\operatorname{sign}(\langle \vec{n_t}, \vec{t_\sigma} \rangle) = \operatorname{sign}(R_1 I_2 - R_2 I_1)$$

A direct computation shows:

$$\begin{aligned} R_1 I_2 - R_2 I_1 &= -\omega \left(e^{2h\sigma}\right) \left(\omega^2 + (\sigma + z)^2\right) \\ &\implies \operatorname{sign}(R_1 I_2 - R_2 I_1) = -1. \end{aligned}$$

Since the sign is constant and negative, the crossing occurs in a consistent direction. This concludes the proof. □

Proof of Proposition 4.4.4

Proof. The curve $\mathcal{K}_0$ is defined as the horizontal axis in the parameter plane (k_p, k_i), which corresponds to $k_i = 0$. To analyze the crossing behavior, we use the implicit function theorem (see, for instance, the Introduction). Consider the characteristic function $\Delta(s; k_p, k_i, h)$. Differentiating implicitly with respect to k_i we find:

$$\frac{ds}{dk_i} = -\frac{\frac{\partial \Delta}{\partial k_i}}{\frac{\partial \Delta}{\partial s}} = \frac{z - s}{d_1 s e^{hs} + b e^{hs} + h k_i (z - s) - k_p d_2 + k_i},$$

where $d_1 = 2a + 3s$, $d_2 = (s(h(s - z) - 2) + z)$. At the point $s = 0$, $k_i = 0$, $k_p \in \mathbb{R}$ we find:

$$\left.\frac{ds}{dk_i}\right|_{s=0, k_i=0} = \frac{z}{b - k_p z}.$$

By definition, $z > 0$. Thus, the sign of $\frac{ds}{dk_i}$ changes exactly when $k_p = b/z$. This observation establishes that the crossing direction changes at that point, completing the proof. $\square$

Proof of Proposition 4.4.5

Proof. We begin by considering the change of variable $s \to s - \sigma$. Evaluating the corresponding equation over the imaginary axis gives:

$$Q(\boldsymbol{i}\omega - \sigma) + ((\boldsymbol{i}\omega - \sigma) - z)(k_p(\boldsymbol{i}\omega - \sigma) + k_i)e^{-h(\boldsymbol{i}\omega-\sigma)} = 0.$$

This can be rewritten as:

$$e^{h\sigma}(\cos(h\omega) - \boldsymbol{i}\sin(h\omega))(k_p(\boldsymbol{i}\omega - \sigma) + k_i) = \frac{Q(\boldsymbol{i}\omega - \sigma)(z + \sigma + \boldsymbol{i}\omega)}{\sigma^2 + \omega^2 + z^2 + 2\sigma z}.$$

Separating the real and imaginary parts yields:

$$e^{h\sigma}(\cos(h\omega)(k_i - k_p\sigma) + k_p\omega\sin(h\omega)) = \Re\left\{\frac{Q(\boldsymbol{i}\omega - \sigma)(z + \sigma + \boldsymbol{i}\omega)}{\sigma^2 + \omega^2 + z^2 + 2\sigma z}\right\} =: \gamma,$$

and

$$e^{h\sigma}(\sin(h\omega)(k_p\sigma - k_i) + k_p\omega\cos(h\omega)) = \Im\left\{\frac{Q(\boldsymbol{i}\omega - \sigma)(z + \sigma + \boldsymbol{i}\omega)}{\sigma^2 + \omega^2 + z^2 + 2\sigma z}\right\} =: \beta,$$

From these expressions, the proportional and integral gains k_p and k_i can be expressed as:

$$k_p(\omega, \sigma) = \frac{e^{-h\sigma}(\gamma\sin(h\omega) + \beta\cos(h\omega))}{\omega}, \tag{A.29}$$

and

$$k_i(\omega, \sigma) = \frac{e^{-h\sigma}\cos(h\omega)(\tan(h\omega)(\gamma\sigma - \beta\omega) + \gamma\omega + \beta\sigma)}{\omega}. \tag{A.30}$$

Thus, the curve comprising the points $(k_p, k_i) \in \mathbb{R}^2$ can be written as:

$$\mathcal{K}(\omega, \sigma) := \begin{bmatrix} k_p(\omega, \sigma) \\ \\ k_i(\omega, \sigma) \end{bmatrix} \equiv \frac{e^{-h\sigma}}{\omega} \begin{bmatrix} k_{11} & k_{12} \\ \\ k_{21} & k_{22} \end{bmatrix} \begin{bmatrix} \gamma \\ \\ \beta \end{bmatrix},$$

where

$$k_{11} = \sin(h\omega), \quad k_{21} = \cos(h\omega)(\sigma\tan(h\omega) + \omega),$$

$$k_{12} = \cos(h\omega), \quad k_{22} = \cos(h\omega)(\sigma - \omega\tan(h\omega)).$$

Next, introduce the function $u : \mathbb{R}_+ \times \mathbb{R}^2 \times \mathbb{R}_+ \to \mathbb{R}$ and $v : \mathbb{R}_+ \times \mathbb{R}^2 \times \mathbb{R}_+ \to \mathbb{R}$:

$$u(\omega; k_p, k_i, \sigma) := e^{h\sigma}(\cos(h\omega)(k_i - k_p\sigma) + k_p\omega\sin(h\omega)) - \gamma,$$

$$v(\omega; k_p, k_i, \sigma) := e^{h\sigma}(\sin(h\omega)(k_p\sigma - k_i) + k_p\omega\cos(h\omega)) - \beta$$

such that:

$$\Delta(\boldsymbol{i}\omega - \sigma; h) = u(\omega; k_p, k_i, \sigma) + \boldsymbol{i}v(\omega; k_p, k_i, \sigma).$$

The total derivatives of u and v are:

$$\begin{aligned} e^{h\sigma}(\omega\sin(h\omega) - \sigma\cos(h\omega))dk_p + e^{h\sigma}\cos(h\omega)dk_i + \frac{\partial u}{\partial\sigma}d\sigma + \frac{\partial u}{\partial\omega}d\omega = 0, \\ e^{h\sigma}(\sigma\sin(h\omega) + \omega\cos(h\omega))dk_p - e^{h\sigma}\sin(h\omega)dk_i + \frac{\partial v}{\partial\sigma}d\sigma + \frac{\partial v}{\partial\omega}d\omega = 0. \end{aligned}$$

Using the Cauchy-Riemann equations $\frac{\partial u}{\partial\sigma} = \frac{\partial v}{\partial\omega}$ and $\frac{\partial u}{\partial\omega} = -\frac{\partial v}{\partial\sigma}$ we can write:

$$\begin{bmatrix} dk_p \\ \\ dk_i \end{bmatrix} = \frac{-1}{e^{h\sigma}\omega} \begin{bmatrix} a_{11} & a_{12} \\ \\ a_{21} & a_{22} \end{bmatrix} \begin{bmatrix} \frac{\partial u}{\partial\sigma} & \frac{\partial u}{\partial\omega} \\ \\ -\frac{\partial u}{\partial\omega} & \frac{\partial u}{\partial\sigma} \end{bmatrix} \begin{bmatrix} d\sigma \\ \\ d\omega \end{bmatrix},$$

where:

$$a_{11} = \sin(h\omega), \quad a_{21} = \omega\cos(h\omega) + \sigma\sin(h\omega), \quad a_{12} = \cos(h\omega), \quad a_{22} = \sigma\cos(h\omega) - \omega\sin(h\omega).$$

The Jacobian determinant is then:

$$\begin{aligned} \det\left(J(\mathcal{K}(\omega,\sigma))\right) &= -\frac{e^{-h\sigma}}{\omega}\left(-\omega\sin^2(h\omega) - \omega\cos^2(h\omega)\right)\left[\left(\frac{\partial u}{\partial\sigma}\right)^2 + \left(\frac{\partial u}{\partial\omega}\right)^2\right] \\ &= e^{-h\sigma}\left[\left(\frac{\partial u}{\partial\sigma}\right)^2 + \left(\frac{\partial u}{\partial\omega}\right)^2\right]. \end{aligned}$$

Since this is always positive, the curve $\mathcal{K}(\omega,\sigma)$ preserves orientation as (ω,σ) vary. This concludes the proof. □

Proof of Theorem 4.4.1

Proof. We begin by noting that, according to Proposition 4.4.5, if a stable region exists, it is unique and corresponds to the *innermost* region in the parameter space. As $\sigma \in \mathbb{R}_+$ increases, the curve $\mathcal{K}_0$ remains a straight line, but its slope increases. This line corresponds to the locus of simple real roots. For sufficiently large σ, the only σ-stable point will be where $\mathcal{K}_\omega$ intersects the line $\mathcal{K}_0$. Specifically, the initial point of the $\mathcal{K}_\omega$ curve, at $\omega = 0$, and a point on the line $\mathcal{K}_0$ will define this stable configuration. At the optimal value of σ, the spectral abscissa corresponds to a triple real root. This configuration arises because two real roots coincide at $\omega = 0$ at the start of $\mathcal{K}_\omega$, and a third root lies on the line $\mathcal{K}_0$. This condition is described by the following system of equations:

$$\Delta(-\sigma; h) = 0, \tag{A.31}$$

$$\left.\frac{d\Delta}{ds}\right|_{s=-\sigma;h} = 0, \tag{A.32}$$

$$\left.\frac{d^2\Delta}{ds^2}\right|_{s=-\sigma;h} = 0. \tag{A.33}$$

To complete the proof, we solve the system of equations (A.31)-(A.33) for σ under the constraint $\sigma \in \mathbb{R}_+$. □

Appendix B

Matlab and python codes

B.1 Step method in Matlab

```
clear
clc
%% Using dde23
close all
% Define the delay
h = 1;  % Delay h
% Define the initial condition function for t < 0
phi = @(t) 1 - t;
% Define the delay differential equation
% dydt = x(t-h)
my_dde = @(t, y, Z) Z;  % Z is the delayed variable x(t-h)
% Solve the equation using dde23
tspan = [0 2];  % Time interval for the solution
sol = dde23(my_dde, h, phi, tspan);
% Plot the solution
figure(1)
plot(sol.x, sol.y, LineWidth = 2);
xlabel('Time $t$', interpreter='latex', FontSize=14);
ylabel('$x(t)$', interpreter='latex', FontSize=14);
grid on;
hold on
%% Anlytical solution
% Define the delay tau
tau = 1;
% Create a time vector from -tau to 2*tau with a step size of 0.00001
t = -tau:0.00001:2*tau;
```

```
% Call the solution function to compute x(t) for the given time vector and tau
x = solution(t, tau);
% Set the limits for the x-axis from 0 to 2*tau
xlim([0, 2*tau]);
% Plot the solution with a dashed line and a linewidth of 2
plot(t, x, '--', 'LineWidth', 2);
% Add a legend to the plot to label the curves
% The 'interpreter' option allows LaTeX formatting in the legend text
legend('Solution using dde23', 'Solution using the step method', ...
       'Interpreter', 'latex', 'Location', 'SouthEast', 'FontSize', 12);
% Define the solution function that computes x(t) based on the conditions
function x = solution(t, tau)
    % Initialize the solution vector x with zeros of the same size as t
    x = zeros(size(t));
    % Apply the initial condition for t <= 0
    % For t <= 0, x(t) = 1 - t
    x(t <= 0) = 1 - t(t <= 0);
    % Apply the formula for 0 < t <= tau
    % This formula is derived from the step method
    x(t > 0 & t <= tau) = 1 + t(t > 0 & t <= tau) - t(t > 0 & t <= tau).^2 / 2 ...
                          + tau * t(t > 0 & t <= tau);
    % Apply the formula for tau < t <= 2*tau
    % This formula is also derived from the step method and considers the delay
    x(t > tau & t <= 2 * tau) = 1 + t(t > tau & t <= 2 * tau) ...
                          - t(t > tau & t <= 2 * tau).^3 / 6 ...
                          + tau^2 + 2 * tau^3 / 3 ...
                          + t(t > tau & t <= 2 * tau).^2 * (1 / 2 + tau) ...
                          - t(t > tau & t <= 2 * tau) * tau * (2 + 3 * tau) / 2;
end
```

Listing B.1: Step method and dde23 for Example 10 in Matlab.

B.2 Step method in Python

```python
import numpy as np
import matplotlib.pyplot as plt
# Parameters
tau = 1
t = np.arange(-tau, 2*tau, 0.00001)  # Time vector
# Solution function in Python
def solution(t, tau):
    x = np.zeros_like(t)
    # For t <= 0, apply the initial condition
    x[t <= 0] = 1 - t[t <= 0]
    # For 0 < t <= tau
    mask1 = (t > 0) & (t <= tau)
    x[mask1] = 1 + t[mask1] - t[mask1]**2 / 2 + tau * t[mask1]
    # For tau < t <= 2 * tau
    mask2 = (t > tau) & (t <= 2*tau)
    x[mask2] = (1 + t[mask2] - t[mask2]**3 / 6 + tau**2
                + 2 * tau**3 / 3 + t[mask2]**2 * (1 / 2 + tau)
                - t[mask2] * tau * (2 + 3 * tau) / 2)
    return x
# Compute the solution
x = solution(t, tau)
# Plotting the result
plt.plot(t, x, '--', linewidth=2)
plt.xlim([0, 2*tau])
plt.title('Solution using the Step Method', fontsize=14)
plt.xlabel('Time t', fontsize=12)
plt.ylabel('x(t)', fontsize=12)
plt.grid(True)
plt.show()
```

Listing B.2: Step method for Example 10 in Python.

B.3 Symbolic QPmR in Python

```
from lib2to3.pygram import Symbols
import numpy as np
import sympy as sp
from sympy import exp
from matplotlib.pyplot import contour
import matplotlib.pyplot as plt
def QPmR(M,Reg,d,e):
    b_min = Reg[0] - 3*d
    b_max = Reg[1] + 3*d
    w_min = Reg[2] - 3*d
    w_max = Reg[3] + 3*d
    """
    m = M.shape
    if m[0]>1:
        M = poly(M,s)
    """
    P='No roots in the selected region'
    nW = round((w_max-w_min)/d + 1)
    nB = round((b_max-b_min)/d + 1)
    W = np.linspace((w_min), (w_max), nW)
    B = np.linspace((b_min), (b_max), nB)
    W = np.reshape(W, (1, nW))
    B = np.reshape(B, (1, nB))
    oB = np.ones((1, nW))
    oW = np.ones((1, nB))
    WW = np.matmul(np.transpose(oW), W)
    BB = np.matmul(np.transpose(oB), B)
    D = BB + np.transpose(WW)*1j
    s = sp.MatrixSymbol("s", D.shape[0], D.shape[1])
    func = sp.utilities.lambdify(s, M,'numpy') # returns a numpy-ready function
    MM = func(D)
    #MM = M.subs({s: sp.Matrix(D)})
    #MM = M.double(MM)
    R = MM.real
    I = MM.imag
    Cr = contour(B[0], W[0],R,[0])
    Cr = Cr.allsegs
    aux = np.empty((0, 2))
    for seg in Cr[0]:
        aux = np.append(aux, np.array(seg), axis=0)
    Cr = np.transpose(aux)
```

```
    pCr=Cr.shape
    pCr=pCr[1]
    Crr=Cr
    Cr=Cr[0,:] + Cr[1,:]*1j
    IIc=np.imag(func(Cr))
    Np=1
    ch=1
    Pp = np.empty((0))
    n = -1
    for no in range(2, pCr-1):
        if((IIc[no-2]*IIc[no])<0) and (ch==1):
            if (Reg[0] <= np.real(Cr[no-1])) and (Reg[1] >= np.real(Cr[no-1])) and (Reg[2] <=
                np.imag(Cr[no-1])) and (Reg[3] >= np.imag(Cr[no-1])):
                if (abs(Crr[0][no-1]-Crr[0][no]) < 2*d) and (abs(Crr[1][no-1]-Crr[1][no]) < 2*d):
                    Pp = np.append(Pp, np.array(Cr[no - 1]))
                    Np = Np + 1
                    ch = 0
        else:
            ch=1
    P=np.empty((0))
    #numeric calculation of poles
    if not (isinstance(P, str) and len(P) == 1):
        H = M
        s = sp.symbols("s")
        dH = sp.diff(M, s)
        dfunc = sp.utilities.lambdify(s, dH,'numpy') # returns a numpy-ready function
        n = Pp.shape
        n = n[0]
        for o in range(1,n+1):
            a = Pp[o-1]
            Newton_run = 1
            while Newton_run:
                a_k1 = a
                #s = a
                a = a - func(a) / dfunc(a)
                Newton_run = (abs(a - a_k1) > e)
            if (not np.isreal(a)) and (abs(np.imag(a)) < 0.1*e):
                a = np.real(a)
            P = np.append(P, a)
    Pmax = max(abs(P))
    PM = np.empty((0))
    for k in range(n):
```

```
        o = np.where(np.abs(P) == np.amin(np.abs(P)))
        o = o[0][0]
        PM = np.append(PM, P[o])
        P[o]=2*Pmax
    for elem in PM:
        print(elem)
    return PM
```

Listing B.3: Symbolic QPmR in Python.

B.4 Improperly-posedness and crossing detection in python

```
from sympy import symbols, exp, I, pi, Sum, solve, Eq, re, im, simplify, sign, N

def compute_crossings():
    try:
        # Prompt user for input
        n = int(input("Enter an integer value for n: "))
        if n <= 0:
            raise ValueError("n must be a positive integer.")
    except ValueError as e:
        print(f"Invalid input: {e}")
        return

    # Define symbolic variables
    w, alpha = symbols('w alpha', real=True)
    k = symbols('k', integer=True)

    # Define functions
    F = Sum((1 - exp(-I * w))**k / k, (k, 1, n)).doit()
    s = -F / (1 + alpha * exp(-I * w) * Sum((1 - exp(-I * w))**(k - 1), (k, 1, n)).doit())

    # Solve for w where Re(F) = 0
    real_F = re(F)
    solutions = solve(Eq(real_F, 0), w, domain=(-10 * pi, 10 * pi))

    # Check and process each solution
    print(f"\nNumber of solutions for n = {n}: {len(solutions)}")
    for sol in solutions:
        w_sol = sol.evalf()  # Numerical solution for w
        if N(w_sol) == 0:
            print(w_sol)
        else:
            imag_part = simplify(im(F.subs(w, w_sol)))
            alpha_val = -simplify(w_sol / imag_part)
            crossing = sign(re(s.subs({w: w_sol, alpha: alpha_val})))
            print(f"w = {w_sol}, alpha = {alpha_val}, crossing = {crossing}")
```

Listing B.4: Improperly-posedness and crossing detection.

B.5 Crossing curves plot function

```
function plotRegion(a, b, z, h, sigma, myColor, w)
    x1 = w.*(-b-a*z+2*z*sigma+sigma^2+w.^2);
    x2 = (z+sigma)*(b+sigma*(sigma-a))-(a+z-sigma)*w.^2;
    kiw = exp(-h*sigma)*(sigma^2+w.^2).*(cos(h*w).*x1-sin(h*w).*x2)./(w.*((z+sigma)^2+w.^2));
    y1 = -w.*(-b*z+sigma*(2*a*z+a*sigma-3*z*sigma-2*sigma^2)+(a+z-2*sigma)*w.^2);
    y2 = (sigma*(z+sigma)*(b+sigma*(-a+sigma))+(b+a*z-(a+3*z)*sigma)*w.^2-w.^4);
    kpw = exp(-h*sigma)*(cos(h*w).*y1-sin(h*w).*y2)./(w.*((z+sigma)^2+w.^2));
    plot(kpw, kiw, LineStyle="-", LineWidth=2, Color=myColor)
    hold on
    kp0 = linspace(min(kpw), max(kpw), length(w));
    ki0 = sigma*(kp0-(exp(-h*sigma)*(sigma*(sigma-a)+b))/(sigma+z));
    plot(kp0, ki0, LineStyle="-", LineWidth=2, Color=myColor)
    xlim([min(kpw), max(kpw)])
    ylim([min(kiw), max(kiw)])
    xlabel('$k_p(\omega, \sigma)$', Interpreter='latex', FontSize=16)
    ylabel('$k_i(\omega, \sigma)$', Interpreter='latex', FontSize=16)
end
```

Listing B.5: Matlab function to plot the stability crossing cruves introduced in Chapter 4.

Bibliography

[1] J. Alvarez-Ramirez, I. Cervantes, G. Espinosa-Perez, P. Maya, and A. Morales. A stable design of pi control for dc-dc converters with an rhs zero. *IEEE Transactions on Circuits and Systems I: Fundamental Theory and Applications*, 48(1):103–106, 2001.

[2] Q. An, E. Beretta, Y. Kuang, C. Wang, and H. Wang. Geometric stability switch criteria in delay differential equations with two delays and delay dependent parameters. *Journal of Differential Equations*, 266(11):7073–7100, 2019.

[3] P. Appeltans, H. Silm, and W. Michiels. Tds-control: A matlab package for the analysis and controller-design of time-delay systems. *IFAC-PapersOnLine*, 55(16):272–277, 2022.

[4] K. G. Begum, A. S. Rao, and T. Radhakrishnan. Enhanced imc based pid controller design for non-minimum phase (nmp) integrating processes with time delays. *ISA transactions*, 68:223–234, 2017.

[5] E. Beretta and Y. Kuang. Geometric stability switch criteria in delay differential systems with delay dependent parameters. *SIAM Journal on Mathematical Analysis*, 33(5):1144–1165, 2002.

[6] I. Boussaada, G. Mazanti, S.-I. Niculescu, J. Huynh, F. Sim, and M. Thomas. Partial pole placement via delay action: A python software for delayed feedback stabilizing design. In *2020 24th International Conference on System Theory, Control and Computing (ICSTCC)*, pages 196–201. IEEE, 2020.

[7] C. Canuto and A. Tabacco. *Mathematical Analysis II*, volume 85. Springer, 2015.

[8] Z. Chen, W. Gao, J. Hu, and X. Ye. Closed-loop analysis and cascade control of a nonminimum phase boost converter. *IEEE Transactions on power electronics*, 26(4):1237–1252, 2010.

[9] C. Christensen. Newton's method for resolving affected equations. *The College Mathematics Journal*, 27(5): 330–340, 1996.

[10] R. Datko. A paradigm of ill-posedness with respect to time delays. *IEEE transactions on automatic control*, 43 (7):964–967, 1998.

[11] A. Datta, M.-T. Ho, and S. P. Bhattacharyya. *Structure and synthesis of PID controllers.* Springer Science & Business Media, 1999.

[12] I. I. Delice and R. Sipahi. Inventory dynamics models of supply chains with delays; system-level connection & stability. In *Topics in Time Delay Systems*, pages 349–358. Springer, 2009.

[13] O. A. Egaji, A. Griffiths, and M. S. Hasan. Delay optimisation for multimedia application in a wireless network control system (wncs). In *2020 11th IEEE Annual Information Technology, Electronics and Mobile Communication Conference (IEMCON)*, pages 0267–0275. IEEE, 2020.

[14] K. Engelborghs, T. Luzyanina, G. Samaey, et al. Dde-biftool: a matlab package for bifurcation analysis of delay differential equations. *TW Report*, 305(1), 2000.

[15] E. Fridman. *Introduction to Time-Delay Systems: Analysis and Control.* Springer, 2014.

[16] T. T. Georgiou and M. C. Smith. w-stability of feedback systems. *Systems & Control Letters*, 13(4):271–277, 1989.

[17] T. T. Georgiou and M. C. Smith. w-stability of feedback systems. *Systems & Control Letters*, 13(4):271–277, 1989.

[18] E. N. Gryazina and B. T. Polyak. Stability regions in the parameter space: D-decomposition revisited. *Automatica*, 42(1):13–26, 2006.

[19] E. N. Gryazina, B. T. Polyak, and A. A. Tremba. D-decomposition technique state-of-the-art. *Automation and Remote Control*, 69(12):1991–2026, 2008.

[20] J. Hadamard. Sur les problèmes aux dérivées partielles et leur signification physique. *Princeton university bulletin*, pages 49–52, 1902.

[21] J.-A. Hernández-Gallardo, C.-F. Méndez-Barrios, J.-E. Escalante-Martínez, and E. J. Gonzalez-Galvan. Stabilizing second-order non-minimum phase systems via pδi controller. In *2024 10th International Conference on Control, Decision and Information Technologies (CoDIT)*, pages 1849–1854, 2024. doi: 10.1109/CoDIT62066.2024.10708290.

[22] M. A. Hossain and J. Tanimoto. A microscopic traffic flow model for sharing information from a vehicle to vehicle by considering system time delay effect. *Physica A: Statistical Mechanics and its Applications*, 585: 126437, 2022.

[23] D. Ivanov, S. Sethi, A. Dolgui, and B. Sokolov. A survey on control theory applications to operational systems, supply chain management, and industry 4.0. *Annual Reviews in Control*, 46:134–147, 2018.

[24] C. Jin, K. Gu, S.-I. Niculescu, and I. Boussaada. Stability analysis of systems with delay-dependent coefficients subject to some particular delay structure. In *2018 European Control Conference (ECC)*, pages 1206–1213. IEEE, 2018.

[25] M. Keyvan-Ekbatani, R. C. Carlson, V. L. Knoop, and M. Papageorgiou. Optimizing distribution of metered traffic flow in perimeter control: Queue and delay balancing approaches. *Control Engineering Practice*, 110: 104762, 2021.

[26] V. Kharitonov, S.-I. Niculescu, J. Moreno, and W. Michiels. Static output feedback stabilization: necessary conditions for multiple delay controllers. *IEEE Trans. Automat. Cont.*, 50(1):82–86, 2005.

[27] H. Kokame and T. Mori. Stability preserving transition from derivative feedback to its difference counterparts. *IFAC Proceedings Volumes*, 35(1):129–134, 2002.

[28] S. G. Krantz and H. R. Parks. *The implicit function theorem: history, theory, and applications.* Springer Science & Business Media, 2002.

[29] A. Mamizadeh, N. Genc, and R. Rajabioun. Optimal tuning of pi controller for boost dc-dc converters based on cuckoo optimization algorithm. In *2018 7th international conference on renewable energy research and applications (ICRERA)*, pages 677–680. IEEE, 2018.

[30] A. Martínez González. *Perturbation Analysis of Eigenvalues for LTI Delay Systems. Regular and Singular Cases.* PhD thesis, Université Paris-Saclay, 2021. URL http://www.theses.fr/2021UPASG017.

[31] A. Martínez-González, C.-F. Méndez-Barrios, S.-I. Niculescu, J. Chen, and L. Félix. Weierstrass approach to asymptotic behavior characterization of critical imaginary roots for retarded differential equations. *SIAM Journal on Control and Optimization*, 57(1):1–22, 2019.

[32] C.-F. Méndez-Barrios, S.-I. Niculescu, A. Martínez-González, and A. Ramírez. Characterizing some improperly posed problems in proportional-derivative control. *International Journal of Robust and Nonlinear Control*, 32 (18):9452–9474, 2022.

[33] C.-F. Méndez-Barrios, J.-D. Torres-García, and S.-I. Niculescu. Delay-difference approximations of pd-controllers. improperly-posed systems in multiple delays case. *International Journal of Robust and Nonlinear Control*, 34(10):6431–6454, 2024.

[34] W. Michiels. To filter or not to filter? impact on stability of delay-difference and neutral equations with multiple delays. *IEEE Transactions on Automatic Control*, 2022.

[35] W. Michiels and S.-I. Niculescu. *Stability, Control, and Computation for Time-Delay Systems. An Eigenvalue-Based Approach (2. ed.).* Advances in design and control. SIAM, Philadelphia, 2014. ISBN 978-1-611-97362-4.

[36] W. Michiels, S. Mondié, D. Roose, and M. Dambrine. The effect of approximating distributed delay control laws on stability. In *Advances in Time-Delay Systems*, pages 207–222. Springer, 2004.

[37] W. Michiels, S.-I. Niculescu, I. Boussaada, and G. Mazanti. On the relations between stability optimization of linear time-delay systems and multiple rightmost characteristic roots. *Mathematics of Control, Signals, and Systems*, pages 1–24, 2024.

[38] Y. I. Neimark. Structure of the d-partition of the space of polynomials and the diagram of vishnegradskii and nyquist. In *Dokl Akad Nauk SSSR*, volume 59, page 853, 1948.

[39] I. Newton and D. T. Whiteside. *The Mathematical Papers of Isaac Newton, volume 1 of The Mathematical Papers of Sir Isaac Newton*. Cambridge University Press, 2008.

[40] S.-I. Niculescu and W. Michiels. Stabilizing a chain of integrators using multiple delays. *IEEE Transactions on Automatic Control*, 49(5):802–807, 2004.

[41] V. A. Oliveira, L. V. Cossi, M. C. Teixeira, and A. M. Silva. Synthesis of pid controllers for a class of time delay systems. *Automatica*, 45(7):1778–1782, 2009.

[42] S. K. Pandey, S. L. Patil, and S. Phadke. Regulation of nonminimum phase dc–dc converters using integral sliding mode control combined with a disturbance observer. *IEEE Transactions on Circuits and Systems II: Express Briefs*, 65(11):1649–1653, 2017.

[43] E. Pinney. *Ordinary difference-differential equations*. Univ of California Press, 1958.

[44] V. Puiseux. Recherches sur les fonctions algébriques. *Journal de mathématiques pures et appliquées*, 15:365–480, 1850.

[45] A. Ramírez, S. Mondié, R. Garrido, and R. Sipahi. Design of proportional-integral-retarded (pir) controllers for second-order lti systems. *IEEE Transactions on Automatic Control*, 61(6):1688–1693, 2015.

[46] C. Riddalls and S. Bennett. The stability of supply chains. *International journal of production research*, 40(2): 459–475, 2002.

[47] A. P. Seyranian and A. A. Mailybaev. *Multiparameter stability theory with mechanical applications*, volume 13. World Scientific, 2003.

[48] G. J. Silva, A. Datta, and S. P. Bhattacharyya. *PID controllers for time-delay systems*. Springer Science & Business Media, 2007.

[49] R. Sipahi, S.-I. Niculescu, C. Abdallah, W. Michiels, and K. Gu. Stability and stabilization of systems with time delay. *IEEE Control Systems Magazine*, 31(1):38–65, 2011.

[50] R. P. Sree and M. Chidambaram. *Control of unstable systems.* Alpha Science International Ltd., 2006.

[51] I. H. Suh and Z. Bien. Proportional minus delay controller. *IEEE Transactions on Automatic Control*, 24(2): 370–372, 1979.

[52] I. H. Suh and Z. Bien. Use of time-delay actions in the controller design. *IEEE Transactions on Automatic Control*, 25(3):600–603, 1980.

[53] G. M. Swisher and S. Tenqchen. Design of proportional-minus-delay action feedback controllers for second-and third-order systems. In *1988 American control conference*, pages 254–260. IEEE American control conference, 1988.

[54] P. Tchébychev. *Sur les questions de minima qui se rattechent a la raprésentation aproximative des fonctions (in French).* Imprimerie de l'Academie Impériale des Sciences, 1858.

[55] A. N. Tikhonov. *Solutions of Ill-Posed Problems.* VH Winston and Sons, 1977.

[56] Y. Tipsuwan and M.-Y. Chow. Control methodologies in networked control systems. *Control engineering practice*, 11(10):1099–1111, 2003.

[57] D. Torres-García, C.-F. Méndez-Barrios, S.-I. Niculescu, and A. Martínez-González. Delay-difference approximation of pd-controllers. insights into improperly-posed closed-loop systems. *IFAC-PapersOnLine*, 55 (40):79–84, 2022.

[58] D. Torres-García, F. Méndez-Barrios, and A. Ramírez. Maximum exponential decay rate for first-order time-delay systems with pi controllers. In *Advances in Automation and Robotics Research: Proceedings of the 3rd Latin American Congress on Automation and Robotics, Monterrey, Mexico 2021*, pages 34–42. Springer, 2022.

[59] D. Torres-García, C. F. M. Barrios, and S.-I. Niculescu. Some remarks on the implementation of a derivative action via a delay-difference approximation. In *2023 European Control Conference (ECC 2023)*, 2023.

[60] D. Torres-García, C. F. M. Barrios, S.-I. Niculescu, and M. Hernández-Gómez. Pi control for optimal spectral abscissa in general non-minimum phase systems with time delay. In *CoDIT 2024-10th International Conference on Control, Decision and Information Technologies*, 2024.

[61] D. Torres-García, C.-F. Méndez-Barrios, and S.-I. Niculescu. Impact of delay-difference approximation on pid controllers: Stability and performance insights. In *2024 32nd Mediterranean Conference on Control and Automation (MED)*, pages 616–621. IEEE, 2024.

[62] D. Torres-García, C.-F. Méndez-Barrios, and S.-I. Niculescu. Stabilization of second-order non-minimum phase system with delay via pi controllers: Spectral abscissa optimization. *IEEE Access*, 12:170851–170867, 2024. doi: 10.1109/ACCESS.2024.3499748.

[63] D. Torres-García, C.-F. Méndez-Barrios, and S.-I. Niculescu. Insights into the stabilization of a chain of integrators via delay-difference approximations*. *IFAC-PapersOnLine*, 58(27):19–24, 2024. ISSN 2405-8963. doi: https://doi.org/10.1016/j.ifacol.2024.10.293. URL https://www.sciencedirect.com/science/article/pii/S2405896324020822. 18th IFAC Workshop on Time Delay Systems TDS 2024.

[64] D. Torres-García[1], J.-A. Hernández-Gallardo[1], C.-F. Méndez-Barrios[1], and S.-I. Niculescu. Exploring delay-based controllers. a comparative study for stabilizing angular positioning. In *Advances in Automation and Robotics Research: Proceedings of the 4th Latin American Congress on Automation and Robotics, San Salvador, El Salvador 2023*, volume 940, page 123. Springer Nature, 2024.

[65] L. N. Trefethen. *Approximation Theory and Approximation Practice, Extended Edition*. SIAM, 2019.

[66] H. U. Ünal, D. Melchor-Aguilar, D. Üstebay, S.-I. Niculescu, and H. Özbay. Comparison of pi controllers designed for the delay model of tcp/aqm networks. *Computer Communications*, 36(10-11):1225–1234, 2013.

[67] T. Vyhlídal and P. Zítek. Quasipolynomial mapping based rootfinder for analysis of time delay systems. *IFAC Proceedings Volumes*, 36(19):227–232, 2003. ISSN 1474-6670. doi: https://doi.org/10.1016/S1474-6670(17)33330-X. URL https://www.sciencedirect.com/science/article/pii/S147466701733330X. 4th IFAC Workshop on Time Delay Systems (TDS 2003), Rocquencourt, France, 8-10 September 2003.

[68] T. Vyhlídal and P. Zítek. Qpmr-quasi-polynomial root-finder: Algorithm update and examples. In *Delay systems*, pages 299–312. Springer, 2014.

[69] C. T. C. Wall. *Singular points of plane curves*. Cambridge University Press, 2004.

[70] K. Walton and J. Marshall. Direct method for tds stability analysis. *IEE Proceedings D-Control Theory and Applications*, 134(2):101–107, 1987.

[71] P. Warrier, P. Shah, and R. Sekhar. A comparative performance evaluation of a complex-order pi controller for dc–dc converters. *Results in Control and Optimization*, 15:100414, 2024.

[72] Z. Wu, G.-P. Liu, J. Hu, H. Yu, and D. Chen. Optimal control strategies for a supply chain system with delay and reference price effects. *International Journal of Control, Automation and Systems*, pages 1–12, 2024.

[73] W. Zhang, M. S. Branicky, and S. M. Phillips. Stability of networked control systems. *IEEE control systems magazine*, 21(1):84–99, 2001.

[74] S. Zhao and Z. Gao. Active disturbance rejection control for non-minimum phase systems. In *Proceedings of the 29th Chinese control conference*, pages 6066–6070. IEEE, 2010.